AN ABSTRACT OF THE THESIS OF

Sanket S. Chiplunkar for the degree of Master of Sciences in Comparative Health Sciences presented on May 29, 2018.

Title: Characterization of Membrane Vesicles Released by the Opportunistic Human Pathogen *Mycobacterium avium subsp. hominissuis* (MAH) in Response to an *in vitro* System Mimicking the Phagosomal Environment

Abstract approved:

_____

Luiz E. Bermudez Lia Danelishvili

Mycobacterium avium subsp. hominissuis (MAH) belongs to the most-clinically significant non-tuberculous mycobacterial (NTM) pathogens with constant increase in disease prevalence, mainly in several industrialized western countries where tuberculosis is less prevalent. Upon entry into the alveolar space, MAH is engulfed by resident-macrophages, where the pathogen adapts to the hostile phagosomal environment and proliferates. Mycobacteria bypass host immune defenses by secreting virulence factors. Several intracellular pathogens including mycobacteria are known to form membrane vesicles (MVs) in response to intracellular stress, helping bacteria to

deliver virulence effectors in the host cell. MVs are bacterial membrane-derived spheres filled with the cargo of biologically active materials such as proteins, lipids and nucleic acids. MVs play important role in bacterial pathogenesis, nutrient acquisition, biofilm formation and immunomodulation essential for bacterial survival within the host. Macrophage phagosomal environment, partly consisting of elemental mixture and low pH, activates several virulence mechanisms of MAH. Using the *in vitro* model mimicking the phagosomal environment of MAH (metal mix), we characterized cargo of MVs and investigated whether MV-associated bacterial virulence effectors are delivered to the cytosol of the host macrophages. Scanning electron microscopy of MAH exposed to the *in vitro* phagosomal model revealed formation of MVs on bacterial surface. Further, transmission electron microscopy confirmed presence of MVs in the purified samples of isolated vesicles. Using mass spectrometric analysis, 202 proteins were identified in MVs of minimal media of starvation model and 263 proteins were found in the *in vitro* model mimicking phagosome environment. Out of 263 cargo proteins, 211 are unique to the metal mix and are enriched in several virulence factors including enzymes involved in lipid and fatty acid metabolism and cell wall-associated processes. Non-canonical amino acid metabolic labeling and click chemistry-based enrichment assay confirmed that at least 5 proteins found in the *in vitro* phagosomal model are also present in the cytosol of THP1 macrophages during MAH infection at 24h. Lipidomic analysis showed presence of outer cell wall lipids with no compositional differences between MVs of minimal media and metal mix. Using PicoGreen assay, we demonstrate that MVs of both minimal media and metal mix harbor dsDNA; however, the concentration was found to be significantly lower in

the *in vitro* phagosomal model. Similar results are observed by laser confocal microscopy of MVs stained with lipophilic nucleic acid dye SYTO-61. Our study suggests that MAH produces MVs in phagosomes and carry important virulence factors with potential roles in bacterial intracellular survival and in the immunomodulation of host cellular defenses.

Characterization of Membrane Vesicles Released by the Opportunistic Human Pathogen *Mycobacterium avium subsp. hominissuis* (MAH) in Response to an *in vitro* System Mimicking the Phagosomal Environment

by
Sanket S. Chiplunkar

A THESIS

submitted to

Oregon State University

in partial fulfillment of
the requirements for the
degree of

Master of Science

Presented May 29, 2018
Commencement June 2018

Master of Science thesis of Sanket S. Chiplunkar presented on May 29, 2018.

APPROVED:

Major Professor, representing Comparative Health Sciences

Co-Major Professor, representing Comparative Health Sciences

Dean of the College of Veterinary Medicine

Dean of the Graduate School

I understand that my thesis will become part of the permanent collection of Oregon State University libraries. My signature below authorizes release of my thesis to any reader upon request.

Sanket S. Chiplunkar, Author

ACKNOWLEDGEMENTS

I am very grateful to Dr. Luiz Bermudez for believing in my potential and giving me this opportunity of working in his laboratory. I am also thankful to him for providing me helpful feedback and suggestions for my research and postgraduate studies. I am very grateful to Dr. Lia Danelishvili for her continuous mentorship and assistance provided during conducting experiments, writing thesis and postgraduate studies. I would like to thank the committee members Dr. Claudia Hase and Dr. Sean Newsom for agreeing to be on my committee and for providing me helpful feedback during committee meetings. I want to thank Dr. Liping Yang and Jeff Morre of OSU Mass Spectrometry Center, Teresa Sawyer of OSU Electron Microscopy Facility, Anne-Marie Girard Pohjanpelto of CGRB confocal laser scanning microscope facility and other CGRB staff for their technical assistance. I am thankful of Dr. Virginia Weis for providing me teaching assistantship. I wish to thank my lab-mates, administrative staff of department of Biomedical Sciences and Integrative Biology, TA-coordinators, friends and family who continuously supported me throughout this journey. Big thank you to my mom and dad for their continuous moral support and encouragement.

This work was supported by the Oregon State University Foundation FS062E-VF01 and by the Oregon State University Incentive Programs VBS330-001100 (Lia Danelishvili). The proteomic sequencing was conducted by the Oregon State University's Mass Spectrometry Center supported in part by OSU's Research Office and institutional funds. The procurement of the Orbitrap Fusion Lumos was made possible by NIH grant S10 OD020111.

CONTRIBUTION OF AUTHORS

Sanket S. Chiplunkar contributed to experimental design, conducted experiments, analyzed data and wrote manuscript. Dr. Lia Danelishvili contributed to experimental design, conducted experiments, data analysis and manuscript preparation and funding of the project. Dr. Luiz Bermudez contributed to experimental design, manuscript preparation and project funding.

TABLE OF CONTENTS

LIST OF FIGURES

LIST OF FIGURES (Continued)

Figure Page

LIST OF TABLES

Chapter 1.

INTRODUCTION

Mycobacterium avium subspecies *hominissuis* (MAH) is one of the members of the group *Mycobacterium avium* complex (MAC), which is a part of the non-tuberculous mycobacterial (NTM) pathogens. MAC consist of two mycobacterial species: *M. avium* and *Mycobacterium intracellulare* (1). Within *M. avium*, there are four distinct subspecies which are MAH, *M. avium subsp. paratuberculosis*, *M. avium subsp. avium*, and *M. avium subsp. silvaticum* (2). These MAC members produce highly antigenic, typeable serovar-specific glycopeptidolipids (GPLs) which are involved in MAC pathogenesis, and are also used for their characterization (3). Worldwide disease incidence and prevalence of NTM is on a constant rise, making these pathogens a significant global health issue. Among the four *M. avium* subspecies, MAH is the most clinically-significant pathogenic subspecies, in terms of human disease burden (2). While, MAC are ubiquitous in the environment, the typical infection sources include tap waters, bathrooms, garden soil, where they may exist in biofilms or also within the protozoa. MAC are very hardy microbes, showing high tolerance to starvation, extremes of temperature, numerous antibiotics and also anthropogenic chlorine-containing disinfectants and bioacids. This is partly due to their characteristic waxy, lipid-rich, thick and impermeable cell wall, and partly due to their slow growth rate that gives them time to adapt to the stressful environment. Urban water supplies serve as an ideal source of MAC where MAC forms biofilm inside the pipes, showerheads, taps, spa-system, ice machine and other water transporting appliances (2), (4). Infection occurs through both respiratory and

gastrointestinal routes. Disseminated MAC infection and/or MAC bacteremia, while uncommon in healthy people, is commonly seen in people living with the acquired immunodeficiency syndrome (AIDS) (1). MAC central nervous system infections (including meningitis) have also been reported in AIDS patients (5). MAC epidemic saw sharp rise in the number of infection cases with the dawn of human immunodeficiency virus caused AIDS epidemic, because the major risk factor of disseminated MAC disease is impaired immunity as reflected by having abnormally low numbers of $CD4^+$ T cells, which is commonly seen in people living with the AIDS. Disseminated MAC infection is among the leading causes of mortality in AIDS patients (6). However, this does not mean that infection of MAC is restricted only to the AIDS patients, but it occurs also in immunocompetent people with certain underlying pulmonary conditions such as chronic obstructive pulmonary disease, bronchiectasis, cystic fibrosis, recurrent pneumonia, pneumoconiosis, lung cancer and latent or active pulmonary tuberculosis. All of these conditions put a person at a high risk of contracting pulmonary MAC infection (1). Moreover, MAC pulmonary infection cases have also been documented in middle aged and elderly women without any underlying immunodeficiency, lung condition, and any history of lung diseases. MAC-caused progressive parenchymal lung disease and bronchiectasis led to respiratory failure and even death in few of these cases in elderly immunocompetent women. MAC lung disease led mortality, in this non-AIDS group, is also quite high. Similarly, MAC is also significant for the livestock industry, being important pathogens of swine, cattle and, poultry (7).

Being ubiquitously present in the environment, with the respiratory and gastrointestinal routes, being the main routes of entry, MAC may be acquired through droplet inhalation, ingestion and also through cutaneous exposure (2). MAC infect a variety of cells including mucosal cells such as intestinal, oropharyngeal and pulmonary epithelial cells, mononuclear phagocytes and fibroblasts (1). Nevertheless, the most-preferred host cell target of MAC, where bacteria establish chronic infection is the specific-tissue (mainly pulmonary)-resident professional phagocyte called macrophage (8). MAC strains isolated from AIDS patients are virulent and survive within human and murine macrophages, where they deal with the bactericidal oxidative burst and superoxide radical, partly by producing superoxide dismutase and heat shock proteins (1). A function of a professional phagocyte such as tissue-resident and blood macrophages, is to engulf/phagocytose and ultimately kill the invading pathogens, where initially the pathogen is attached to a specific macrophage receptor before getting phagocytosed. Complement receptor 3 (CR3), fibronectin and mannosyl-fucosyl are among the known macrophage receptors that are responsible for uptake of *M. avium* by human macrophages (9). After entering the macrophage, *M. avium* persists in a membrane-bound vacuole. Mycobacterial pathogens have adapted to use virulence mechanisms, which enable them to persist and replicate intracellularly in otherwise very hostile environment in a macrophage. Pathogenic mycobacteria prevent phagosome maturation through modulation of several host cell processes that, in turn, make the phagosomal environment favorable for bacterial survival and replication (10). The phagosome goes through a series of sequential fusion events with several vesicles, originated during endocytic pathways. Through

this process, the phagosome matures into a phagolysosome, which has numerous bactericidal properties such as acidic pH (through acquisition of vacuolar proton ATPase), and being filled with numerous hydrolytic enzymes, which are capable of degrading engulfed bacteria (11). *M. avium* prevents phagosome maturation into the phagolysosome through secretion of numerous effector proteins that interfere with the host cell protein trafficking involved in the phagosome maturation (12). As part of preventing phagosome maturation, *M. avium* inhibits fusion of MAC-containing phagosome with the hydrolytic enzymes-containing lysosome (13), and also suppresses phagosome acidification needed for the pathogen killing. *M. avium*-containing phagosomal membrane do not show vacuolar proton ATPase and fail to acidify below the pH of 6.3-6.5 (14). This virulence strategy is shared among numerous mycobacterial pathogens including *M. tuberculosis* (11). Following macrophage infection, *M. tuberculosis* break open/ruptures the phagosome using ESX1 secreted ESAT6 effector, in turn, escape the phagosome and, ultimately lead to the host immune response-mediated granuloma formation, which helps the *M. tuberculosis* bacilli to spread to new uninfected areas within the human host (15). While *M. avium* has also been shown to induce granuloma formation, following *in vivo* macrophage infection (16), (17), (18), it lacks ESX1/ESAT6 secretion system (15). Nevertheless, MAH does have other ESX secretion systems, including ESX-5 which is involved in mycobacterial pathogenesis (19), described in more details in the next paragraph. Virulent *M. tuberculosis* suppresses macrophage apoptosis, at least, during the early stage of infection (20) whereas, MAH has been shown to induce macrophage apoptosis, as a way of spreading to other host cells. Viable *M. avium*

bacilli are present in macrophage apoptotic bodies, which are engulfed by healthy macrophages and in the process, get infected with the MAH (21), (22).

Ability of secreting virulence factors dictates bacterial pathogenicity. These virulence factors may be exported on bacterial cell surface, secreted into the extracellular milieu or injected directly into the host cell (23). Secreted proteins that are destined to enter host cells, also called as effector proteins and/or secreted virulence factors are indeed infection effecters that bind to host cell targets (usually a host protein) and interfere with and/or modulate specific host cell processes and/or signaling pathways, in order to colonize and/or infect the host cell (24). General secretion system, which is also termed as Sec pathway is a highly conserved and hence common secretion systems present in all eubacteria, archaea and eukaryotes. Proteins secreted through Sec system harbor amino-terminal signal peptide, which serves as a signal for translocation of that protein through Sec system, across the bacterial membrane. During the process of translocation, the signal peptide is cleaved of from the translocated/secreted protein. In many pathogenic gram-positive bacteria, including pathogenic mycobacteria, accessory Sec systems are also present such as SecA2-only and SecA2/SecY2. Twin-arginine translocation (tat) system is another conserved bacterial secretion system which is present in most of the eubacterial species, which has the characteristic ability to secrete fully folded proteins (25). Gram negative bacteria translocate proteins across their inner and outer membrane, with highly diverse secretion machineries, which are classified into six different pathways, namely type I to VI secretion systems. Among these, type I, III, IV and VI, protein translocation across inner and outer membrane occurs in a single step whereas mainly

in case of type II and V, proteins are initially exported to periplasmic space via Sec or tat pathway and then across the outer membrane in a second step. Few of these six distinct secretion pathways are also present in gram positive bacteria (24). In addition, gram positive bacteria, particularly mycobacteria possess a unique specialized secretion apparatus termed as type VII secretion system (T7SS) (23). Before understanding this specialized mycobacterial secretion system, it is important to understand two unique gene families, present in most of the mycobacteria, with further genomic expansion seen in pathogenic mycobacteria. These are PE and PPE gene families, named so because of proline-glutamic acid and proline-proline-glutamic acid motifs present in the proximity of N-terminus of the proteins encoded by members of PE and PPE gene families respectively. Importance of these two families can be highlighted by the observation that around 10% of the coding potential of virulent *M. tuberculosis* genome has been invested in these two families (26). PPE genes are present in numerous pathogenic mycobacteria including fish pathogen *Mycobacterium marinum*, and also *M. avium*; however, it is absent in non-pathogenic *Mycobacterium smegmatis*, suggesting strong selection for PPE proteins only in the pathogenic mycobacteria (27). PPE expansion in pathogenic mycobacteria is correlated with the members of 6kDa early secretory antigenic target (ESAT-6) protein family secretion pathways which are also termed as ESX systems. PE and PPE proteins have similarities with the ESAT6 and 10kDa culture filtrate protein (CFP-10) in the context that they are secreted out without a classical signal peptide, which means their secretion cannot occur through Sec system but, must occur through a novel and unique mechanism. Most mycobacterial genomes harbor five such

distinct ESX pathways termed as ESX- 1, 2, 3, 4 and 5 – which collectively refers to the T7SS. Of these, ESX-1 and ESX-5 are significant for the mycobacterial pathogenesis. While ESX1 is indispensable for the virulence of few prominent mycobacterial pathogens including *M. tuberculosis*, *Mycobacterium leprae* and *Mycobacterium bovis*, and that, attenuation of the *M. bovis* vaccine strain BCG is the result of loss of the ESX1 encoding genomic region; however, ESX1 is absent in other important mycobacterial pathogens including *Mycobacterium microti* – a member of the *M. tuberculosis* complex, *Mycobacterium ulcerans*, which is a causative agent of Buruli ulcers, and *M. avium* (27), (28), (23). In contrast, ESX-5 is a highly conserved T7SS in the pathogenic mycobacteria, but absent in non-pathogenic *M. smegmatis*. Interestingly, *M. marinum* mutants of ESX-5 failed to efficiently spread to uninfected macrophages (27). ESX-5 serves as a secretion mechanism for the proteins of PE and PPE family. It is also thought to be involved in the translocation of cell envelope proteins, essential for the nutrient uptake, substituting function of MspA-like porins that are absent in slow growing mycobacteria (28). In case of *M. avium*, there is also experimental evidence for the interaction of a specific bacterial protein (mmpL4) with a host porin (phagosome bound voltage dependent anion channel) to translocate effectors, including myco-lipid molecules. This interaction is crucial for *M. avium* pathogenesis since inactivation of the host porin caused decreased intracellular survival of the *M. avium* (29).

Proteins and other virulence factor secretion can also occur through extracellular vesicle (EV) release, which is a novel secretion mechanism to carry not only proteins but also nucleic acids (DNA, RNA), lipids and other bio-active

molecules, collectively referred to as EV cargo, in the extracellular space. This type of secretion, where effector molecules are packaged inside a membrane bag, is advantageous over direct protein secretion for three main reasons: 1. The effector molecules can travel to their target site in a secured and concentrated manner, 2. The cargo is directed to a specific target (such as specific host cells/tissue) with the use of specific receptors and, 3. This membrane packaging allows the cargo of effector molecules to travel long distances without their natural and host induced degradation and/or dilution (30), (31). EVs may be defined as spherical closed membrane particles, made up of bacterial membranes, that are in a size range of 20-500 nm in diameter. They are formed on a bacterial membrane as bulges and/or blebs, which are then released from the parent cell as closed membrane bags, filled with the cargo of various biologically active molecules. EV production and release is a highly conserved physiological phenomenon that occurs in cells from all three domains of life *i.e.* bacteria, archaea and eukaryota (32), (33), (34). EVs produced by eukaryotic cells are called as exosomes. In prokaryotes, EVs produced by gram negative bacteria are called outer membrane vesicles (OMVs) since gram negative bacteria possess two membranes – outer and inner, and that EVs originate from the outer membrane. Since gram positive bacteria have single membrane, EVs produced by them are simply called as membrane vesicles (MVs). OMV release from a gram negative bacterium was documented, for the first time, around four decades ago, and since then, it has been extensively researched mainly in gram negative bacteria (35). In case of gram positive bacteria, including mycobacteria, people have just begun to appreciate the importance of MV release (34). Bacterial vesiculation (*i.e.* the act of releasing EVs)

response is a natural response that occurs under all physiological and growth conditions. Nevertheless, this response is considered as a part of the bacterial stress response because upon detecting both external and internal stress stimuli (such as host environment, thermal stress, starvation, exogeneous and endogenous oxidative stress, misfolded proteins, DNA damage), vesiculation is triggered that enables bacteria to cope with the stress. Vesiculation is involved in bacterial survival and persistence in stressful environment, nutrient acquisition, biofilm formation, pathogenesis and host immunomodulation (30), (31). Bacterial EV cargo may contain DNA, RNA, lipopolysaccharide (LPS), proteins, bacterial toxins, active enzymes, peptidoglycan, communication molecules such as those involved in quorum sensing and other biologically active bacterial products. In other words, they harbor most of the biological material present in the parent bacterium, in a non-replicative form (35). In the context of bacterial pathogenesis and induction of host immune responses, bacterial EVs may not act in the same way as whole bacteria or extracts of bacterial membrane or bacterial membrane products such as purified peptidoglycan or LPS and/or pieces of lysed bacteria, because the EV membrane composition is markedly different from that of the membrane of the parent bacterium. These differences arise from selective enrichment and/or exclusion of specific membrane proteins and LPS modifications (33), that gives bacterial EVs special importance in playing unique roles, which cannot be performed by the whole parent bacteria and/or their freely secreted effector molecules. Bomberger *et al.* (36) found that only intact OMVs of *Pseudomonas aeruginosa* were cytotoxic to host airway epithelial cells; however, upon incubation with the same OMVs in a lysed form, airway epithelial cell toxicity

was not detected. These MVs transported a notable *P. aeruginosa* virulence factor named Cif (cystic fibrosis transmembrane conductance regulator inhibitory factor) to the airway epithelial cells. Interestingly, Cif seems to work only when transported through intact OMVs, and not when they are lysed (36). Similarly, OMVs derived from another opportunistic pathogen *Acinetobacter baumannii* upregulated the transcription of pro-inflammatory immune mediators (IL-1β, MIP1α, IL6, IL8, and monocyte chemoattractant protein-1) in host epithelial cells, in a dose dependent manner. However, when those same OMVs were lysed or treated with proteinase-K (which wipes out all the surface protein decoration of the OMV membrane), the transcriptional response of pro-inflammatory immune mediators was not detected, in both of these treatments. In case of intact OMVs, the pro-inflammatory transcriptional response was followed by the detachment of epithelial cells and neutrophilic infiltration in the OMV-injected lungs of mice (37). These studies not only underscore the importance of bacterial EVs as the delivery vehicles of the bacterial virulence cargo, but also the significance of their interaction with the host cell membrane, and the underlining mechanism through which the cargo is delivered, as prematurely lysed EVs did not work.

Studies in gram negative bacteria have shown that OMVs interact with the host cell endocytic pathways and lipid rafts. Endocytic system is broadly divided into two categories: 1. phagocytosis (restricted to professional phagocytes such as macrophages) and 2. endocytosis (occurs in all nucleated cells). These endocytic pathways are further subdivided into four subcategories according to the size of the endocytic vesicle: caveolin-mediated (~60nm), clathrin/caveolin -independent

(~90nm), clathrin-mediated (~120nm) and micropinocytosis (>1μm) (38), (39). Lipid rafts are specific host cell plasma-membrane subdomains, which are enriched in cholesterol, sphingolipids and specific membrane proteins such as caveole. Heat-labile enterotoxin (LT) carrying OMVs from enterotoxigenic *Escherichia coli* were endocytosed using lipid rafts (40). OMVs from enterohemorrhagic *E. coli* exported LPS to the host cell cytosol through OMVs, where the OMVs got internalized into the host cell, via clathrin-mediated endocytosis. LPS reached cytosol through early endocytic compartment and activated LPS-detecting pathway that resulted in host cell pyroptosis (41). Periodontal pathogen *Porphyromonas gingivalis* derived-OMVs get internalized by using lipid raft mediated endocytic pathway. Additionally, they also employ host cell regulatory GTPase for entry into the host cell (42). OMVs from a gastrointestinal pathogen, *Helicobacter pylori*, use clathrin-mediated endocytosis for OMVs internalization whereas when the OMVs harbor vacuolating cytotoxin A, a known *H. pylori* virulence factor, then the OMVs managed to get internalized into the gastric epithelial cells, through several endocytic mechanisms (43). OMVs from *H. pylori*, *P. aeruginosa*, *P. gingivalis*, and, the causative agent of gonorrhea, *Neisseria gonorrhoeae* all utilize host cell lipid rafts for internalization into the host cell (36), (42), (44). In addition to using lipid rafts, OMVs from multidrug-resistant nosocomial pathogen, *A. baumannii* also internalize into the host cells by direct fusion with the host cell membrane and through interaction with the receptor-mediated endocytosis (45).

Despite of enormous ongoing research efforts, we still do not have a clear-cut understanding of EV biogenesis. As per one proposed model, OMV formation and

release occurs on the outer membrane sites with locally reduced levels of crosslinks between the outer membrane and peptidoglycan, and decreased peptidoglycan hydrolase activity. Gram negative bacteria may coordinate OMV production via controlling the number of crosslinks between Lpp and peptidoglycan, which occurs through the regulation of peptidoglycan remodeling. Thus, Lpp appears to be an important factor, involved in the OMV biogenesis; it is among the most common lipoprotein, copiously present in the outer membrane; one-third of this Lpp is covalently crosslinked to the peptidoglycan (46). There is also an alternative mechanism proposed, based on mutant studies. As per this mechanism which sees vesiculation as an outcome of stress response to misfolded proteins. Bacterial envelope components such as proteins, pieces of peptidoglycan and/or LPS build-up in the "nanoterritories" that are free of Lpp, compared to the other areas of the outer membrane. This buildup of damaged and/or unwanted products leads to the bulging in those specific outer membrane areas, ultimately leading to budding off of those bulges as OMVs. Lipids and lipid-binding molecules also significantly influence OMV biogenesis (46). However, these proposed models are limited as they are dependent on genetic manipulation and presence of stress, and that they may not be applicable, in general, to all of the bacterial species. More recent evidence suggested role for genes encoding highly conserved ATP binding cassette (ABC) transport system, in the OMV biogenesis. This system does not let phospholipids to accumulate in the outer leaflet of the outer membrane. Downregulation of this system results in phospholipid rearrangement and accumulation in the specific outer membrane areas and causes vesicle formation (47), (48).

Unlike gram negative bacteria, gram positive bacteria possess single thick peptidoglycan cell wall, surrounding their cell membrane. In mycobacteria, layer of peptidoglycan is covalently attached to arabinogalactan, which is surrounded by a layer of mycolic acids. The upper layers of this cell wall contain free lipids, including glycolipids, that are covered with an outermost capsule made up of polysaccharides, proteins and lipids (34), (49). Paucity of studies exploring vesiculation in gram positive bacteria, including mycobacteria partly stems from the notion that these single, thick-membrane containing bacteria may not be able to vesiculate at all, which has now proven to be wrong, as numerous studies have shown vesiculation in several gram positive bacteria (34). Among these, few reports are also on mycobacteria, highlighting the importance of vesiculation in mycobacterial pathogenesis. For example, *M. tuberculosis* MVs have been shown to be involved in iron acquisition (50), TLR2-dependent immune modulation (51) and inhibition of T cell activation (52).

Obtaining sufficient amount of EVs, in a pure and reproducible form, has been a major obstacle in the field of EV biology. Earlier investigators have used a variety of stress stimuli, during an *in vitro* culture, to obtain adequate EV sample. This includes nutrient depletion, iron limitation, oxidative stress-induced by addition of sub-lethal concentration of hydrogen peroxide in the culture media, temperature stress, and chemical and, biochemical agents that compromise bacterial cell envelope integrity. Lastly, people have also used genetic manipulation techniques to generate hypervesiculating phenotypes (53). In case of *M. avium* infection, the host macrophage intra-phagosomal environment is the key to understanding numerous

bacterial virulence responses, that ultimately lead to the macrophage infection. Through novel X-ray microprobe technology, Wagner *et al.* (54) identified presence of single elements, (including iron, calcium, chlorine, potassium, manganese, copper, zinc) and their specific concentrations, present in the phagosomal microenvironment, following *M. avium* infection. Based on this data, our group developed an *in vitro* system (metal mix) that mimics the phagosomal environment of *M. avium* containing phagosome at 1 hour and 24 hours following macrophage infection. Exposure of metal mix leads to an intracellular phenotype of *M. avium*, characterized by induction of several virulence factors known to be upregulated during *M. avium* infection of macrophages (21). Recently, our group also demonstrated that several *M. avium* effector proteins, that are usually secreted in the host cell cytosol by the intracellular *M. avium* (including ESAT-6 like proteins), were also secreted upon exposure to the metal mix (55). Our present study is the first report that demonstrates vesiculation in *M. avium*, in response to 24h post-infection phagosome environment. We characterized the cargo of metal mix induced MVs and compared it with the cargo of MVs released in response to starvation stress. We found various free lipids, present in the outermost layers of the mycobacterial cell wall, in the MVs. Mass spectrometric analysis revealed common as well as unique sets of proteins found in the metal mix- and minimal media- derived MVs. Some of metal mix MV cargo proteins were also found to be released in the host cell cytosol. Moreover, our study revealed DNA export through MVs. Overall, this research establishes MVs as delivery vehicles of several *M. avium* virulence-associated products, using the phagosomal microenvironment mimicking *in vitro* system.

Chapter 1

MATERIALS & METHODS

Bacterial Cultures and Exposure Media

Mycobacterium avium subspecies hominissuis 104 (hereafter referred to as MAH104) used in this study were harvested from the blood of an AIDS patient. MAH104 were cultured on 7H9 liquid broth, supplemented with 10% oleic acid, albumin, dextrose and catalase (OADC, Hardy Diagnostics, Santa Maria, CA) at 37º C, until mid-log phase (which is 7-8 days, in case of MAH104). Mid-log phase MAH104 cultures were centrifuged at 2000 × g for 20 min, and bacterial pellets were resuspended in the minimal medium or 24h post-infection metal mix. Number of bacteria in each medium were standardized by matching turbidity to McFarland standard #1 (3×10^8 CFU/ml). Minimal media was prepared as described previously (56), which is an established nutrient starvation medium, known to stimulate vesiculation in mycobacteria. Metal mix was made as described previously (21). Contents of minimal media and metal mix are listed in table 1. Bacteria were incubated in minimal media for 2 weeks or for 24 hours in the metal mix in a shaker rotating at 50 rpm at 37º C. MAH104 viability was tested in terms of colony forming units per milliliter (cfu/ml) over the period of 2 weeks in both minimal media and metal mix and compared to the control which was 10% OADC supplemented 7H9 broth.

Table 1: Contents of minimal media, a chemically defined nutrient starvation media, and metal mix which represents 24h post infection environment of MAH104 containing phagosome of macrophage

Minimal Media	**Metal Mix**
For 1L medium, materials added to 975ml deionized H_2O (pH 7.0)	For 1L medium, solutions added to 1L Middlebrook 7H9 broth (pH 5.8)
1 g KH_2PO_4	1.85ml of 1 M KCl
2.5 g Na_2HPO_4	2.5ml of 1 M $CaCl_2$
500 mg Asparagine	23.8ml of 1 M $MnCl_2$
14ml of 50% (v/v) glycerol	11µl of 1 M $CuSO_4$
100µl of 500mg/L ferric ammonium citrate	117.4µl of 1 M $ZnCl_2$
100µl of 5mg/L $CaCl_2$	4ml of 0.25 M ferric pyrophosphate
100µl of 1mg/L $ZnSO_4$	10µl of 1 M $NiCl_2$

Isolation and purification of MAH104 membrane vesicles (MVs)

MVs were isolated and purified as described previously (56), with few modifications. Briefly, the experimental media were centrifuged at 2000 × g for 20 min, at 4º C, and then, the supernatant was vacuum filtered through 0.22 µm pore-size membrane. The filtrate was concentrated using ultrafiltration concentrators, having 100kDa exclusion filters (Thermo Fisher Scientific, Waltham, MA). The concentrate was centrifuged at 15000 × g for 15 min. at 4º C, followed by ultracentrifugation at 100,000 × g for 1h at 4º C, to pellet the MVs. After this ultracentrifugation, the supernatant was discarded and the pellet was resuspended in 2ml of 35% (w/v) Optiprep solution, diluted in PBS. Starting with this, as the densest layer on the

bottom of an ultra-clear centrifuge tube (Beckman Coulter, Brea, CA), less dense layers were overlaid in descending order of 30%, 25%, 20%, 15% and 10% respectively. These density gradients were ultra-centrifuged for 16h at 4º C. After that, 3rd and 4th fraction (consisting of 20% and 25% diluted Optiprep) were combined and retained, whereas other fractions were discarded; see figure 1 for more details. These pure MV containing fractions were diluted in PBS and centrifuged at 38,000 × g for 2h at 4º C; supernatant containing Optiprep was discarded and the MV pellet was resuspended in PBS for further analysis.

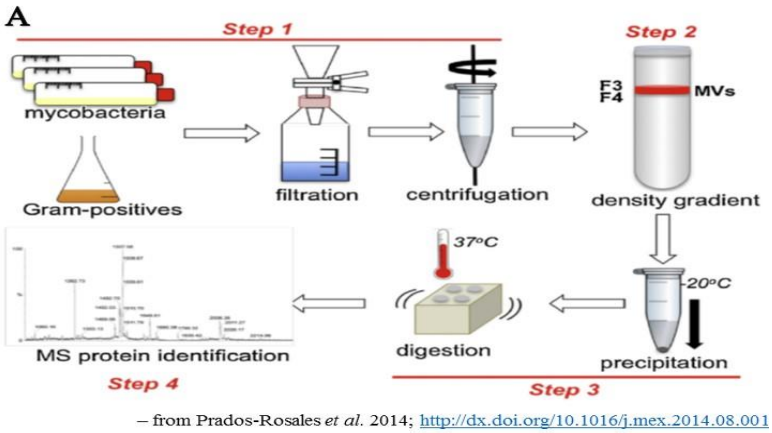

Figure 1: A. Diagrammatic representation of procedure of isolating and purifying membrane vesicles from mycobacteria and subsequent mass spectrometric analysis of cargo proteins (Photo credit: Prados-Rosales *et al.* 2014; http://dx.doi.org/10.1016/j.mex.2014.08.001). B. Optiprep density gradients purify MVs from other macromolecular contaminants by separating them into the fractions of specific Optiprep solution densities.

Scanning and transmission electron microscopy

Scanning electron microscopy was used to ensure that the experimental treatment media (*i.e.* minimal media and metal mix) induce vesiculation response in MAH104. 24h after incubation of MAH104 in metal mix, or 2 weeks after their incubation in minimal media, the bacterial samples were collected and fixed with the Karnovsky fixative (5% glutaraldehyde and 4% formaldehyde freshly made from paraformaldehyde in 80mM cacodylate buffer at pH 7.3, added with 5mM $CaCl_2$) (Ted Pella Ince., Redding, CA). Samples were critical point dried using an EMS 850 (Hatfield, PA) and dehydrated at room temperature, using graded solutions of ethanol and liquid CO_2. Micrographs were taken at the Oregon State University Electron Microscopy Facility, using the FEI Quant 600 FEG scanning electron microscope.

Transmission electron microscopy was used to ensure purity of MVs in the sample, following MV isolation and purification steps, described earlier. The MV samples were fixed with the Karnovsky fixative (5% glutaraldehyde and 4% formaldehyde freshly made from paraformaldehyde in 80mM cacodylate buffer at pH 7.3, added with 5mM $CaCl_2$) (Ted Pella Ince., Redding, CA) overnight at 4º C. Fixation was followed by sample washing, using the same buffer. Next, the samples were treated with cold 1% osmium tetroxide for 90min and dehydrated in an acetone gradient, made with an ascending order of series of concentrations 10%, 30%, 50%, 70%, 90%, 100% and 100% respectively, and then, fixed in the epoxy resin. Ultrathin sections (80mm) were cut out of blocks and were mounted on grids. Staining was done by using uranyl acetate and lead citrate. Micrographs were taken at the Oregon

State University Electron Microscopy Facility, using the FEI Titan Chemi STEMT transmission electron microscope, operating at 200kV.

Proteomics of MVs

MV samples were prepared for mass spectrometric protein identification as described previously (56) with few modifications. MV samples were incubated with 4 volumes of acetone at 20º C for overnight, and then, incubated at -20º C for 4 hours. The precipitate was centrifuged at 8000 × g at 4º C for 10 minutes and then treated with 50mM ammonium bicarbonate with 0.1% RapiGest SF surfactant. Subsequently, the samples were incubated with 5mM DTT solution at 56º C for 1h to reduce disulfide bonds, and then, with 5mM iodoacetamide, again for 1h in dark condition, to prevent the formation of disulfide bonds. Sample was overnight digested with trypsin at 37º C and analyzed in the Mass Spectrometry Center at Oregon State University. LC-MS/MS experiments were performed, using a Thermo Orbitrap Fusion Lumos MS coupled with a Waters nano-Acquity UPLC system. All raw files were analyzed by Proteome Discoverer 2.2 software. The identified *M. avium* proteins were classified into distinct groups, based on their function. This functional classification was conducted by blasting the amino acid sequence of found *M. avium* proteins against the protein sequence database of well-studied *M. tuberculosis* strain H37Rv, using the Institute Pasteur's TubercuList web server (http://genolist.pasteur.fr/TubercuList/). The *M. avium* proteins that did not match with the H37Rv proteins were classified based on their predicted or known function.

Lipidomics of MVs

MV Lipidomic analysis was conducted at the Oregon State University, Mass Spectrometry Center. MVs were disrupted by sonication and lipids were extracted by using dichloromethane (DCM): isopropyl alcohol (IPA): methanol (MeOH) ratio of 20:10:65, by volume, at room temperature, vortexed and the organic DCM layer was collected for the lipid analysis. Chromatographic separation was carried out by using a Waters HSS T3 column and the lipid extracts were measured by using an Applied Biosystems 5600 Triple TOF mass spectrometer coupled to a Shimadzu Nexera UHPLC.

Host cell culture and growth media

Human THP1 cells were purchased from the American Type Culture Collection (ATCC, Manassas, VA). THP1 cells were maintained in Roswell Park Memorial Institute medium-1640 (RPMI 1640 Corning) supplemented with 10% fetal bovine serum (FBS, Gemini) at 37º C with 5% CO_2. THP1 cells were used for infection experiments.

Bioorthogonal non-canonical amino acid tagging (BONCAT) of MAH104 and macrophage infection

The method of BONCAT was used to label MAH104 proteins with L-Azidohomoalanine (AHA) (Click Chemistry Tools, Scottsdale, AZ), an amino acid analog of methionine, containing an azide moiety. MAH104 were grown in 10% OADC supplemented 7H9 broth with or without 2Mm AHA for 7 days at 37º C.

THP1 human host cells, grown and maintained as described above, were differentiated from monocytic cells to macrophages through the treatment of 10ng/ml of phorbol-12-myristate-13-acetate (PMA, Sigma Aldrich) for 24h at 37º C with 5% CO_2 and, seeded at 80% confluency in T-200 tissue culture flasks. Following this 24h PMA treatment, the PMA containing cell culture media was replaced with fresh cell culture media and the THP1 cells were allowed to fully differentiate into macrophages for further 48h at 37º C with 5% CO_2. Next, infection was carried out using 7 day-grown MAH104 with AHA or without AHA (used as control) for 2h. The multiplicity of infection (MOI) was kept at around 10 bacteria per macrophage cell. Extracellular bacteria that failed to internalize into the macrophages, during the 2h period, were removed by washing with the Hank's Balanced Salt Solution (HBSS, Life Technologies) for three times. Infected macrophages were incubated in 10% FBS supplemented RPMI for 24h at 37º C with 5% CO_2.

Protein enrichment using click chemistry

Following 24h incubation, the cell culture media was removed and the infected macrophages were resuspended into 3ml of 0.1% triton X-100 in PBS using a cell scraper. The cells were mechanically lysed by passing the concentrated cell suspension through a 27-gauge needle, several times. This cell lysate was syringe-filtered to remove cell debris and whole bacteria. Clear lysate was processed for the enrichment of AHA-labeled (azide-modified) MAH104 proteins by using Click-iT® Protein Enrichment kit (Molecular Probes, Eugene, OR), following manufacturer's protocol, with few modifications. Briefly, the click reaction was set up by adding

lysate and catalyst solution over the agarose resin slurry. The reaction was allowed to take place for overnight, at room temperature, in a rotator. Next morning, the resin bound proteins were reduced and alkylated by treatment of resin bound proteins with DTT and then, iodoacetamide solutions in SDS wash buffer. Then several washing steps were performed initially with the SDS wash buffer, and then, with 8M Urea/100mM Tris (pH 8.00), and with 20% acetonitrile, in order to wash out any proteins non-specifically bound to the resin. Subsequently, the resin-bound proteins were overnight digested at 37º C, using trypsin. Following this on-resin digestion, the peptides were separated from the resin using centrifugation, and were processed for protein sequencing at Oregon State University Mass Spectrometry Facility.

Quantification of external and internal MV-associated DNA

PicoGreen dsDNA assay (Molecular Probes, Eugene, OR) was used to quantify double stranded DNA associated externally with the MVs and, the double stranded DNA present inside the vesicles (internally associated MV DNA) as described previously (57), with few modifications. Purified MV samples were incubated with or without DNase I (Promega, Madison, WI), by following manufacturer's instructions, to get rid of any externally-associated DNA. Next, the MVs were either lysed by using bead homogenizer (OMNI International Inc., Kennesaw, GA) to release internally associated DNA or kept intact. Subsequently, the samples were assayed using the PicoGreen dsDNA kit, by following the manufacturer's instructions. Fluorescence was measured using *infinite 200q* fluorescent plate reader (Tecan, Zürich, Switzerland), using the fluorescein

wavelengths ~480nm for excitation and, ~520nm for emission. Fluorescence measurement values were converted into the DNA concentrations by using the low-range standard curve, plotted using the fluorescence measurements of dilutions of a DNA standard, provided by the manufacturer.

Laser confocal microscopic visualization of MV-associated DNA

Purified MV samples were incubated with or without DNase I (Promega, Madison, WI), by following manufacturer's instructions, to get rid of any externally-associated DNA. Then, these samples were stained with a lipophilic nucleic acid stain, SYTO®-61 (Molecular Probes, Eugene, OR) in a ratio of 1:1000. The samples were visualized in the Center for Genome Research and Biocomputing (CGRB) microscopy facility, at Oregon State University, using Zeiss LSM 780 NLO confocal microscope system (Carl Zeiss, Thornwood, NY). Samples were excited with 633nm Helium-Neon laser (of power of 5%) and, emission of 636-758 nm was collected with a Zeiss plan Apochromat 40x / 1.4 oil DIC M27 objective. Zen 2012 software was used to capture and merge images.

Construction of MAH104 FLAG-tag overexpression clones

To supplement BONCAT-mediated MAH104 secreted protein identification and to link it with the proteins found in the MVs released in response to the metal mix (hereafter referred to as MX proteins), this molecular cloning-based approach was used. Based on previous literature, 11 out of the 260 MX proteins were selected and primers for them were designed, for the purpose of PCR amplification. The DNA

sequence of GATTACAAGGATGACGACGATAAG codes for the peptide FLAG-tag, having an amino acid sequence of DYKDDDDK, which was used in primer design, in order to incorporate this peptide tag in selected MX proteins. Genes for these 11 MX proteins and their primers are listed in table 2. Either two forward (F) or two reverse (R) primers were designed for each of the protein, depending on whether the FLAG-tag sequence was inserted at the beginning or at the end of the gene. Initially PCR amplification was carried out using the pair of first primer (either F1 or R1) and the coupled respective R or F primer. For this round of amplification, MAH104 genomic DNA was used as a template, obtained as previously described (58), (59). Following that, the second round of PCR amplification was done using the pair of second primer (either F2 or R2) and the coupled respective R or F primer, in which the template used was the PCR product of the first round of amplification. All amplicons were tested by using electrophoresis on 1% agarose gel. PCR products were purified with the QIAquick PCR purification kit (Qiagen, Venlo, Netherlands), by following manufacturer's instructions. All genes were cloned in the restriction sites EcoRI and HpaI (except MAV_2964, cloned in PstI and HpaI) of pMV261-BlaC vector, harboring kanamycin resistance cassette. Digestion of the vector and the PCR products, was carried out by using the respective restriction enzymes (Thermo Fisher Scientific, Waltham MA) in a buffered solution at 37º C for 3h; following that, the enzymes were heat inactivated at 65º C for 10min and the ligation of the vector-PCR product was carried out for overnight at 17º C, using the T4 DNA ligase (Invitrogen, Carlsbad, CA).

Table 2: Primers used in the study

Gene name	Primer	Sequence (5′ to 3′)
MAV_5153	F1	AGTGAGTTCACAATTCCG
	F2	TTTTTGAATTCGATTACAAGGATGACGACGATAAGAGTGAGTTCA
	R	TTTTTGTTAACTCAGGATTTGCCG
MAV_1082	F	TTTTTGAATTCCGCGAGATTACGA
	R1	ACCGGTGGTGACGGTGGC
	R2	TTTTTGTTAACGATTACAAGGATGACGACGATAAGACCGGTGGTG
MAV_2909	F1	TTCTATGGGGCCTTTCCG
	F2	TTTTTGAATTCGATTACAAGGATGACGACGATAAGTTCTATGGGG
	R	TTTTTGTTAACTCAACCCAACTGG
MAV_2345	F1	GCGTTCAGTAAGCCACCG
	F2	TTTTTGAATTCGATTACAAGGATGACGACGATAAGGCGTTCAGTA
	R	TTTTTGTTAACCTAGTTGTTGCCC
MAV_4365	F1	AGCAAGATCATTGAGTAC
	F2	TTTTTGAATTCGATTACAAGGATGACGACGATAAGAGCAAGATCA
	R	TTTTTGTTAACTCAGTGATGGTGA
MAV_2833	F1	CAAGGGGATCCGGAAGTT
	F2	TTTTTGAATTCGATTACAAGGATGACGACGATAAGCAAGGGGATC
	R	TTTTTGTTAACTCAGCTCGGTGGC
MAV_2964	F	TTTTTCTGCAGTCGCGGGGGTGGC
	R1	CTAGCCGCCCAGCCCCTT
	R2	TTTTTGTTAACGATTACAAGGATGACGACGATAAGGCCGCCCAGC
MAV_3813	F1	GCCGACAACCCCAAACGT
	F2	TTTTTGAATTCGATTACAAGGATGACGACGATAAGGCCGACAACC
	R	TTTTTGTTAACTCACATGGCGGCC
MAV_3310	F	TTTTTGAATTCTCTGCCAGCTGTC
	R1	TCATCCGCCGTGGCCGGG
	R2	TTTTTGTTAACGATTACAAGGATGACGACGATAAGTCCGCCGTGG
MAV_0740	F1	AACAACCTCTACCGCGAT
	F2	TTTTTGAATTCGATTACAAGGATGACGACGATAAGAACAACCTCTA
	R	TTTTTGTTAACTCACGAAGTGAGC
MAV_2054	F1	ACGTCGGCTCAAAATGAG
	F2	TTTTTGAATTCGATTACAAGGATGACGACGATAAGACGTCGGCTC
	R	TTTTTGTTAACTCACTTGTACTCA

Transformation and colony screening

Ligation products were multiplied by transforming them into the electrocompetent *E. coli* (Invitrogen, Carlsbad, CA) by pulsing them with the voltage of 1700V and the *E. coli* were grown in LB agar plates, containing 50µg/ml of kanamycin. The molecular cloning steps of digestion, ligation and transformation were evaluated by performing *E. coli* colony PCR amplifications and only those colonies were selected that showed presence of the cloned gene, detected by gel electrophoresis. Positive colonies were further grown in LB broth containing 50µg/ml of kanamycin for overnight and the vector was extracted by using GeneJET Plasmid Miniprep kit ((Thermo Fisher Scientific, Waltham MA), by following manufacturer's instructions. Cloning of the construct, along with the FLAG tag, at the correct site was ensured by the vector DNA sequencing. These vectors were used for MAH104 transformation. MAH104 competent cells were prepared, and then, transformed as described previously (55) with few changes. Briefly, MAH104 cultures were washed three times with a wash buffer (10% glycerol and 0.1% Tween-20) using centrifugation at 2000 × g for 15 min. the resulting pellet was resuspended in 10% glycerol and electroporated with vector DNA, and then, plated on 7H10 plates, containing 400µg/ml kanamycin. The plates were incubated at 37º C for 2 weeks. Subsequently, MAH104 colonies were tested for the presence of kanamycin resistance cassette (and hence the vector) using the kanamycin primers and PCR program described in (55). Positive colonies were further grown in 10% OADC supplemented 7H9 broth, containing 2mM AHA and 400µg/ml of kanamycin, and used in the western blotting experiments.

Isolation of exosomes from infected macrophages

THP1 cells, differentiated into macrophages as described above, were infected with the MAH104 (grown until mid-log phase), with the moi of 10 bacteria per THP1 macrophage, as described above. Infected macrophages were incubated at 37º C, with 5% CO_2, for 72h. This cell culture media was harvested at two-time points – 24h post infection and 72h post infection in order to isolate exosomes of infected macrophages with the total exosome isolation reagent (Invitrogen, Carlsbad, CA), by following manufacturer's instructions. Briefly, the harvested cell culture media was centrifuged at 2000 × g for 20min to remove bigger cell debris, and the supernatant was filtered through a 0.22µm syringe filter. The culture filtrate was transferred to a new tube and mixed with the 0.5 volumes of the total exosome isolation reagent, into a homogeneous solution by gentle pipetting. This solution was incubated overnight at 4º C, then was centrifuged at 10,000 × g for 1h at 4º C to pellet the exosomes. The supernatant was discarded and the pellet was washed twice with PBS. Finally, the pellet was resuspended in 500µl of PBS and processed for sequencing at mass spectrometric facility, Oregon State university.

Data Analysis

All the experiments were repeated at least two times. GraphPad PRISM version 7.04 was used to plot MAH104 survival plot and DNA concentration plot. Venn diagrams were created by using Ghent University, Gent, Belgium operated Bioinformatics & Evolutionary Genomics website (http://bioinformatics.psb.ugent.be/webtools/Venn/). All other charts were made using the Microsoft Excel 2016.

Chapter 1

RESULTS

Exposure of MAH to minimal media (for 2 weeks) and metal mix (for 24h) induced robust vesiculation response in MAH104

Minimal media is a starvation media, deprived in most of the essential nutrients whereas metal mix mimics the intracellular environment of phagosomes formed during 24h MAH infection of macrophages. Both of these experimental media induced vigorous vesiculation in MAH104. SEM micrographs clearly showed membrane bulges that were about to bud off, on MAH104 membranes (fig. 2). This result was further substantiated by TEM micrographs that showed the intact MAH104 MVs, in their naïve form, following MV isolation and sample purification (fig. 3). TEM micrographs also validated our experimental procedure of MV isolation and sample purification. To rule out the possibility of bacterial death, bacterial survival and/or viability was measured, in both of these experimental media, for up to 2 weeks, in terms of colony forming units per milliliter (cfu/ml). Compared to the 10% OADC supplemented 7H9 nutrient-rich medium (control), MAH104 survival was slightly impacted in both of these experimental media, over the course of 2-week period. Nonetheless, 95% of bacteria survived in these media and were completely viable, after 14^{th} day of exposure to minimal media and metal mix (fig. 4).

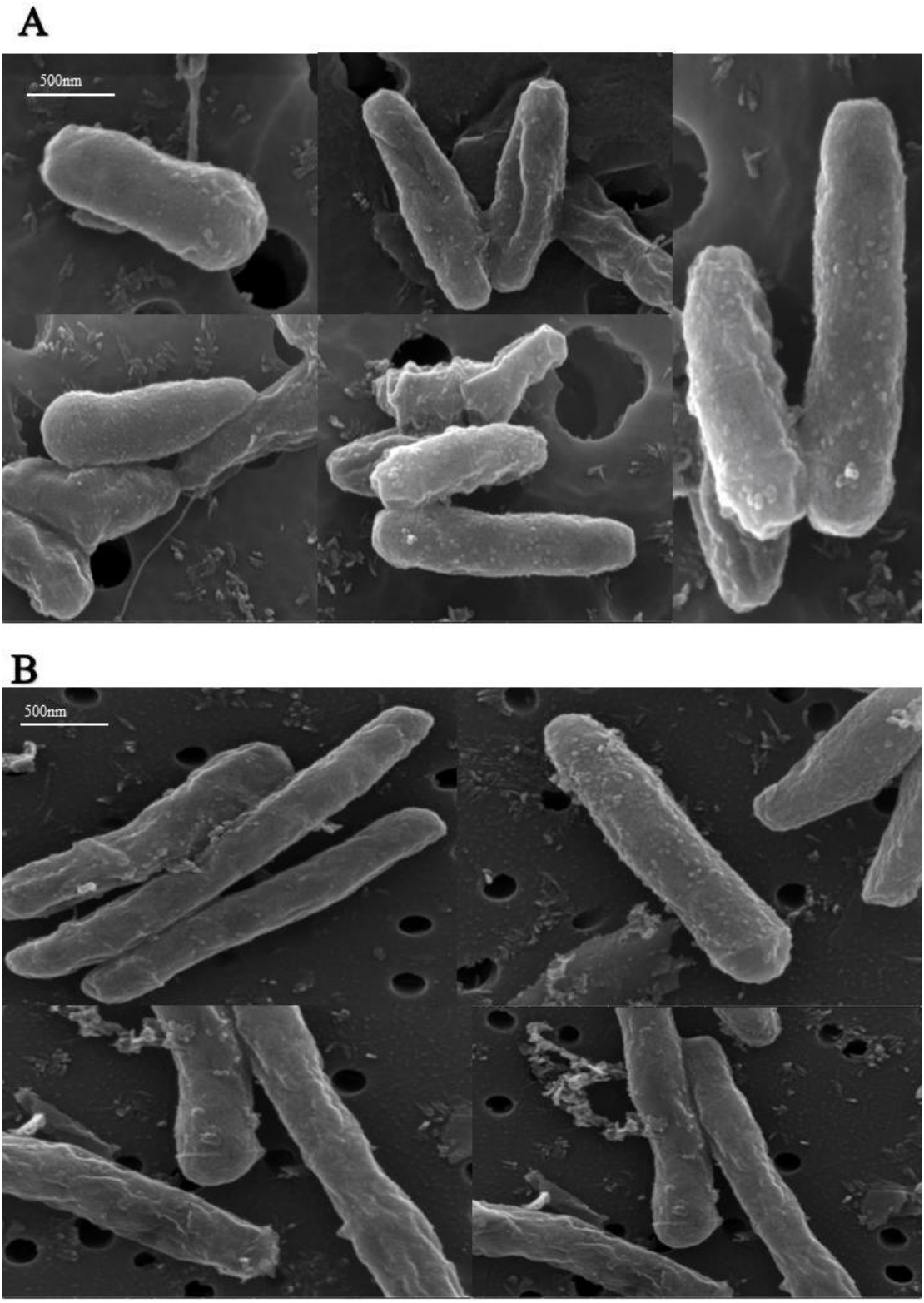

Figure 2: SEM micrographs of MAH104 exposed to minimal media for 2-weeks (A) and metal mix for 24h (B). SEM micrographs demonstrate bulges on the bacterial membranes, that are about to bud off from the membrane. Scale bar: 500 nm

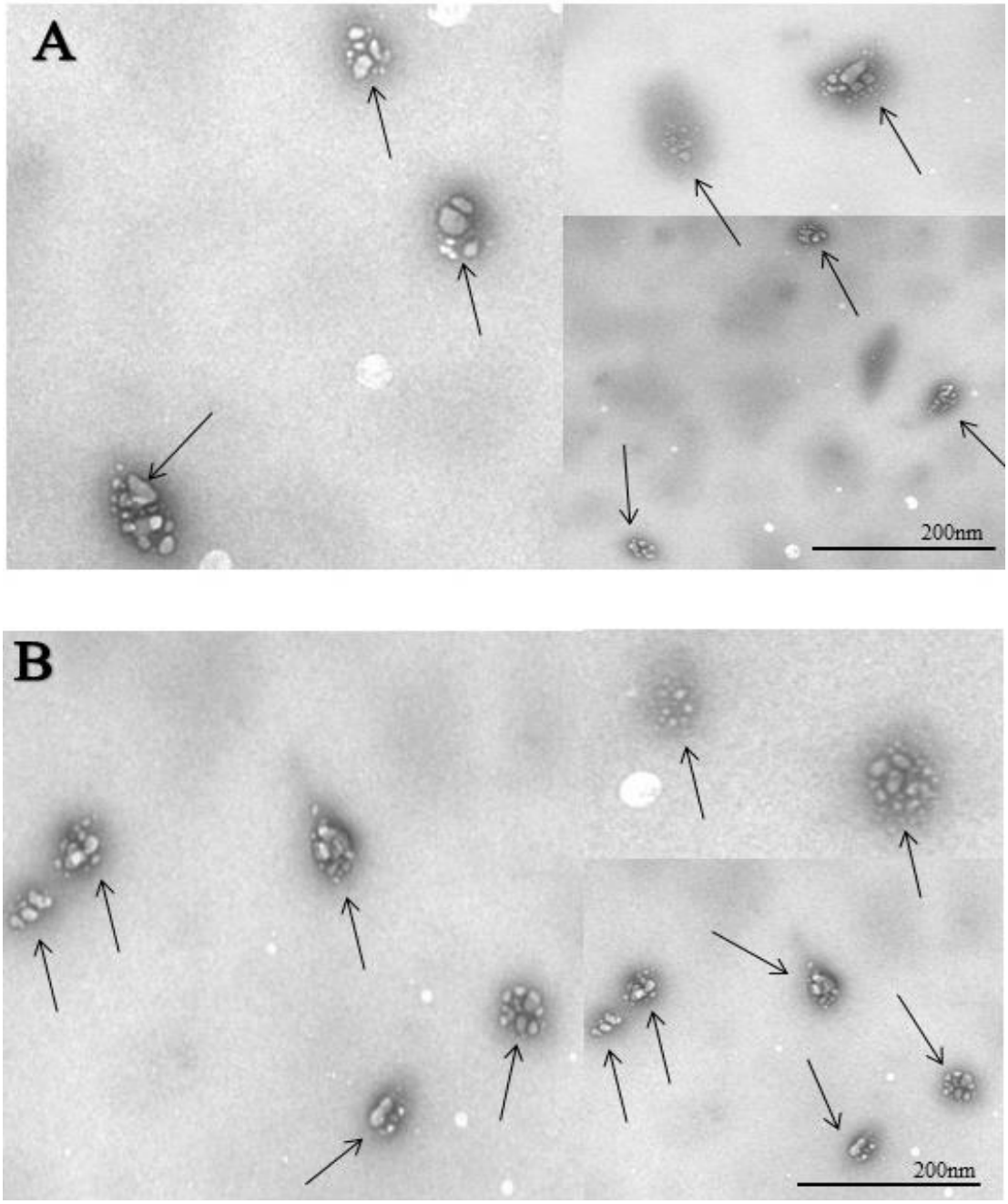

Figure 3: TEM micrographs of purified MV samples with closed membrane structure. MVs are indicated by arrows. (A) Purified MV sample from MAH104 exposed to the minimal media for 2-weeks. (B) Purified MV sample from MAH104 exposed to the metal mix for 24h. Scale bar: 200nm

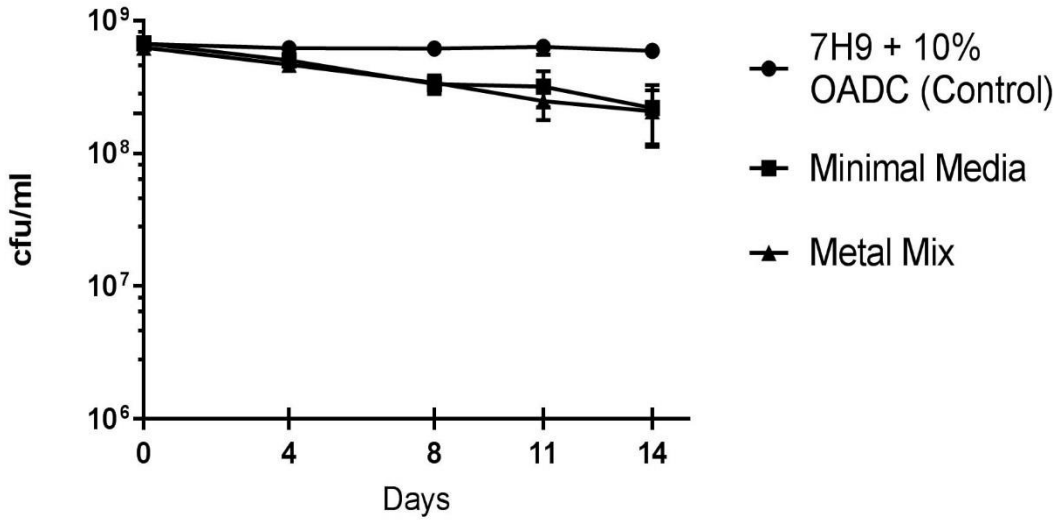

Figure 4: Survival and/or viability of MAH104 was tested in both minimal media and metal mix for up to 2-weeks. Compared to the 10% OADC supplemented 7H9 control, CFUs of bacteria exposed to both minimal media and metal mix slightly decreased, over the 2-week course. Nevertheless, even by the last day of the experiment (day 14), the bacterial counts were quite high in both experimental media. Data was plotted as mean (of two independent trials) and standard deviation.

Proteomic profile of MAH104 MVs of minimal media and metal mix

Mass spectrometric analysis of purified MAH104 MV samples found a total of 202 cargo proteins, from 2-week minimal media exposure (hereafter referred to as MM proteins; table 3), and 263 cargo proteins from 24h metal mix exposure (hereafter referred to as MX proteins; table 4). Proteins were categorized based on their function, as described in the methods. In case of the MM proteins, among the most represented categories, 63 proteins involved in cell wall and cell processes (31.18%), 41 proteins involved in intermediate metabolism and respiration (20.29%), 51 conserved hypothetical proteins (25.24%) and 25 proteins associated with the information pathways (12.37%) were found. Among the least represented categories, 10 regulatory proteins (4.95%), 8 proteins involved in lipid metabolism (3.96%) and 4 proteins related to virulence, detoxification and adaptation (1.98%) were found (fig.

5A). In case of MX proteins, among the most represented categories, 103 proteins involved in intermediate metabolism and respiration (39.16%), 41 proteins involved in lipid metabolism (15.58%), 32 proteins involved in cell wall and cell processes (12.16%), 41 conserved hypothetical proteins (15.58%) and 27 proteins related to information pathways (10.26%), were found. Among the least represented categories, 14 proteins involved in virulence, detoxification and adaptation (5.32%), 4 regulatory proteins (1.52%) and 1 PE/PPE family protein (0.38%), were found (fig. 5B). Relative contribution of MX proteins to virulence, detoxification and adaptation was more than that of MM proteins. This was also true for lipid metabolism, PE/PPE proteins and intermediary metabolism and respiration. In contrast, relative contribution of MM proteins to cell wall and cell processes, conserved hypotheticals and regulatory pathways was more than that of MX proteins. Proteins associated with information pathways were almost equally represented in both minimal media and metal mix (fig. 6). Among MM and MX proteins, 52 were common whereas 211 proteins were unique to metal mix and 150 were unique to minimal media (figure 7). Proteome of MVs released in response to 2-week exposure to metal mix, was also analyzed. The list of proteins (table S1) and a Venn diagram (figure S1) showing common and unique proteins among 2-week minimal media exposure, 2-week metal mix exposure and 24h metal mix exposure, are given in the supplementary material.

Table 3: MAH104 proteins found in the MVs, released in response to 2-week minimal media exposure. Their functional classification into the categories are based on the function of matching *M. tuberculosis* (strain H37Rv) homolog proteins, which are also listed here.

Accession no.	Gene name	Description	Functional Category	MW [kDa]	Peptides	H37Rv homolog
A0A0H2ZQZ9	MAV_0558	Uncharacterized protein	conserved hypotheticals	26.533	4	-
A0A0H2ZR87	MAV_4459	Uncharacterized protein	cell wall and cell processes	33.91	5	Rv0713
A0A0H2ZRK6	MAV_4161	Cobyrinic Acid a,c-diamide synthase	cell wall and cell processes	28.117	2	Rv3213c
A0A0H2ZS38	MAV_0306	Lipoprotein LpqH	cell wall and cell processes	15.268	4	Rv3763
A0A0H2ZSF7	MAV_4443	Signal peptide peptidase SppA,	cell wall and cell processes	62.755	2	Rv0724
A0A0H2ZSP5	MAV_0209	Bifunctional udp-galactofuranosyl transferase glft	cell wall and cell processes	70.115	5	Rv3808c
A0A0H2ZSP7	MAV_1424	LprC protein	cell wall and cell processes	20.151	2	Rv1275
A0A0H2ZSQ6	MAV_1782	Sulfate ABC transporter, sulfate-binding protein	cell wall and cell processes	36.078	8	Rv2400c
A0A0H2ZSU9	MAV_1047	Phosphate-binding protein PstS	cell wall and cell processes	37.189	6	Rv0928
A0A0H2ZSZ8	MAV_3726	Peptidase M50	cell wall and cell processes	42.567	2	Rv2869c
A0A0H2ZT06	MAV_0464	Bacterial extracellular solute-binding protein, family protein 5	cell wall and cell processes	57.116	3	Rv3666c
A0A0H2ZTE4	MAV_2412	Uncharacterized protein	cell wall and cell processes	24.565	2	Rv2091c
A0A0H2ZTE6	MAV_3468	Protein translocase subunit SecD	cell wall and cell processes	63.126	2	Rv2587c
A0A0H2ZTX7	MAV_4738	Peptidase, M28 family protein	cell wall and cell processes	51.519	3	Rv0418
A0A0H2ZU60	MAV_2140	LppO protein	cell wall and cell processes	17.413	2	Rv2290
A0A0H2ZUB9	MAV_4239	Phosphate-binding protein PstS	cell wall and cell processes	37.378	4	Rv0932c
A0A0H2ZUT3	MAV_3910	Periplasmic binding protein	cell wall and cell processes	36.527	7	Rv3044
A0A0H2ZUW2	MAV_3639	FtsK/SpoIIIE family protein	cell wall and cell processes	82.604	3	Rv2748c
A0A0H2ZUZ1	MAV_4675	Heparin binding hemagglutinin hbha	cell wall and cell processes	22.148	8	Rv0475
A0A0H2ZV05	MAV_0938	Uncharacterized protein	cell wall and cell processes	31.997	2	Rv1363c
A0A0H2ZV32	MAV_3698	Uncharacterized protein	cell wall and cell processes	14.596	2	Rv2843
A0A0H2ZV36	MAV_0566	Uncharacterized protein	cell wall and cell processes	28.44	4	Rv3587c
A0A0H2ZV45	MAV_3369	Aminoglycosides/tetracycline-transport integral membrane protein	cell wall and cell processes	55.052	5	Rv1410c
A0A0H2ZV86	MAV_5197	Manganese/iron transporter, nramp family protein	conserved hypotheticals	61.227	5	-
A0A0H2ZVA7	MAV_0569	LpqE protein	cell wall and cell processes	19.139	5	Rv3584
A0A0H2ZVI5	MAV_4011	Nitric-oxide reductase subunit B	intermediary metabolism and respiration	82.943	4	-
A0A0H2ZVL6	MAV_2465	LppI protein	cell wall and cell processes	21.809	2	Rv2046
A0A0H2ZVX0	MAV_4561	LpqN protein	cell wall and cell processes	22.587	2	Rv0583c
A0A0H2ZW85	MAV_1098	Large conductance mechanosensitive channel protein	cell wall and cell processes	16.09	3	Rv0985c
A0A0H2ZWC3	MAV_1078	34 kDa antigenic protein	cell wall and cell processes	29.983	2	Rv0954
A0A0H2ZX51	MAV_4811	LpqJ protein	cell wall and cell processes	19.794	2	Rv0344c
A0A0H2ZXJ3	MAV_4895	Periplasmic binding protein	cell wall and cell processes	33.212	6	Rv0265c
A0A0H2ZXK3	MAV_2394	Uncharacterized protein	cell wall and cell processes	17.356	2	Rv2120c
A0A0H2ZXN1	MAV_5306	ParB-like partition proteins	cell wall and cell processes	35.178	3	Rv3917c
A0A0H2ZXU3	MAV_4920	Glycosyl hydrolase family protein 3	cell wall and cell processes	40.111	4	Rv0237
A0A0H2ZXY5	MAV_3855	LppZ protein	cell wall and cell processes	36.836	3	Rv3006

A0A0H2ZY09	MAV_4666	ErfK/YbiS/YcfS/YnhG family protein	cell wall and cell processes	46.623	7	Rv0483
A0A0H2ZYI9	MAV_4792	Uncharacterized protein	cell wall and cell processes	32.654	3	Rv0383c
A0A0H2ZYQ2	MAV_4968	MmpL3 protein	cell wall and cell processes	101.297	3	Rv0206c
A0A0H2ZYT3	MAV_0759	Uncharacterized protein	cell wall and cell processes	28.318	3	Rv0817c
A0A0H2ZZH2	MAV_0156	Uncharacterized protein	cell wall and cell processes	34.099	2	Rv3888c
A0A0H2ZZI0	MAV_4003	Cell division ATP-binding protein FtsE	cell wall and cell processes	25.801	3	Rv3102c
A0A0H2ZZU4	MAV_2123	PknM protein	cell wall and cell processes	25.424	2	Rv3576
A0A0H3A024	MAV_4942	Uncharacterized protein	cell wall and cell processes	45.27	6	Rv0227c
A0A0H3A049	MAV_4339	Phosphoglycerate mutase family protein	cell wall and cell processes	24.078	7	Rv3390
A0A0H3A0C0	MAV_0012	Cell wall synthesis protein CwsA	cell wall and cell processes	15.661	2	Rv0008c
A0A0H3A0C7	MAV_3813	Uncharacterized protein	cell wall and cell processes	26.675	6	Rv2969c
A0A0H3A0J2	MAV_2276	Uncharacterized protein	conserved hypotheticals	11.285	2	-
A0A0H3A0R3	MAV_1082	Uncharacterized protein	conserved hypotheticals	19.445	10	-
A0A0H3A0V9	MAV_5298	Virulence factor mvin family protein	cell wall and cell processes	126.188	2	Rv3910
A0A0H3A0X5	MAV_5100	ABC transporter, ATP-binding protein	cell wall and cell processes	38.967	3	Rv0655
A0A0H3A198	MAV_4325	ABC transporter, ATP-binding protein	cell wall and cell processes	90.457	3	Rv1747
A0A0H3A1B6	MAV_2345	Wag31 protein	cell wall and cell processes	26.99	2	Rv2145c
A0A0H3A1L5	MAV_4671	Uncharacterized protein	cell wall and cell processes	37.396	5	Rv0479c
A0A0H3A1Z4	MAV_4944	Uncharacterized protein	cell wall and cell processes	57.059	2	Rv0226c
A0A0H3A281	MAV_0446	Transglycosylase	cell wall and cell processes	82.39	6	Rv3682
A0A0H3A2D7	MAV_4235	Cadmium-translocating P-type ATPase	cell wall and cell processes	75.802	2	Rv3270
A0A0H3A343	MAV_0178	Nuclear export factor GLE1 family protein	cell wall and cell processes	21.258	3	-
A0A0H3A358	MAV_2863	Molybdate ABC transporter, periplasmic molybdate-binding protein	cell wall and cell processes	26.011	5	Rv1857
A0A0H3A3F3	MAV_2471	DoxX subfamily protein, putative	conserved hypotheticals	36.076	2	-
A0A0H3A3P3	MAV_1154	LpqT protein	cell wall and cell processes	22.933	4	Rv1016c
A0A0H3A3R2	MAV_2355	LppL protein	cell wall and cell processes	33.982	3	Rv2138
A0A0H3A3W0	MAV_0467	ABC transporter, ATP-binding protein DppD	cell wall and cell processes	59.634	4	Rv3663c
A0A0H3A402	MAV_0071	Transglycosylase	cell wall and cell processes	91.696	2	Rv0050
A0A0H3A4E8	MAV_0139	Uncharacterized protein	conserved hypotheticals	9.854	3	-
A0A0H3A4L1	MAV_1466	Uncharacterized protein	conserved hypotheticals	22.239	3	-
A0A0H3A4W6	MAV_3367	LprG protein	cell wall and cell processes	24.405	8	Rv1411c
A0A0H3A552	MAV_2699	Uncharacterized protein	conserved hypotheticals	20.417	4	-
A0Q8S8	MAV_0015	Cell division protein CrgA	cell wall and cell processes	10.347	2	Rv0011c
A0QFC0	MAV_2409	Sec-independent protein translocase protein TatA	cell wall and cell processes	9.949	2	Rv2094c
A0QK47	MAV_4137	UPF0182 protein	cell wall and cell processes	107.897	9	Rv3193c
A0A0H2ZRA6	MAV_1241	Uncharacterized protein	conserved hypotheticals	15.166	2	Rv1261c
A0A0H2ZS42	MAV_1131	Uncharacterized protein	conserved hypotheticals	60.44	2	Rv1006
A0A0H2ZSC8	MAV_3188	Uncharacterized protein	conserved hypotheticals	14.966	2	Rv1598c
A0A0H2ZT44	MAV_4595	Mycobacterial family protein 11	conserved hypotheticals	16.307	2	-
A0A0H2ZT76	MAV_3495	Uncharacterized protein	conserved hypotheticals	17.933	2	Rv2616
A0A0H2ZTA8	MAV_3199	Uncharacterized protein	conserved hypotheticals	12.564	2	-
A0A0H2ZTP0	MAV_3073	Uncharacterized protein	conserved hypotheticals	32.028	8	Rv1698
A0A0H2ZTY9	MAV_3588	Uncharacterized protein	conserved hypotheticals	27.411	2	Rv2696c

A0A0H2ZUC8	MAV_1123	Uncharacterized protein	conserved hypotheticals	22.625	2	Rv0999
A0A0H2ZUS2	MAV_0583	Periplasmic solute binding protein family protein	conserved hypotheticals	32.016	4	-
A0A0H2ZUU9	MAV_3984	Uncharacterized protein	conserved hypotheticals	14.023	2	-
A0A0H2ZV18	MAV_1705	Uncharacterized protein	conserved hypotheticals	15.989	5	Rv2468c
A0A0H2ZV54	MAV_2235	Adenylate cyclase, putative	conserved hypotheticals	59.876	2	Rv2226
A0A0H2ZV63	MAV_0741	Dyp-type peroxidase family protein	conserved hypotheticals	36.406	2	Rv0799c
A0A0H2ZVL8	MAV_4623	Uncharacterized protein	conserved hypotheticals	15.401	2	Rv0523c
A0A0H2ZVS7	MAV_3225	Uncharacterized protein	conserved hypotheticals	15.414	3	Rv1546
A0A0H2ZX99	MAV_1134	Uncharacterized protein	conserved hypotheticals	63.718	3	Rv1006
A0A0H2ZXK5	MAV_0529	D-alanyl-D-alanine carboxypeptidase/endopeptidase	conserved hypotheticals	45.809	4	Rv3627c
A0A0H2ZY07	MAV_4151	Uncharacterized protein	conserved hypotheticals	30.719	2	Rv3205c
A0A0H2ZY89	MAV_1665	Conserved ATP-binding protein	conserved hypotheticals	55.479	3	Rv2510c
A0A0H2ZY97	MAV_2940	Uncharacterized protein	conserved hypotheticals	20.428	2	Rv1780
A0A0H2ZYZ3	MAV_0468	Uncharacterized protein	conserved hypotheticals	25.367	2	Rv3662c
A0A0H2ZZ49	MAV_3635	35kd antigen	conserved hypotheticals	29.442	8	Rv2744c
A0A0H2ZZK5	MAV_4514	ABC1 family protein	conserved hypotheticals	49.4	2	Rv0647c
A0A0H2ZZV1	MAV_3332	Uncharacterized protein	conserved hypotheticals	13.937	3	Rv1444c
A0A0H3A0A5	MAV_0700	Uncharacterized protein	conserved hypotheticals	24.292	4	Rv0756c
A0A0H3A0I9	MAV_4496	Uncharacterized protein	conserved hypotheticals	14.037	2	Rv0679c
A0A0H3A0K0	MAV_4803	Uncharacterized protein	conserved hypotheticals	27.09	3	-
A0A0H3A0K4	MAV_4031	YceI like family protein	conserved hypotheticals	19.287	2	-
A0A0H3A0N9	MAV_3624	Uncharacterized protein	conserved hypotheticals	46.211	3	Rv2731
A0A0H3A0S5	MAV_5243	Uncharacterized protein	conserved hypotheticals	17.816	5	Rv0088
A0A0H3A1E4	MAV_3074	Uncharacterized protein	conserved hypotheticals	42.254	3	Rv1697
A0A0H3A1F2	MAV_0384	FAD/FMN-containing dehydrogenase	conserved hypotheticals	53.332	2	Rv3719
A0A0H3A1P7	MAV_1776	CBS domain protein	conserved hypotheticals	15.331	2	Rv2406c
A0A0H3A2N8	MAV_0179	Uncharacterized protein	conserved hypotheticals	23.723	2	Rv3850
A0A0H3A3T4	MAV_2778	Uncharacterized protein	conserved hypotheticals	16.671	3	Rv1919c
A0A0H3A425	MAV_2443	Dienelactone hydrolase family protein	conserved hypotheticals	21.835	2	Rv2054
A0A0H3A484	MAV_4871	ATPase, AAA family protein	conserved hypotheticals	66.985	2	Rv0282
A0A0H3A6D3	MAV_0386	KanY protein	conserved hypotheticals	15.266	2	Rv3718c
A0A0H2ZRI5	MAV_3386	MihF protein	information pathways	11.428	4	Rv1388
A0A0H2ZUC5	MAV_0005	DNA gyrase subunit B	information pathways	74.485	2	Rv0005
A0A0H2ZVM4	MAV_3462	Peptidyl-prolyl cis-trans isomerase (PPIase)	information pathways	31.19	4	Rv2582
A0A0H2ZW89	MAV_0519	DNA topoisomerase 1 (DNA topoisomerase I)	information pathways	102.34	3	Rv3646c
A0A0H2ZXJ2	MAV_4462	30S ribosomal protein S17	information pathways	12.888	2	Rv0710
A0A0H2ZXW8	MAV_4448	30S ribosomal protein S5	information pathways	23.049	2	Rv0721
A0A0H2ZYM4	MAV_3744	30S ribosomal protein S2	information pathways	30.135	4	Rv2890c
A0A0H3A054	MAV_3836	DNA-binding protein HU	information pathways	22.44	4	Rv2986c
A0QDG8	MAV_1729	50S ribosomal protein L21	information pathways	11.025	2	Rv2442c
A0QIW6	MAV_3677	30S ribosomal protein S15	information pathways	10.312	2	Rv2785c
A0QIY2	MAV_3693	Translation initiation factor IF-2	information pathways	95.408	2	Rv2839c
A0QJ48	MAV_3764	30S ribosomal protein S16	information pathways	18.064	3	Rv2909c

A0QKT2	MAV_4385	30S ribosomal protein S9	information pathways	18.147	2	Rv3442c
A0QKT3	MAV_4386	50S ribosomal protein L13	information pathways	16.157	4	Rv3443c
A0QKU6	MAV_4399	30S ribosomal protein S4	information pathways	23.48	2	Rv3458c
A0QKU8	MAV_4401	30S ribosomal protein S13	information pathways	14.3	2	Rv3460c
A0QKZ6	MAV_4449	50S ribosomal protein L18	information pathways	13.267	2	Rv0720
A0QKZ8	MAV_4451	30S ribosomal protein S8	information pathways	14.417	3	Rv0718
A0QL13	MAV_4466	50S ribosomal protein L22	information pathways	19.062	2	Rv0706
A0QL19	MAV_4472	30S ribosomal protein S10	information pathways	11.424	4	Rv0700
A0QL48	MAV_4502	DNA-directed RNA polymerase subunit beta	information pathways	146.936	7	Rv0668
A0QL54	MAV_4508	50S ribosomal protein L10	information pathways	20.176	2	Rv0651
A0QL66	MAV_4520	50S ribosomal protein L1	information pathways	24.883	5	Rv0641
A0QL67	MAV_4521	50S ribosomal protein L11	information pathways	14.976	2	Rv0640
X8B104	I549_1549	50S ribosomal protein L5	information pathways	21.168	3	Rv0716
A0A0H2ZTK2	MAV_0134	Uncharacterized protein	conserved hypotheticals	32.165	4	-
A0A0H2ZQZ2	MAV_2964	Uncharacterized protein	conserved hypotheticals	20.159	5	-
A0A0H2ZQZ6	MAV_4862	Subtilase family protein	intermediary metabolism and respiration	46.328	2	Rv0291
A0A0H2ZSH1	MAV_0758	Thioredoxin	intermediary metabolism and respiration	14.822	2	Rv0816c
A0A0H2ZSI9	MAV_4817	Ferredoxin, 4Fe-4S	intermediary metabolism and respiration	104.436	5	Rv0338c
A0A0H2ZSP8	MAV_3341	Glyceraldehyde-3-phosphate dehydrogenase	intermediary metabolism and respiration	36.073	13	Rv1436
A0A0H2ZSX9	MAV_0275	Adenine specific DNA methylase Mod	intermediary metabolism and respiration	74.233	2	Rv3396c
A0A0H2ZT29	MAV_1384	Short chain alcohol dehydrogenase	intermediary metabolism and respiration	28.955	2	Rv1245c
A0A0H2ZUI0	MAV_2376	Short chain dehydrogenase	intermediary metabolism and respiration	32.037	3	Rv2129c
A0A0H2ZV74	MAV_5147	Aldehyde dehydrogenase	intermediary metabolism and respiration	51.37	3	Rv0147
A0A0H2ZVV5	MAV_1153	Retinol dehydrogenase 13	intermediary metabolism and respiration	31.038	3	-
A0A0H2ZW96	MAV_0121	Carbonate dehydratase	intermediary metabolism and respiration	52.068	2	Rv3273
A0A0H2ZWB0	MAV_2273	Dihydrolipoamide acetyltransferase	intermediary metabolism and respiration	61.732	2	Rv2215
A0A0H2ZX25	MAV_4124	Dehydrogenase	intermediary metabolism and respiration	67.174	3	Rv0068
A0A0H2ZX34	MAV_0459	Serine protease	intermediary metabolism and respiration	41.212	9	Rv3671c
A0A0H2ZX42	MAV_4796	FAD dependent oxidoreductase domain protein	intermediary metabolism and respiration	111.138	2	-
A0A0H2ZXS5	MAV_1285	3-Hydroxyacyl-CoA dehydrogenase	intermediary metabolism and respiration	26.396	2	Rv1144
A0A0H2ZYG8	MAV_4818	Aspartate aminotransferase	intermediary metabolism and respiration	45.621	2	Rv0337c
A0A0H2ZYI7	MAV_0654	short chain dehydrogenase/reductase family protein	intermediary metabolism and respiration	29.746	2	Rv3502c
A0A0H2ZZV9	MAV_4909	Succinate dehydrogenase	intermediary metabolism and respiration	70.481	8	Rv0248c
A0A0H3A0A3	MAV_5142	Alanine dehydrogenase/pyridine nucleotide transhydrogenase	intermediary metabolism and respiration	37.28	4	Rv0155
A0A0H3A0H6	MAV_4098	Aldo/keto reductase	intermediary metabolism and respiration	34.893	4	Rv2298
A0A0H3A0H8	MAV_2990	Oxidoreductase	intermediary metabolism and respiration	35.114	2	Rv2781c
A0A0H3A169	MAV_3265	Putative glycosyl transferase	intermediary metabolism and respiration	46.744	2	Rv1524

A0A0H3A1C3	MAV_4278	Glycerol-3-phosphate dehydrogenase	intermediary metabolism and respiration	63.034	6	Rv3302c
A0A0H3A1I1	MAV_4619	Uncharacterized protein	intermediary metabolism and respiration	21.051	3	Rv0526
A0A0H3A1K0	MAV_4813	Uncharacterized protein	conserved hypotheticals	22.41	3	-
A0A0H3A230	MAV_4910	Succinate dehydrogenase	intermediary metabolism and respiration	28.619	4	Rv0247c
A0A0H3A290	MAV_3633	Uncharacterized protein	intermediary metabolism and respiration	15.848	2	Rv2740
A0A0H3A2U3	MAV_4248	Biotin-[acetyl-CoA-carboxylase] ligase	intermediary metabolism and respiration	26.687	2	Rv3279c
A0A0H3A3H5	MAV_3876	Electron transfer protein, beta subunit	intermediary metabolism and respiration	27.83	3	Rv3029c
A0A0H3A3K1	MAV_0524	Nucleoside-diphosphate-sugar epimerase	intermediary metabolism and respiration	33.079	4	Rv3634c
A0A0H3A3N4	MAV_1046	Short chain dehydrogenase	intermediary metabolism and respiration	27.161	2	Rv0927c
A0A0H3A3R8	MAV_2297	Putative ubiquinol-cytochrome c reductase, iron-sulfur subunit QcrA	intermediary metabolism and respiration	43.746	2	Rv2195
A0A0H3A4A1	MAV_2279	Probable cytosol aminopeptidase	intermediary metabolism and respiration	53.436	4	Rv2213
A0QCX5	MAV_1524	ATP synthase subunit b-delta	intermediary metabolism and respiration	48.45	4	Rv1307
A0QCX6	MAV_1525	ATP synthase subunit alpha	intermediary metabolism and respiration	59.956	6	Rv1308
A0QCX7	MAV_1526	ATP synthase gamma chain	intermediary metabolism and respiration	33.556	11	Rv1309
A0QCX8	MAV_1527	ATP synthase subunit beta	intermediary metabolism and respiration	53.064	5	Rv1310
A0QDH1	MAV_1732	Glutamate 5-kinase	intermediary metabolism and respiration	37.818	2	Rv2439c
A0QJV0	MAV_4036	NADH-quinone oxidoreductase subunit D	intermediary metabolism and respiration	48.327	2	Rv3148
A0QLV0	MAV_4761	F420-dependent glucose-6-phosphate dehydrogenase	intermediary metabolism and respiration	37.331	2	Rv0407
A0A0H2ZS36	MAV_5229	Methyltransferase type 11	intermediary metabolism and respiration)	26.295	2	Rv1523
A0A0H2ZQY9	MAV_4891	Acyl-CoA synthase	lipid metabolism	60.812	11	Rv0270
A0A0H2ZS23	MAV_2193	Acyl carrier protein (ACP)	lipid metabolism	12.477	4	Rv2244
A0A0H2ZUY7	MAV_4915	Acetyl-CoA acetyltransferase	lipid metabolism	44.657	5	Rv0243
A0A0H2ZUZ7	MAV_0217	Acyl-CoA synthase	lipid metabolism	69.304	8	Rv3801c
A0A0H2ZYK2	MAV_2965	Uncharacterized protein	conserved hypotheticals	17.262	2	-
A0A0H2ZYK6	MAV_1351	Acyl-CoA synthase	lipid metabolism	63.823	2	Rv1206
A0A0H2ZZD1	MAV_2307	Putative acyl-CoA dehydrogenase	lipid metabolism	64.545	4	Rv2187
A0A0H3A1U7	MAV_2190	Propionyl-CoA carboxylase beta chain	lipid metabolism	50.071	2	Rv2247
A0A0H3A2P2	MAV_4916	Oxidoreductase	lipid metabolism	47.243	6	Rv0242c
A0A0H2ZZY4	MAV_2054	Major membrane protein 1	cell wall and cell processes	33.651	5	-
A0A0H2ZTL7	MAV_2542	Regulatory protein GntR, HTH	regulatory proteins	28.812	2	Rv3060c
A0A0H2ZU77	MAV_0185	Transcriptional regulator	regulatory proteins	33.343	2	-
A0A0H2ZXW5	MAV_4678	Transcriptional regulator, TetR family protein	regulatory proteins	25.254	2	Rv0472c
A0A0H2ZYD4	MAV_3299	MoxR protein	regulatory proteins	40.705	5	Rv1479
A0A0H2ZYE5	MAV_0453	Transcriptional regulator, Crp/Fnr family protein	regulatory proteins	24.78	8	Rv3676
A0A0H2ZYJ3	MAV_1022	Two component response transcriptional regulatory protein prra	regulatory proteins	25.009	2	Rv0903c
A0A0H3A1Q7	MAV_1176	Two component transcriptional regulator trcr	regulatory proteins	28.509	2	Rv1033c
A0A0H3A2H2	MAV_1290	Regulatory protein GntR, HTH	regulatory proteins	13.224	2	Rv1152
A0A0H3A389	MAV_0023	FHA domain protein	regulatory proteins	14.431	3	Rv0019c

A0A0H3A3I3	MAV_0017	Serine/threonine protein kinase	regulatory proteins	66.322	2	Rv0014c
A0A0H2ZSE9	MAV_0740	29 kDa antigen Cfp29	virulence, detoxification, adaptation	28.601	11	Rv0798c
A0A0H3A0B2	MAV_3310	27 kDa lipoprotein antigen	virulence, detoxification, adaptation	25.074	5	-
A0A0H3A1X7	MAV_2043	[Cu-Zn] superoxide dismutase	virulence, detoxification, adaptation	20.467	4	-
A0A0H3A3S5	MAV_4722	Superoxide dismutase [Cu-Zn]	virulence, detoxification, adaptation	22.424	2	Rv0432

Table 4: MAH104 proteins found in the MVs, released in response to 24h metal mix exposure. Their functional classification into the categories was based on the function of their significantly matching *M. tuberculosis* (strain H37Rv) homolog proteins, which are also listed here.

Accession no.	Gene names	Description	Functional Category	MW [kDa]	Peptides	H37Rv homolog
A0A0H2ZU28	MAV_0542	ATP-dependent zinc metalloprotease FtsH	cell wall and cell processes	86	9	Rv3610c
A0A0H3A1B6	MAV_2345	Wag31 protein	cell wall and cell processes	27	5	Rv2145c
A0A0H3A198	MAV_4325	ABC transporter, ATP-binding protein	cell wall and cell processes	90.5	5	Rv1747
A0A0H2ZSF7	MAV_4443	Signal peptide peptidase SppA	cell wall and cell processes	62.8	3	Rv0724
A0A0H2ZZ15	MAV_3290	Secreted protein	cell wall and cell processes	40.8	3	Rv1488
A0A0H2ZQZ2	MAV_2964	Uncharacterized protein	conserved hypotheticals	20.2	3	-
A0A0H3A074	MAV_1135	Chain length determinant protein	conserved hypotheticals	51.1	5	-
A0A0H3A0S7	MAV_3776	Signal recognition particle receptor FtsY	cell wall and cell processes	44.7	3	Rv2921c
A0A0H2ZZH2	MAV_0156	Uncharacterized protein	cell wall and cell processes	34.1	4	Rv3888c
A0QJ93	MAV_3810	Phosphopantetheine adenylyltransferase	cell wall and cell processes	17.4	4	Rv2965c
A0QDF1	MAV_1712	Trigger factor	cell wall and cell processes	50.6	4	Rv2462c
A0A0H2ZVA7	MAV_0569	LpqE protein	cell wall and cell processes	19.1	3	Rv3584
A0A0H3A0H4	MAV_2917	Uncharacterized protein	cell wall and cell processes	44.1	3	Rv1797
A0A0H3A0V9	MAV_5298	Virulence factor mvin family protein	cell wall and cell processes	126.2	3	Rv3910
A0A0H3A1N0	MAV_1373	Uncharacterized protein	cell wall and cell processes	16.2	3	Rv1234
A0A0H3A1B9	MAV_2896	SbmA protein	cell wall and cell processes	71.2	2	Rv1819c
A0A0H3A4F0	MAV_2041	Uncharacterized protein	cell wall and cell processes	68.8	3	Rv2345
A0A0H2ZSX3	MAV_0229	Probable arabinosyltransferase A	cell wall and cell processes	112.4	3	Rv3793
A0A0H3A4C4	MAV_3261	Methyltransferase MtfC	conserved hypotheticals	30	3	-
A0A0H2ZTE6	MAV_3468	Protein translocase subunit SecD	cell wall and cell processes	63.1	3	Rv2587c
A0A0H3A4W6	MAV_3367	LprG protein	cell wall and cell processes	24.4	2	Rv1411c
A0A0H2ZVI5	MAV_4011	Nitric-oxide reductase subunit B	intermediary metabolism and respiration	82.9	2	-
A0A0H3A076	MAV_4608	Uncharacterized protein	cell wall and cell processes	59.4	2	Rv0537c
A0A0H3A1U0	MAV_3583	TrkB protein	cell wall and cell processes	23.6	2	Rv2692

A0A0H3A107	MAV_3414	Uncharacterized protein	cell wall and cell processes	23	2	Rv2536
A0A0H3A3W0	MAV_0467	ABC transporter, ATP-binding protein DppD	cell wall and cell processes	59.6	2	Rv3663c
A0A0H2ZX20	MAV_2932	Ftsk/spoiiie family protein	cell wall and cell processes	150.8	2	Rv2748c
A0A0H3A024	MAV_4942	Uncharacterized protein	cell wall and cell processes	45.3	2	Rv0227c
A0A0H2ZXJ3	MAV_4895	Periplasmic binding protein	cell wall and cell processes	33.2	2	Rv0265c
A0A0H3A2A2	MAV_3565	Uncharacterized protein	cell wall and cell processes	49.1	2	Rv2673
A0A0H3A0M0	MAV_4799	Uncharacterized protein	conserved hypotheticals	38.1	2	-
A0A0H2ZV45	MAV_3369	Aminoglycosides/tetracycline-transport integral membrane protein	cell wall and cell processes	55.1	2	Rv1410c
A0A0H3A3Q4	MAV_4005	Transporter, small conductance mechanosensitive ion channel (MscS) family protein	cell wall and cell processes	31.1	2	Rv3104c
A0A0H2ZTR9	MAV_0208	UDP-galactopyranose mutase	cell wall and cell processes	45.9	2	Rv3809c
A0A0H2ZUW2	MAV_3639	FtsK/SpoIIIE family protein	cell wall and cell processes	82.6	2	Rv2748c
A0A0H2ZZI0	MAV_4003	Cell division ATP-binding protein FtsE	cell wall and cell processes	25.8	2	Rv3102c
A0QGP2	MAV_2894	Protein translocase subunit SecA	cell wall and cell processes	85	2	Rv1821
A0A0H2ZZ49	MAV_3635	35kd antigen	conserved hypotheticals	29.4	10	Rv2744c
A0A0H2ZWB5	MAV_1780	Glycoside hydrolase	conserved hypotheticals	76.7	14	Rv2402
A0A0H2ZSN9	MAV_3643	Ribonuclease J	conserved hypotheticals	59.6	14	Rv2752c
A0A0H2ZXF9	MAV_1050	Non-homologous end joining protein Ku	conserved hypotheticals	34	8	Rv0937c
A0QF43	MAV_2327	Transcriptional regulator MraZ	conserved hypotheticals	15.8	6	Rv2166c
A0A0H3A2C4	MAV_0274	Uncharacterized protein	conserved hypotheticals	94.4	7	Rv1179c
A0A0H3A2T3	MAV_1190	Patatin	conserved hypotheticals	36.2	8	Rv1063c
A0A0H2ZV18	MAV_1705	Uncharacterized protein	conserved hypotheticals	16	5	Rv2468c
A0A0H2ZU55	MAV_0883	Putative cyclase superfamily protein	conserved hypotheticals	35.9	5	-
A0A0H2ZRZ7	MAV_0068	Transcriptional regulator, PadR family protein	conserved hypotheticals	20.4	6	Rv0047c
A0A0H2ZRN7	MAV_0407	Transcriptional regulator, PadR family protein	conserved hypotheticals	27.5	4	-
A0A0H2ZQS1	MAV_1588	Dihydrodipicolinate synthetase family protein	conserved hypotheticals	37.1	6	-
A0A0H3A0U9	MAV_3650	Uncharacterized protein	conserved hypotheticals	26.8	5	Rv1682
A0A0H2ZV54	MAV_2235	Adenylate cyclase, putative	conserved hypotheticals	59.9	7	Rv2226
A0A0H2ZSW1	MAV_0646	Amidohydrolase family protein	conserved hypotheticals	30.4	4	Rv3510c
A0A0H2ZX36	MAV_1416	Uncharacterized protein	conserved hypotheticals	21.5	4	Rv1265
A0A0H2ZZG2	MAV_0276	Uncharacterized protein	conserved hypotheticals	16.5	4	Rv0269c
A0A0H3A0K0	MAV_4803	Uncharacterized protein	conserved hypotheticals	27.1	3	-
A0A0H2ZSN6	MAV_1652	Peptidase M20	conserved hypotheticals	46.7	4	Rv2522c
A0A0H3A1Y3	MAV_3981	HpcH/HpaI aldolase/citrate lyase family protein, putative	conserved hypotheticals	33.2	3	Rv3075c
A0A0H2ZWT4	MAV_4615	Uncharacterized protein	conserved hypotheticals	46.1	2	Rv0530
A0A0H2ZTY1	MAV_1494	Cadmium inducible protein cadi	conserved hypotheticals	18.4	3	Rv2641
A0A0H2ZZV4	MAV_4288	Uncharacterized protein	conserved hypotheticals	47.6	3	Rv3311
A0A0H2ZXK5	MAV_0529	D-alanyl-D-alanine carboxypeptidase/D-alanyl-D-alanine-endopeptidase	conserved hypotheticals	45.8	2	Rv3627c
A0A0H3A321	MAV_3608	Uncharacterized protein	conserved hypotheticals	35.8	2	Rv2714
A0A0H2ZW37	MAV_2209	GTP cyclohydrolase 1 type 2 homolog	conserved hypotheticals	39.4	2	Rv2230c
A0A0H2ZS30	MAV_4065	CheR methyltransferase, SAM binding domain protein	conserved hypotheticals	69.2	2	-

A0A0H2ZY07	MAV_4151	Uncharacterized protein	conserved hypotheticals	30.7	2	Rv3205c
A0A0H3A2D0	MAV_1300	Uncharacterized protein	conserved hypotheticals	28.5	2	Rv1682
A0QL48	MAV_4502	DNA-directed RNA polymerase subunit beta'	information pathways	146.9	17	Rv0668
A0A0H3A2S9	MAV_3119	Phenylalanine--tRNA ligase beta subunit	information pathways	87.7	13	Rv1650
A0A0H2ZT47	MAV_0006	DNA gyrase subunit A	information pathways	92.3	12	Rv0006
A0QIW5	MAV_3676	Polyribonucleotide nucleotidyltransferase	information pathways	79.5	7	Rv2783c
A0QL35	MAV_4489	Elongation factor Tu	information pathways	43.7	8	Rv0685
A0A0H3A054	MAV_3836	DNA-binding protein HU	information pathways	22.4	4	Rv2986c
A0QKU5	MAV_4398	DNA-directed RNA polymerase subunit alpha	information pathways	37.7	7	Rv3457c
A0A0H2ZY16	MAV_3152	30S ribosomal protein S1	information pathways	53	7	Rv1630
A0QL49	MAV_4503	DNA-directed RNA polymerase subunit beta	information pathways	129.7	5	Rv0667
A0A0H2ZXZ2	MAV_3913	Ribonucleoside-diphosphate reductase subunit beta	information pathways	37.3	6	Rv3048c
A0A0H2ZX40	MAV_3919	Ribonucleoside-diphosphate reductase	information pathways	80.3	4	Rv3051c
A0A0H2ZUC5	MAV_0005	DNA gyrase subunit B	information pathways	74.5	3	Rv0005
A0QL15	MAV_4468	50S ribosomal protein L2	information pathways	30.4	4	Rv0704
A0QHB6	MAV_3120	Phenylalanine--tRNA ligase alpha subunit	information pathways	37.4	3	Rv1649
A0QL12	MAV_4465	30S ribosomal protein S3	information pathways	30.6	3	Rv0707
A0A2A3A104	lysS CKJ75_07550	Lysine--tRNA ligase	information pathways	130.4	3	Rv1640c
A0A0H3A0Q1	MAV_0002	Beta sliding clamp	information pathways	39.8	2	Rv0002
A0QID4	MAV_3490	Threonine--tRNA ligase	information pathways	76.3	3	Rv2614c
A0QIB8	MAV_3474	Holliday junction ATP-dependent DNA helicase RuvA	information pathways	20.3	2	Rv2593c
A0QJD4	MAV_3859	Glutamyl-tRNA(Gln) amidotransferase subunit A	information pathways	51.2	2	Rv3011c
A0QL36	MAV_4490	Elongation factor G	information pathways	77.2	2	Rv0684
A0A0H2ZVH1	MAV_1446	Nudix hydrolase	intermediary metabolism and respiration	22.5	2	-
A0A202G104	rplO	50S ribosomal protein L15	information pathways	15.7	2	Rv0723
A0A0H2ZXZ9	MAV_1728	Rne protein	information pathways	102.4	2	Rv2444c
A0QJ27	MAV_3743	Elongation factor Ts	information pathways	29.1	2	Rv2889c
A0QL11	MAV_4464	50S ribosomal protein L16	information pathways	15.7	2	Rv0708
A0A0H3A140	MAV_5027	Type I restriction-modification system, M subunit	information pathways	55.4	2	Rv2756c
A0QL17	MAV_4470	50S ribosomal protein L4	information pathways	22.9	2	Rv0702
A0A0H2ZV52	MAV_0434	Anti-anti-sigma factor	conserved hypotheticals	33	6	-
A0A0H2ZY71	MAV_5153	Starvation-induced DNA protecting protein	conserved hypotheticals	20	3	-
A0A0H3A0J8	MAV_4373	Glutamate decarboxylase	intermediary metabolism and respiration	51	12	Rv3432c
A0A0H2ZV13	MAV_1737	Glutamine-dependent NAD(+) synthetase	intermediary metabolism and respiration	75.5	11	Rv2438c
A0A0H3A1C3	MAV_4278	Glycerol-3-phosphate dehydrogenase	intermediary metabolism and respiration	63	8	Rv3302c
A0A0H2ZVV6	MAV_2267	Glutamine synthetase	intermediary metabolism and respiration	53.7	8	Rv2220
A0A0H2ZRC1	MAV_4211	Adenosylhomocysteinase	intermediary metabolism and respiration	54.5	11	Rv3248c
A0QCX8	MAV_1527	ATP synthase subunit beta	intermediary metabolism and respiration	53.1	10	Rv1310
A0QGK3	MAV_2855	Probable phosphoketolase	intermediary metabolism and respiration	89.3	10	-

A0A0H2ZZP6	MAV_0406	Glycerol kinase	intermediary metabolism and respiration	55.1	7	Rv3696c
A0A0H2ZVK4	MAV_4963	Phosphoenolpyruvate carboxykinase [GTP]	intermediary metabolism and respiration	67.6	8	Rv0211
A0A0H2ZT75	MAV_4652	Pyrroline-5-carboxylate reductase	intermediary metabolism and respiration	30.1	6	Rv0500
A0A0H2ZY31	MAV_2779	Limonene 1,2-monooxygenase	intermediary metabolism and respiration	42	7	-
A0QCX5	MAV_1524	ATP synthase subunit b-delta	intermediary metabolism and respiration	48.5	10	Rv1307
A0A0H2ZZV9	MAV_4909	Succinate dehydrogenase	intermediary metabolism and respiration	70.5	11	Rv0248c
A0Q994	MAV_0188	Prephenate dehydratase	intermediary metabolism and respiration	32.5	5	Rv3838c
A0A0H2ZX42	MAV_4796	FAD dependent oxidoreductase domain protein	intermediary metabolism and respiration	111.1	4	-
A0A0H2ZQM4	MAV_0593	Extradiol ring-cleavage dioxygenase	intermediary metabolism and respiration	33.8	8	Rv3568c
A0QCX6	MAV_1525	ATP synthase subunit alpha	intermediary metabolism and respiration	60	8	Rv1308
A0QBX4	MAV_1164	Enolase	intermediary metabolism and respiration	44.8	6	Rv1023
A0A0H2ZU78	MAV_0742	Probable M18 family aminopeptidase 2	intermediary metabolism and respiration	46	8	Rv0800
A0A0H3A227	MAV_3021	Biphenyl-2,3-diol 1,2-dioxygenase 1	intermediary metabolism and respiration	33.2	8	-
A0A0H2ZSI9	MAV_4817	Ferredoxin, 4Fe-4S	intermediary metabolism and respiration	104.4	6	Rv0338c
A0A0H2ZYT8	MAV_2781	Isocitrate lyase	intermediary metabolism and respiration	85.2	7	Rv1916
A0QLK3	MAV_4662	2,3-bisphosphoglycerate-dependent phosphoglycerate mutase	intermediary metabolism and respiration	27.1	5	Rv0489
A0A0H2ZWB0	MAV_2273	Dihydrolipoamide acetyltransferase component of pyruvate dehydrogenase complex	intermediary metabolism and respiration	61.7	7	Rv2215
A0A0H2ZRQ6	MAV_0425	Dehydrogenase	intermediary metabolism and respiration	36.5	5	-
A0A0H2ZXW1	MAV_3170	Pyruvate kinase	intermediary metabolism and respiration	48.2	7	Rv1617
A0A0H3A3Q6	MAV_4352	Glycoside hydrolase family protein 65, central catalytic	intermediary metabolism and respiration	87.5	6	Rv3401
A0A0H2ZXN0	MAV_2829	Glutamine synthetase, catalytic domain	intermediary metabolism and respiration	46.6	6	Rv1878
A0A0H2ZXD2	MAV_5140	NAD(P) transhydrogenase subunit beta	intermediary metabolism and respiration	48.4	5	Rv0157
A0QIC8	MAV_3484	Pyridoxal 5'-phosphate synthase subunit PdxS	intermediary metabolism and respiration	31.9	5	Rv2606c
A0A0H3A0N1	MAV_1221	Fumarate hydratase class II	intermediary metabolism and respiration	49.7	6	Rv1098c
A0A0H2ZRT1	MAV_1696	NAD-glutamate dehydrogenase	intermediary metabolism and respiration	178.7	7	Rv2476c
A0A0H2ZR92	MAV_3329	Glucose-6-phosphate 1-dehydrogenase	intermediary metabolism and respiration	54.4	5	Rv1447c
A0A0H2ZYT7	MAV_1549	Alpha-glucan phosphorylase	intermediary metabolism and respiration	96	6	Rv1328
A0A0H2ZWU6	MAV_4637	Delta-aminolevulinic acid dehydratase	intermediary metabolism and respiration	30.9	3	Rv0512
A0A0H3A0E2	MAV_2196	Pyruvate dehydrogenase E1 component	intermediary metabolism and respiration	103.3	5	Rv2241
A0A0H3A5C4	MAV_3327	Transketolase	intermediary metabolism and respiration	75.4	6	Rv1449c
A0A0H2ZSP8	MAV_3341	Glyceraldehyde-3-phosphate dehydrogenase	intermediary metabolism and respiration	36.1	5	Rv1436
A0A0H3A0M2	MAV_2733	Glucose-6-phosphate 1-dehydrogenase	intermediary metabolism and respiration	56.5	4	Rv1447c
A0A0H2ZYF1	MAV_4773	O-succinylhomoserine sulfhydrylase	intermediary metabolism and respiration	43.4	3	Rv0391

A0A0H2ZTI5	MAV_3117	Arginine biosynthesis bifunctional protein ArgJ	intermediary metabolism and respiration	40.9	3	Rv1653
A0A0H2ZYW5	MAV_3330	OpcA protein	intermediary metabolism and respiration	32.9	3	Rv1446c
A0A0H2ZSS7	MAV_1156	Ribose-phosphate pyrophosphokinase	intermediary metabolism and respiration	35.4	5	Rv1017c
A0A0H2ZQN4	MAV_1714	ATP-dependent Clp protease proteolytic subunit	intermediary metabolism and respiration	23.3	3	Rv2460c
A0A0H3A005	MAV_5301	Thioredoxin reductase	intermediary metabolism and respiration	38.6	4	Rv3913
A0QGM8	MAV_2880	Malate synthase G	intermediary metabolism and respiration	80.3	4	Rv1837c
A0A0H2ZVY7	MAV_1016	Citrate synthase	intermediary metabolism and respiration	40.3	4	Rv0889c
A0A0H3A0A3	MAV_5142	Alanine dehydrogenase/pyridine nucleotide transhydrogenase	intermediary metabolism and respiration	37.3	4	Rv0155
A0A0H2ZSY8	MAV_0633	Rieske [2Fe-2S] domain protein	intermediary metabolism and respiration	44.1	2	Rv3526
A0A0H3A3R8	MAV_2297	Putative ubiquinol-cytochrome c reductase, iron-sulfur subunit QcrA	intermediary metabolism and respiration	43.7	6	Rv2195
A0A0H2ZX09	MAV_1103	Molybdopterin biosynthesis protein moeA	intermediary metabolism and respiration	44.5	3	Rv0994
A0A0H2ZU32	MAV_2281	Branched-chain-amino-acid aminotransferase	intermediary metabolism and respiration	40	4	Rv2210c
A0A0H3A1A9	MAV_4687	Dihydrolipoyl dehydrogenase	intermediary metabolism and respiration	49.5	5	Rv0462
A0QBI3	MAV_1012	Putative phosphoserine aminotransferase	intermediary metabolism and respiration	39.7	4	Rv0884c
A0A0H2ZV08	MAV_1201	Cystathionine beta-synthase	intermediary metabolism and respiration	49.2	4	Rv1077
A0QI26	MAV_3382	S-adenosylmethionine synthase	intermediary metabolism and respiration	43.3	4	Rv1392
A0QMB9	MAV_4936	Succinate-semialdehyde dehydrogenase [NADP(+)]	intermediary metabolism and respiration	50	4	Rv0234c
A0QCX4	MAV_1523	ATP synthase subunit b	intermediary metabolism and respiration	18.9	4	Rv1306
A0A0H2ZZ08	MAV_3747	Lactate 2-monooxygenase	intermediary metabolism and respiration	41.1	3	-
A0QC23	MAV_1215	Serine hydroxymethyltransferase	intermediary metabolism and respiration	44.9	3	Rv1093
A0A0H3A4L5	MAV_3875	Electron transfer flavoprotein, alpha subunit	intermediary metabolism and respiration	31.3	3	Rv3028c
A0A0H2ZYG8	MAV_4818	Aspartate aminotransferase	intermediary metabolism and respiration	45.6	3	Rv0337c
A0QMH2	MAV_4989	Dihydroxy-acid dehydratase	intermediary metabolism and respiration	59.5	3	Rv0189c
A0QGN2	MAV_2884	Glycine dehydrogenase (decarboxylating)	intermediary metabolism and respiration	99.9	3	Rv1832
A0A0H2ZU95	MAV_2994	Putative class II aldolase	intermediary metabolism and respiration	28.2	3	-
A0A0H3A414	MAV_2291	Cytochrome c oxidase, subunit 2	intermediary metabolism and respiration	37.1	3	Rv2200c
A0A0H3A363	MAV_2730	Citrate lyase beta chain (Citrase beta chain) (Citrate(Pro-3S)-lyase beta chain)	intermediary metabolism and respiration	30.9	3	-
A0QHB0	MAV_3114	Ornithine carbamoyltransferase	intermediary metabolism and respiration	33.6	3	Rv1656
A0A0H2ZV88	MAV_3847	D-3-phosphoglycerate dehydrogenase	intermediary metabolism and respiration	54.5	3	Rv2996c
A0A0H3A3F8	MAV_3655	Oxidoreductase, short chain dehydrogenase/reductase family protein	intermediary metabolism and respiration	26.8	3	Rv2766c
A0A0H2ZRI7	MAV_3470	4-aminobutyrate transaminase	intermediary metabolism and respiration	47.2	2	Rv2589
A0A0H2ZWA3	MAV_4244	N5-carboxyaminoimidazole ribonucleotide mutase	intermediary metabolism and respiration	17.6	2	Rv3275c
A0A0H3A230	MAV_4910	Succinate dehydrogenase	intermediary metabolism and respiration	28.6	3	Rv0247c
A0A0H2ZZR5	MAV_4461	Arylsulfatase	intermediary metabolism and respiration	86.4	3	Rv0711

A0A0H3A2J3	MAV_4304	Taurine-pyruvate aminotransferase	intermediary metabolism and respiration	48	2	Rv3329
A0A0H2ZYT9	MAV_2865	Uncharacterized protein	intermediary metabolism and respiration	33.4	2	Rv1855c
A0QCX7	MAV_1526	ATP synthase gamma chain	intermediary metabolism and respiration	33.6	2	Rv1309
A0A0H2ZQI0	MAV_4682	Isocitrate lyase	intermediary metabolism and respiration	47	2	Rv0467
A0A0H2ZWB2	MAV_4691	Eptc-inducible aldehyde dehydrogenase	intermediary metabolism and respiration	54.7	2	Rv0458
A0A0H2ZUK9	MAV_4409	Putative acyltransferase	intermediary metabolism and respiration	41.2	2	-
A0A0H2ZRA7	MAV_4925	Glucose-methanol-choline	intermediary metabolism and respiration	66.4	2	Rv1279
A0A0H2ZV74	MAV_5147	Aldehyde dehydrogenase	intermediary metabolism and respiration	51.4	2	Rv0147
A0A0H3A663	MAV_4047	NADH-quinone oxidoreductase subunit N	intermediary metabolism and respiration	55.1	2	Rv3158
A0A0H2ZUM9	MAV_1203	Cystathionine beta-lyase MetC	intermediary metabolism and respiration	40.6	2	Rv1079
A0A0H2ZY47	MAV_5203	Thiamine pyrophosphate enzyme, central domain family protein	intermediary metabolism and respiration	61.9	2	-
A0A0H3A3H5	MAV_3876	Electron transfer protein, beta subunit	intermediary metabolism and respiration	27.8	2	Rv3029c
A0A0H2ZW98	MAV_1553	Peptidase family protein T4	intermediary metabolism and respiration	34.4	2	Rv1333
A0A0H3A2U5	MAV_3303	Aconitate hydratase 1	intermediary metabolism and respiration	101.1	2	Rv1475c
A0A0H2ZRT8	MAV_0608	Coenzyme A transferase, subunit B	intermediary metabolism and respiration	27.1	2	Rv3552
A0A0H3A0R9	MAV_1253	6-phosphogluconate dehydrogenase, decarboxylase	intermediary metabolism and respiration	36.5	2	Rv1122
A0QCI6	MAV_1380	Malate dehydrogenase	intermediary metabolism and respiration	34.6	2	Rv1240
A0A0H3A0L0	MAV_2833	Bacterioferritin	intermediary metabolism and respiration	18.5	2	Rv1876
A0A0H2ZRL8	MAV_0067	Myo-inositol-1-phosphate synthase	intermediary metabolism and respiration	40.2	2	Rv0046c
A0A0H2ZTD7	MAV_4039	NADH-quinone oxidoreductase	intermediary metabolism and respiration	84	3	Rv3151
A0A0H3A1S4	MAV_4760	Phosphate acetyltransferase	intermediary metabolism and respiration	73.5	2	Rv0408
A0A0H3A242	MAV_3187	Histidinol dehydrogenase	intermediary metabolism and respiration	48	2	Rv1599
A0A0H2ZZZ9	MAV_2296	Cytochrome b6	intermediary metabolism and respiration	62.4	2	Rv2196
A0QHI0	MAV_3185	Imidazoleglycerol-phosphate dehydratase	intermediary metabolism and respiration	22.6	2	Rv1601
A0QI58	MAV_3413	3-dehydroquinate dehydratase	intermediary metabolism and respiration	15.2	2	Rv2537c
A0QHB4	MAV_3118	N-acetyl-gamma-glutamyl-phosphate reductase	intermediary metabolism and respiration	35.2	2	Rv1652
A0A0H2ZWD3	MAV_1345	2,3,4,5-tetrahydropyridine-2,6-dicarboxylate N-succinyltransferase	intermediary metabolism and respiration	32.4	2	Rv1201c
A0A0H3A1M4	MAV_1090	Acetyl-CoA carboxylase carboxyltransferase	lipid metabolism	56.7	12	Rv0974c
A0A0H2ZZ02	MAV_1650	Fatty acid synthase	lipid metabolism	328	18	Rv2524c
A0A0H3A1U9	MAV_1089	Carbamoyl-phosphate synthase L chain, ATP binding domain	lipid metabolism	70.5	14	Rv0973c
A0A0H2ZZC7	MAV_0218	Polyketide synthase	lipid metabolism	192.9	15	Rv3800c
A0A0H2ZYX8	MAV_4255	Acetyl-/propionyl-coenzyme A carboxylase alpha chain	lipid metabolism	62.4	7	Rv3285
A0QHY0	MAV_3336	Phosphoenolpyruvate carboxylase	lipid metabolism	102.5	7	-
A0A0H2ZZ95	MAV_2729	Hydrolase, peptidase M42 family protein	lipid metabolism	44.3	7	-
A0A0H2ZS23	acpP MAV_2193	Acyl carrier protein	lipid metabolism	12.5	5	Rv2244

A0A0H2ZWE8	MAV_1544	Acetyl-CoA acetyltransferase	lipid metabolism	40.5	6	Rv1323
A0A0H3A0C3	MAV_1671	Acetyl-/propionyl-coenzyme A carboxylase alpha chain	lipid metabolism	71.9	5	Rv2501c
A0A0H2ZSX9	MAV_0275	Adenine specific DNA methylase Mod	lipid metabolism	74.2	6	Rv3396c
A0A0H3A2A7	MAV_1574	L-carnitine dehydratase/bile acid-inducible protein F	lipid metabolism	41.8	5	-
A0A0H3A4K9	MAV_1117	M42 glutamyl aminopeptidase superfamily protein	lipid metabolism	40.2	4	-
A0A0H2ZZY3	MAV_3244	Linear gramicidin synthetase subunit D	lipid metabolism	366.2	4	Rv0101
A0A0H3A2U4	MAV_4681	3-hydroxybutyryl-CoA dehydrogenase	lipid metabolism	31.8	5	Rv0468
A0A0H2ZTA2	MAV_1088	Acyl-CoA dehydrogenase fadE12	lipid metabolism	41.4	4	Rv0972c
A0A0H2ZTC2	MAV_4250	Propionyl-CoA carboxylase beta chain	lipid metabolism	59	3	Rv3280
A0A0H3A275	MAV_1766	Acyl-CoA dehydrogenase domain protein	lipid metabolism	42.6	3	-
A0A0H2ZRE0	MAV_4914	Putative acyl-CoA dehydrogenase	lipid metabolism	66.5	3	Rv0244c
A0A0H2ZXF3	MAV_1765	Pimeloyl-CoA dehydrogenase	lipid metabolism	39.3	3	-
A0A0H3A0U3	MAV_0220	Propionyl-CoA carboxylase beta chain	lipid metabolism	57.3	3	Rv3799c
A0A0M3KKT5	MAV_3689	Enoyl-CoA hydratase	lipid metabolism	27.6	3	Rv2831
A0A0H2ZS53	MAV_0945	L-carnitine dehydratase/bile acid-inducible protein F	lipid metabolism	42.9	3	-
A0A0H2ZR60	MAV_4940	Phosphotriesterase-like protein	lipid metabolism	33.9	3	Rv0230c
A0A0H3A5X8	MAV_4185	FadA6_4	lipid metabolism	40.3	2	-
A0A0H2ZWD4	MAV_1216	Fatty acid desaturase	lipid metabolism	31.5	3	Rv1094
A0A0H2ZZD1	MAV_2307	Putative acyl-CoA dehydrogenase	lipid metabolism	64.5	2	Rv2187
A0A0H2ZSV5	MAV_3294	Enoyl-[acyl-carrier-protein] reductase [NADH]	lipid metabolism	28.7	2	Rv1484
A0A0H2ZXP2	MAV_3309	Putative acyl-CoA dehydrogenase	lipid metabolism	65.8	2	Rv1467c
A0A0H2ZXW9	MAV_2191	3-oxoacyl-[acyl-carrier-protein] synthase 2	lipid metabolism	42.9	2	Rv2246
A0A0H3A0T6	MAV_0909	Acetyl-CoA acetyltransferase	lipid metabolism	39.7	2	-
A0A0H2ZWV9	MAV_1608	Carboxyl transferase domain	lipid metabolism	53.1	2	-
A0A0H3A5Q9	MAV_0343	Malyl-CoA lyase	lipid metabolism	33.4	2	-
A0A0H2ZYK6	MAV_1351	Acyl-CoA synthase	lipid metabolism	63.8	2	Rv1206
A0A0H3A2P5	MAV_3524	Enoyl-CoA hydratase/isomerase family protein	lipid metabolism	30.2	2	-
A0A0H2ZT32	MAV_4343	3-oxoacyl-[acyl-carrier-protein] synthase 2	lipid metabolism	44	2	Rv2246
A0A0H3A3T5	MAV_4517	Cyclopropane-fatty-acyl-phospholipid synthase 1	lipid metabolism	34.3	2	Rv0642c
A0A0H2ZVS4	MAV_0981	Putative acyl-CoA dehydrogenase	lipid metabolism	76	2	Rv0860
A0A0H2ZZ17	MAV_4647	Cyclopropane-fatty-acyl-phospholipid synthase 2	lipid metabolism	34.2	2	Rv0503c
A0A0H2ZUZ7	MAV_0217	Acyl-CoA synthase	lipid metabolism	69.3	2	Rv3801c
A0A0H3A0K4	MAV_4031	YceI like family protein	conserved hypotheticals	19.3	2	-
A0A0H2ZSS8	MAV_0651	Putative acyl-CoA dehydrogenase	lipid metabolism	38	2	Rv3505
A0A0H2ZZY4	MAV_2054	Major membrane protein 1	conserved hypotheticals	33.7	4	-
A0A0H2ZYQ3	MAV_2909	PPE family protein	PE/PPE	47.4	2	-
A0A0H2ZR02	MAV_4801	Uncharacterized protein	conserved hypotheticals	16.2	3	-
A0A0H3A494	MAV_0412	ATPase family protein associated with various cellular activities (AAA)	regulatory proteins	34.9	3	Rv3692
A0A0H2ZYD4	MAV_3299	MoxR protein	regulatory proteins	40.7	5	Rv1479
A0A0H2ZVB5	MAV_1159	Transcriptional regulator, TetR family protein	regulatory proteins	24.2	3	Rv1019

A0A0H2ZZB1	MAV_3679	Iron repressor protein	regulatory proteins	25.5	2	Rv2788
A0A0H3A178	MAV_0277	Uncharacterized protein	unknown	13.1	2	-
A0QLZ6	MAV_4808	Chaperone protein DnaK	virulence, detoxification, adaptation	66.5	9	Rv0350
A0QLP6	MAV_4707	60 kDa chaperonin 2	virulence, detoxification, adaptation	56.6	10	Rv0440
A0A0H2ZXG0	MAV_5186	Trehalose synthase	virulence, detoxification, adaptation	67.6	7	Rv0126
A0QGA4	MAV_2753	Catalase-peroxidase	virulence, detoxification, adaptation	81.6	7	Rv1908c
A0A0H3A2I9	MAV_2839	Alkylhydroperoxide reductase	virulence, detoxification, adaptation	21.6	5	Rv2428
A0A0H2ZXE8	MAV_3701	N-acetyltransferase Eis	virulence, detoxification, adaptation	45.5	5	Rv2416c
A0A0H3A0R3	MAV_1082	Uncharacterized protein	conserved hypotheticals	19.4	3	-
A0A0H2ZZB0	MAV_4069	Catalase	virulence, detoxification, adaptation	80	4	-
A0A0H2ZSE9	MAV_0740	29 kDa antigen Cfp29	virulence, detoxification, adaptation	28.6	4	Rv0798c
A0A0H2ZYB9	MAV_4978	Starvation-inducible DNA-binding protein or fine tangled pili major subunit	conserved hypotheticals	18.6	6	-
A0QKR2	MAV_4365	60 kDa chaperonin 1	virulence, detoxification, adaptation	55.8	5	Rv3417c
A0QKR3	MAV_4366	10 kDa chaperonin	virulence, detoxification, adaptation	10.7	4	Rv3418c
A0A0H2ZVN7	MAV_0182	Superoxide dismutase	virulence, detoxification, adaptation	23	3	Rv3846
A0A0H2ZXX3	MAV_1658	N-acetyltransferase Eis	virulence, detoxification, adaptation	45.1	2	Rv2416c
A0QEJ0	MAV_2118	Chaperone protein HtpG	virulence, detoxification, adaptation	72.8	2	Rv2299c
A0A0H3A0B2	MAV_3310	27 kDa lipoprotein antigen	virulence, detoxification, adaptation	25.1	4	-

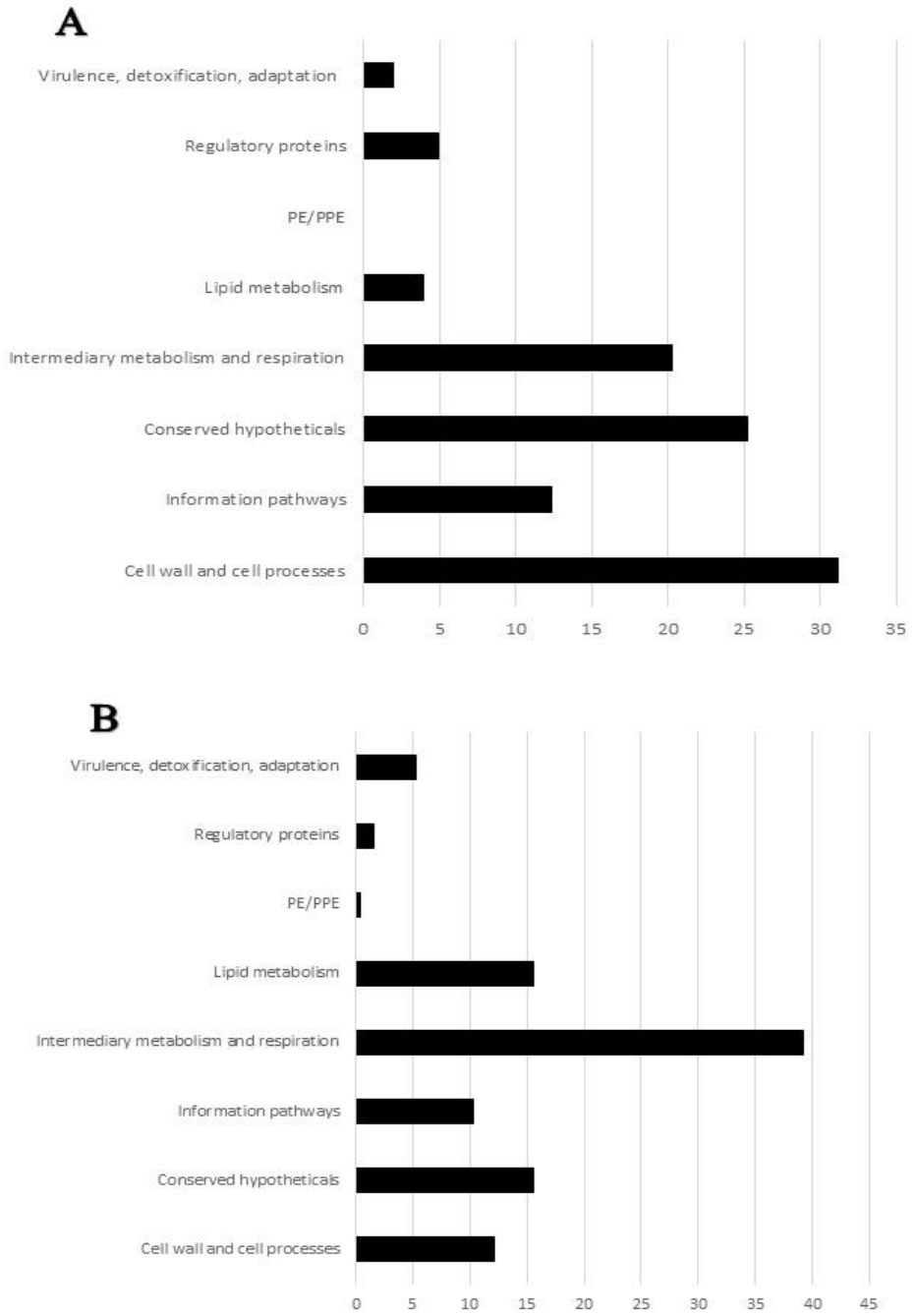

Figure 5: Functional Classification of MV cargo proteins into categories was done by finding the protein homologs of H37Rv strain and using the functional categorization available on TubercuList webserver of Institute Pasteur or based on predicted or known function for those *M. avium* proteins that do not match to any proteins of H37Rv strain. The number of proteins belonging to each functional category, were converted into percentages and the bars show % representation of each category in MV cargo proteins of minimal media (A) and metal mix (B).

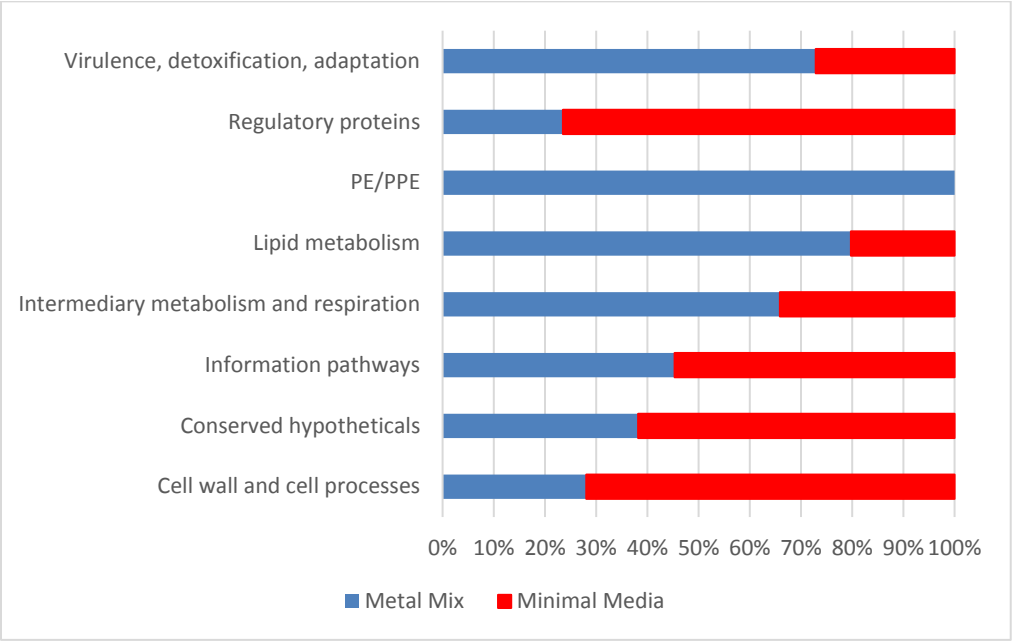

Figure 6: Comparison between % representation of each category in minimal media versus metal mix.

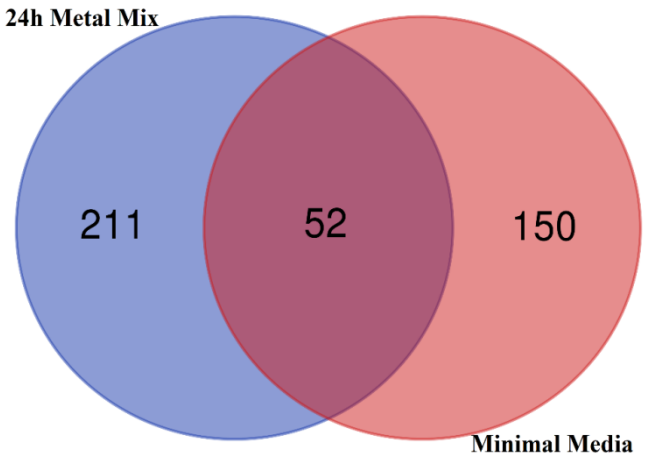

Figure 7: Venn diagram showing common and unique cargo proteins found in MAH104 MVs released in response to minimal media and metal mix. The Venn diagrams were created by using Ghent University, Gent, Belgium operated Bioinformatics & Evolutionary Genomics website (http://bioinformatics.psb.ugent.be/webtools/Venn/)

BONCAT labeling and subsequent protein enrichment revealed MAH104 secreted effectors, translocated into the host cell cytosol, during the first 24h of THP1 macrophage infection

BONCAT labeling with AHA, during MAH104 growth and subsequent click chemistry-based enrichment enabled us to selectively identify MAH104 secreted proteins in the host protein-crowded THP1 cell lysate. This method was used as a complementary approach to the above described discovery of MAH104 MV cargo proteins, identified using the metal mix, that mimics the MAH104 phagosome of 24h post-infected macrophage. AHA labeling during the bacterial growth occurs by incorporation of AHA, in place of methionine, during the active protein synthesis by growing bacteria. Subsequently, AHA labeling allows the proteins to bind to the alkyne agarose resin, through Cu catalyzed click reaction between the alkyne group of the resin and the azide moiety of the AHA. Only the AHA-labeled MAH104 proteins present in the host cell lysate sample bind to the resin by an azide-alkyne covalent bond whereas host proteins, lacking AHA, are washed away. 21 MAH104 proteins were found in the lysate of 24h post-infected THP1 human macrophages (table 5). Same functional categorization approach, described above, was used for these proteins as well. Out of the 21 found proteins, 9 proteins involved in the cell wall and cell processes, 6 proteins were involved in intermediary metabolism and respiration and 3 proteins belonged to the categories of virulence, detoxification and adaptation, and conserved hypotheticals (fig. 8). 5 proteins were common between the MX proteome and AHA-labeled MAH104 secreted effectors, implying MVs as a way

of their export to the host cell cytosol. Remaining 16 proteins (out of 21), were unique to the AHA-secretome (fig. 9).

Table 5: MAH104 secreted proteins found in the lysate of 24h post-infected THP1 macrophage, through AHA-labeling and subsequent click-reaction mediated enrichment. Their functional classification into the categories was based on the function of their significantly matching *M. tuberculosis* (strain H37Rv) homolog proteins, which are also listed here.

Accession no.	Gene name	Description	Functional Category	MW [kDa]	Peptides	H37Rv homolog
A0A0H2ZST3	MAV_1432	OppC ABC transporter, permease protein	cell wall and cell processes	33	2	Rv1282
A0A0H2ZUA4	MAV_3419	ABC transporter permease protein	virulence, detoxification, adaptation	28	2	-
A0A0H2ZWB3	MAV_3084	amt Ammonium transporter	cell wall and cell processes	44	2	-
A0A0H3A0D0	MAV_2087	amino acid transporter	cell wall and cell processes	48	6	Rv2320c
A0A0H3A0X6	MAV_4750	GluB Bacterial extracellular solute-binding protein	cell wall and cell processes	36	2	Rv0411c
A0A0H3A326	MAV_4059	Monoxygenase	intermediary metabolism and respiration	95	2	-
A0A0H3A3W0	MAV_0467	dppD ABC transporter, ATP-binding protein	cell wall and cell processes	60	3	Rv3663c
A0QFE1	MAV_2434	SsuB Aliphatic sulfonates import ATP-binding protein	cell wall and cell processes	28	3	-
A0QHM5	MAV_3231	lspA Lipoprotein signal peptidase	cell wall and cell processes	20	2	Rv1539
A0QK47	MAV_4137	UPF0182 protein	cell wall and cell processes	108	3	Rv3193c
A0A0H2ZYT4	MAV_1694	Single-stranded DNA-binding protein	conserved hypotheticals	17	2	Rv2478c
A0A0H2ZVH6	MAV_2217	TraSA:integrase fusion protein	conserved hypotheticals	43	4	-
A0A0H2ZTJ2	MAV_2056	putative sulfate exporter family transporter	cell wall and cell processes	40	7	-
A0A0H2ZVV6	MAV_2267	glnA Glutamine synthetase	intermediary metabolism and respiration	54	3	Rv2220
A0A0H2ZZP6	MAV_0406	Glycerol kinase	intermediary metabolism and respiration	55	2	Rv3696c
A0A0H2ZZZ9	MAV_2296	Cytochrome b6	intermediary metabolism and respiration	63	2	Rv2196
A0A0H3A2U3	MAV_4248	BPL_C biotin-[acetyl-CoA-carboxylase] ligase	intermediary metabolism and respiration	27	2	Rv3279c
A0QCX7	MAV_1526	ATP synthase gamma chain	intermediary metabolism and respiration	34	2	Rv1309
A0A0H2ZQZ9	MAV_0558	Uncharacterized protein	conserved hypotheticals	27	3	-
A0A0H2ZVL5	MAV_0059	ABC transporter, permease protein, His/Glu/Gln/Arg/opine family protein	virulence, detoxification, adaptation	63	2	-
A0A0H2ZXB8	MAV_2433	SsuC putative aliphatic sulfonates transport permease protein	virulence, detoxification, adaptation	30	2	-

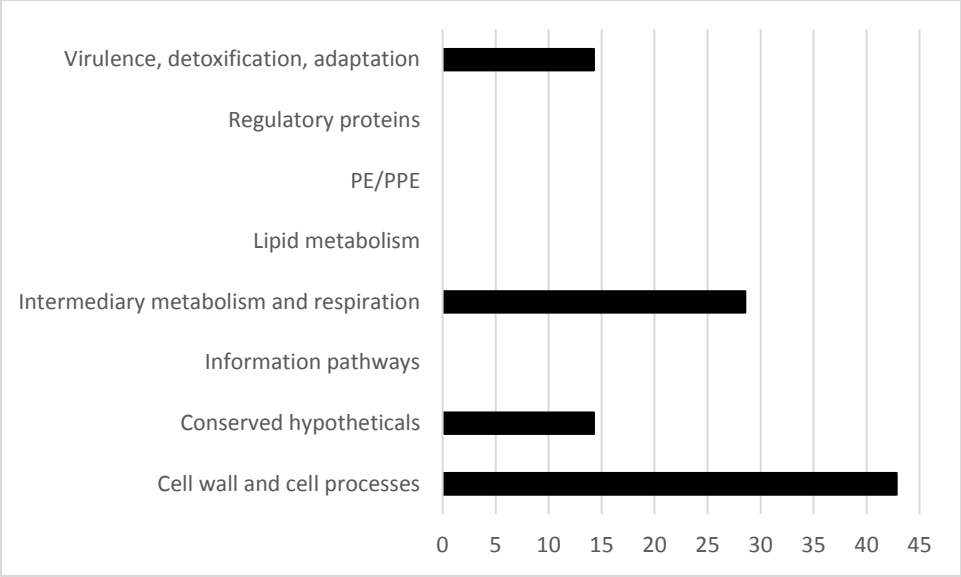

Figure 8: Functional Classification of AHA-labeled MAH104 secreted effectors into categories was done by finding the protein homologs of H37Rv strain and using the functional categorization available on TubercuList webserver of Institute Pasteur or based on predicted or known function for those *M. avium* proteins that do not match to any proteins of H37Rv strain. The number of proteins belonging to each functional category, was converted into percentages and the bars show % representation of each category in secreted proteins found through AHA-labeling and subsequent click reaction-mediated enrichment.

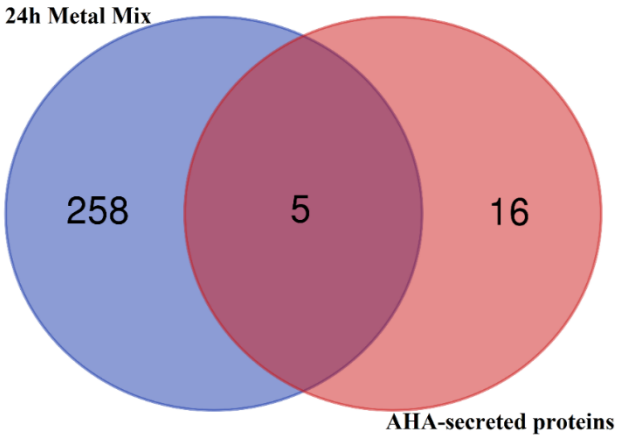

Figure 9: Venn diagram showing common and unique proteins found in MAH104 MVs released in response to metal mix and AHA-labeled MAH104 secreted effectors found in the host cell cytosol, 24h post THP1 macrophage infection. The Venn diagrams were created by using Ghent University, Gent, Belgium operated Bioinformatics & Evolutionary Genomics website (http://bioinformatics.psb.ugent.be/webtools/Venn/)

Lipidomic profile of MAH104 MVs of minimal media and metal mix

Lipidomic analysis of MAH104 MVs from both minimal media and metal mix found similar profile of lipids present in the MVs. Triacylglycerols (TAGs), diacylglycerols (DAGs), phosphatidylethanolamines (PEs), free fatty acid ethyl esters (FFAEEs) and free fatty acid methyl esters were found (fig. 10), present in the uppermost layers of the MAH104 cell wall.

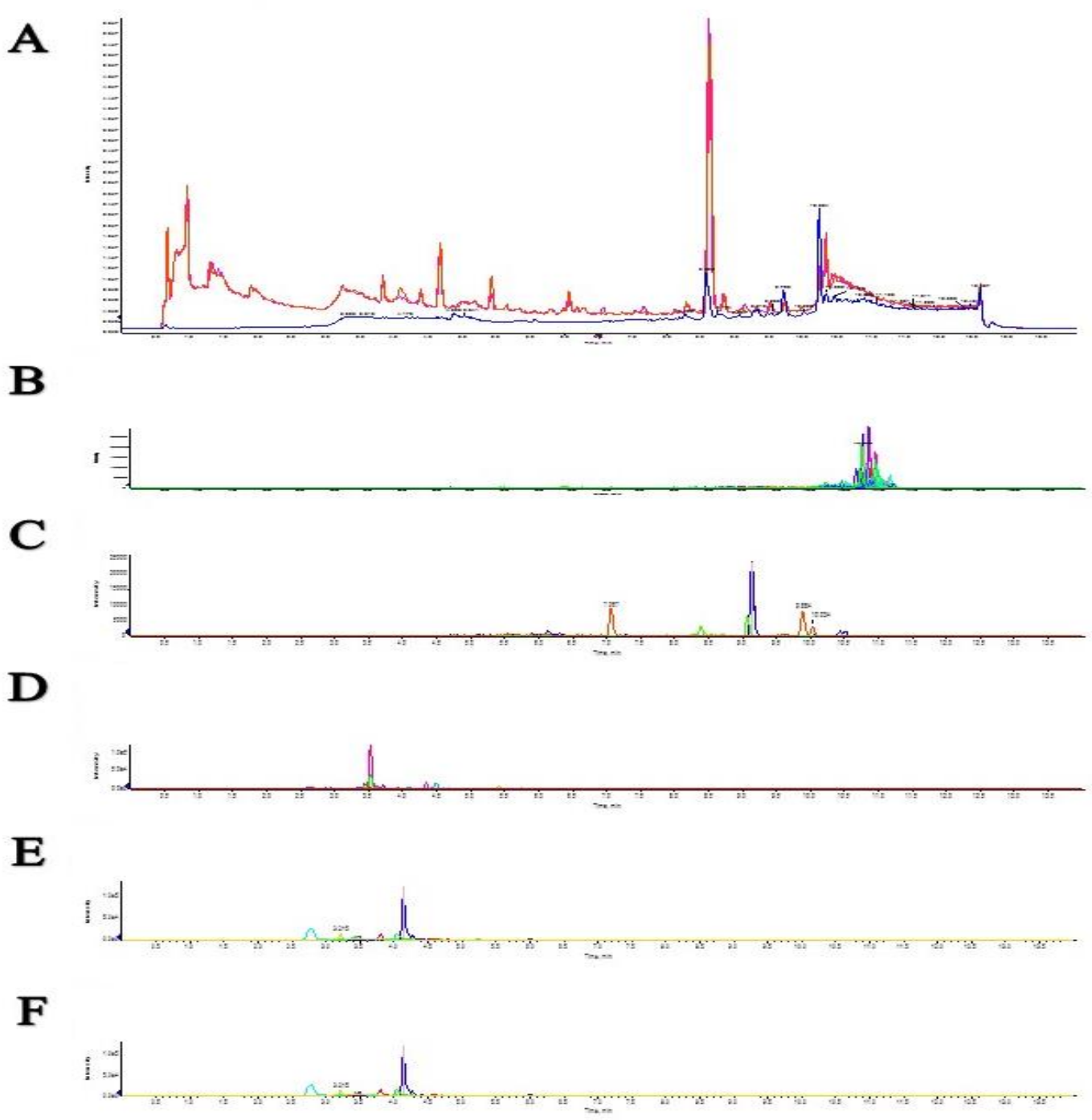

Figure 10: MV lipidomics: A is the total ion chromatogram and the remaining chromatograms are extracted ion chromatograms for individual lipid classes – B: Triacylglycerols (TAGs), C: Diacyl gycerols (DAGs), D: Phosphatidylethanolamines (PEs), E: Free fatty acid ethyl esters (FFEE), F: Free fatty acid methyl esters (FFME).

MAH104 MVs carry DNA as part of the internal cargo as well as externally-associated with the vesicle-membrane.

Double stranded DNA (dsDNA) quantification of purified MV samples, using dsDNA PicoGreen assay found DNA present in MVs released in response to both minimal media and metal mix (table 6, fig. 11). MVs released in response to minimal media carried higher amount of DNA compared to the MVs released in response to metal mix (table 6; fig. 11). Higher amount of DNA was present, associated with the external MV surface, compared to the amount present internally, as part of the MV-packaged cargo. This trend was seen in MVs from both minimal media and metal mix (table 6; figure 11). Results were substantiated by laser confocal microscopic visualization of MV-associated DNA, stained with the lipophilic nucleic acid stain SYTO-61. DNase non-treated MV samples showed high SYTO-61 fluorescence, compared to the MV samples treated with the DNase (fig. 12) in order to remove externally associated DNA, confirming the DNA quantification result that higher amount of DNA was present externally associated with the MV-membrane, compared to the amount of DNA present internally, as part of the MV packaged-cargo.

Table 6: External and internal MV-associated DNA quantification using Quant-iT PicoGreen dsDNA assay (n=3). Internal DNA was measured by treating intact MV sample with DNase before lysing the MVs whereas external DNA was measured by not lysing the MVs. Removal of external DNA, following DNase treatment, was confirmed by running the assay on DNase treated intact MV sample (external removed). Each measurement given below is the mean of 3 independent trials, run in triplicate.

	DNA concentration (ng of DNA/mL)		
	Total (External + Internal)	**Internal Only**	**External Only**
Minimal media	26.46	4.17	22.28
Metal mix	2.94	0.43	2.51

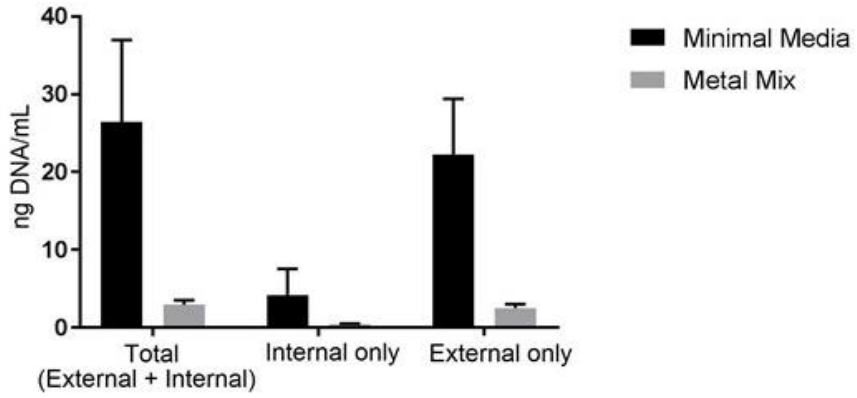

Figure 11: External and internal MV-associated DNA quantification using Quant-iT PicoGreen dsDNA assay (n=3). Internal DNA was measured by treating intact MV sample with DNase before lysing the MVs whereas external DNA was measured by not lysing the MVs, before running the assay. The data was plotted as mean (of 3 independent trials, run in triplicate) and standard deviation.

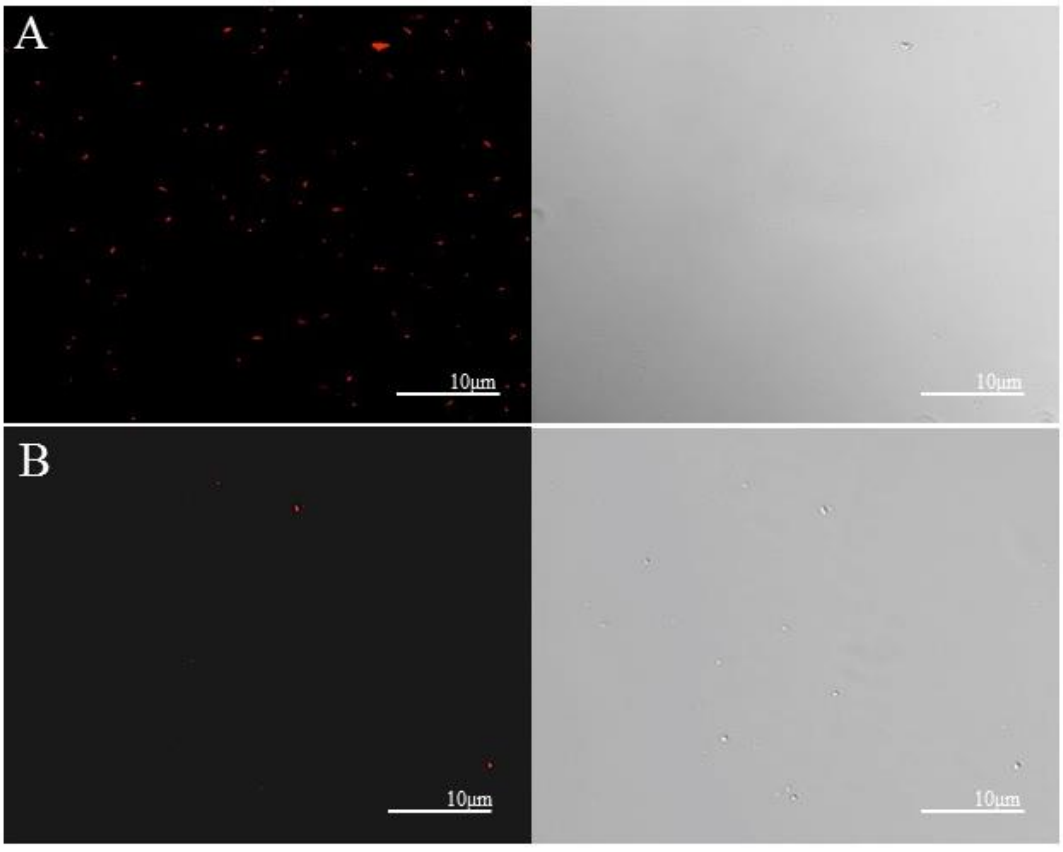

Figure 12: Laser confocal images of MVs either non-treated (A) or DNase treated (B) to remove the external MV-associated DNA. MVs are seen in transmitted light image (right panel), MV sample was treated with a lipophilic nucleic acid stain SYTO-61, which emits red fluorescence, upon DNA binding (left panel). Scale bar: 10µm.

Cloning of MAH104 FLAG-tagged overexpression constructs

FLAG-tag sequence was incorporated into the sequence of 11 MAH104 genes (of proteins selected from the list of MX proteins) and amplified using PCR (see table 2 for the list of primers). All positive constructs (11 in total; fig. 13) that showed DNA band at a site, matching with a specific DNA ladder-band that corresponded with the size of the gene, were cloned into the pMV261 plasmid under hsp60 promoter, via enzymatic digestion and ligation, following which, recombinant vectors were used for the *E. coli* transformations. Upon colony screening PCR, for several colonies, belonging to the 11 out of 11 constructs, DNA bands were found at sites, matching with a specific DNA ladder-band that corresponded with the size of the cloned gene (fig 14). After propagation of these constructs into the *E. coli* cells, cloned pMV261 constructs were extracted from *E. coli* and transformed into the MAH104 cells. Upon MAH104 colony screening PCR, DNA bands belonging to the 8 out of 11 constructs were found at sites, matching with a specific DNA ladder-band that corresponded with the size of the cloned gene (fig 15). However, we did not detect FLAG-tagged MAH104 proteins in the lysate of infected THP1 macrophage, through western blotting in an initial attempt (data not shown), requiring optimization of the experimental procedure.

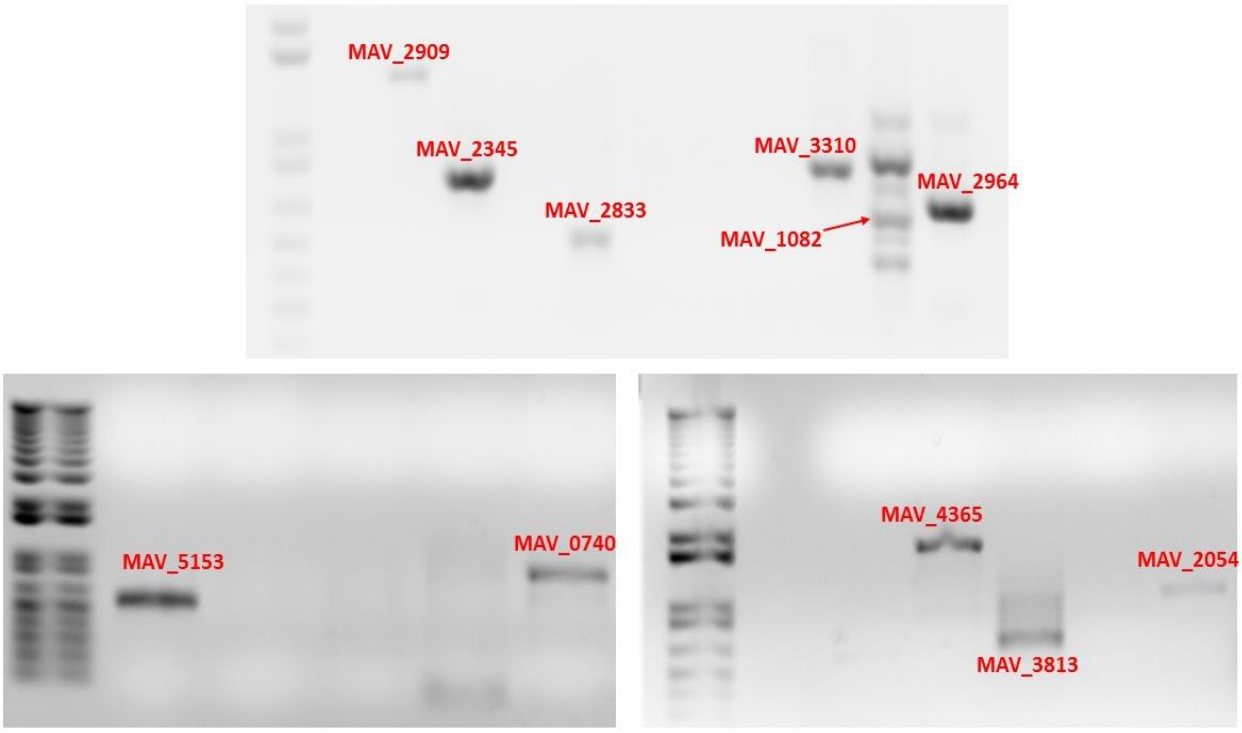

Figure 13: PCR gel electrophoresis images (captured through UV illumination) of initial and repeat experiments, showing positive constructs of initial FLAG-tag sequence incorporated selected MAH104 genes. Forward and reverse primers specific for these genes were used in the PCR amplification cycles. The PCR program was: 95°C for 3 min, 34 cycles of 95°C for 30 s, 59-63°C for 30s (or 2 min for genes which were heavier than 1000 bp), 72°C for 2 min and a final 72°C for 5 min.

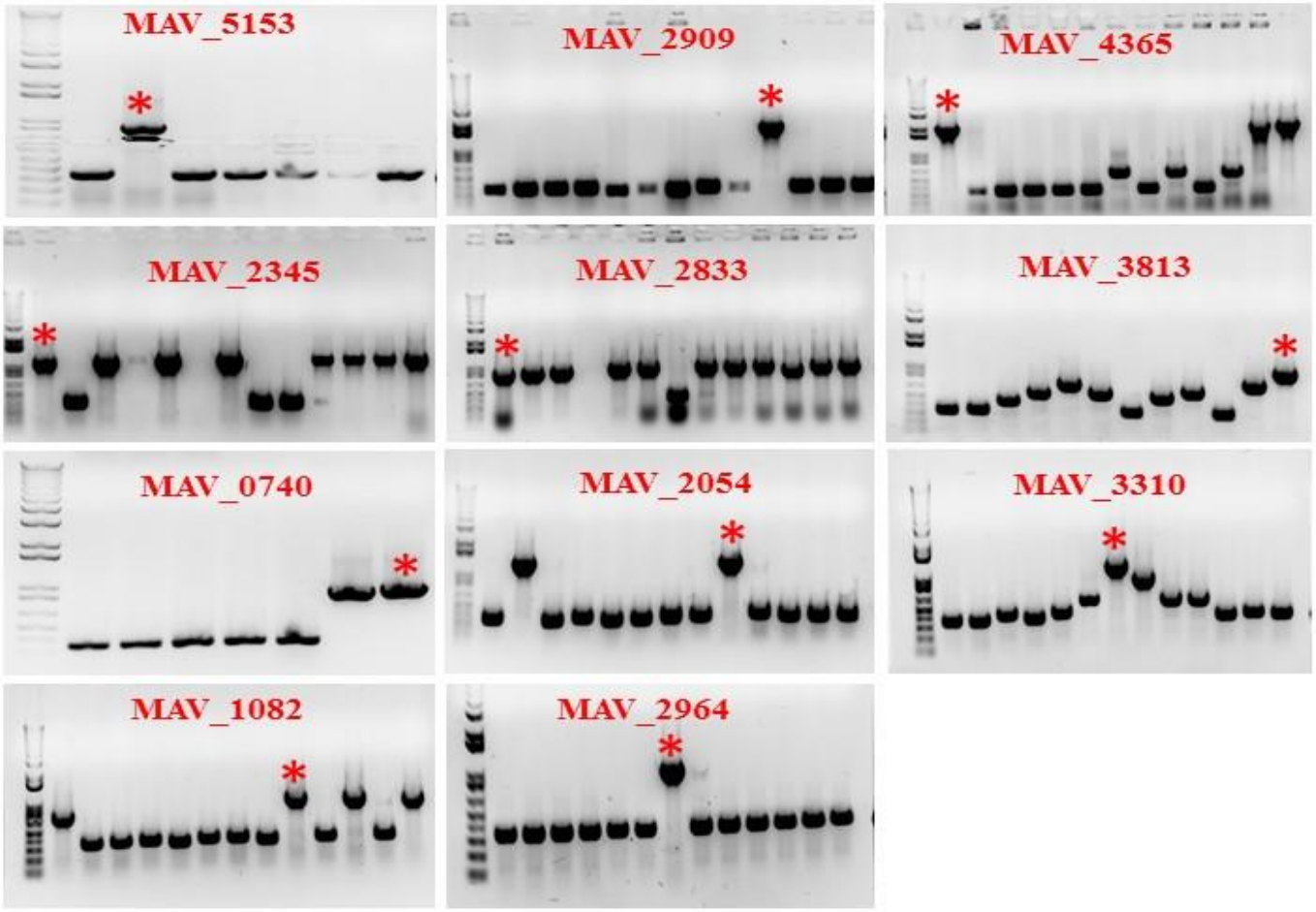

Figure 14: *E. coli* colony screening PCR gel electrophoresis images (captured through UV illumination), showing colonies harboring the pMV261-BlaC vector cloned with the construct of interest – which are FLAG-tag sequence incorporated MAH104 genes. The primers are designed based on the plasmid sequence, amplifying 320bp without having any gene in it. Colonies with positive constructs are shown with red asterisk. Forward and reverse primers specific to pMV261-BlaC vector were used in the PCR amplification cycles. The PCR program was: 95°C for 3 min, 34 cycles of 95°C for 30 s, 57°C for 30s, 72 °C for 2 min and a final 72 °C for 5 min.

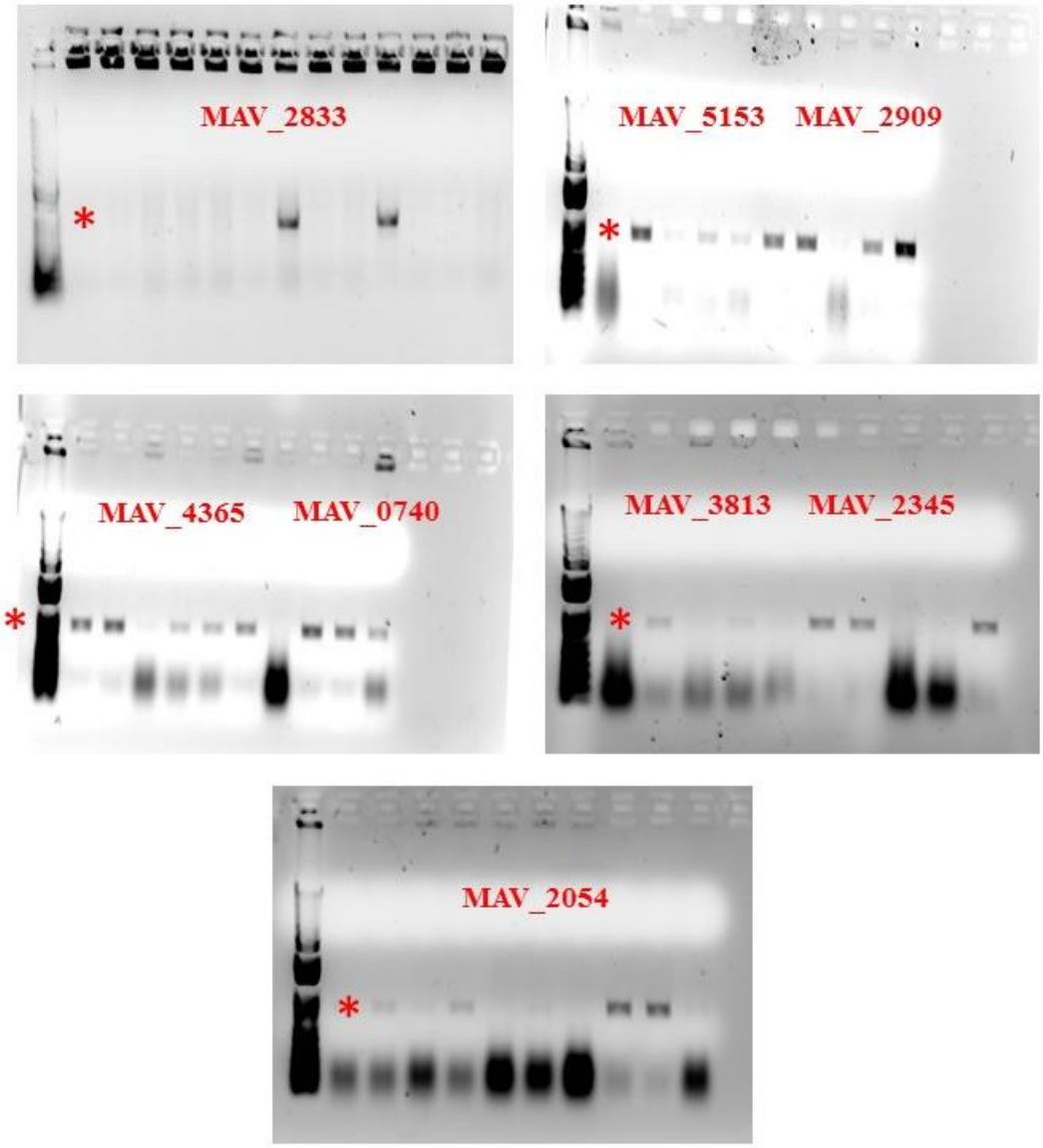

Figure 15: MAH104 colony screening PCR gel electrophoresis images (captured through UV illumination), showing colonies harboring the pMV261-BlaC vector cloned with the construct of interest – which are FLAG-tag sequence incorporated MAH104 genes. Forward and reverse primers specific to the Kanamycin resistance-gene, present on the cloned pMV261-BlaC vector, were used in the PCR amplification cycles. The red asterisk shows the specific location on DNA ladder (corresponding to the size of Kanamycin resistance gene) where the DNA bands of positive colonies should appear. The gel images were labeled with MAH104 genes that represent the positive colonies. The PCR program was: 95°C for 5 min, 35 cycles of 95°C for 30 s, 60°C for 30 s, 68°C for 1 min and a final 68°C for 5 min.

Chapter 1

DISCUSSION

Following entry into the macrophages, MAH104 resides within the vacuole and/or phagosome where it interferes with the host immune defenses, adapts to that otherwise harsh intra-phagosomal environment, replicate and continue its infectious cycle. Export of virulence determinants has a lion's share in this infectious process. While cell-bound secretion systems are important (19), (28), involvement of extracellular vehicles (EVs, also termed as membrane vesicles or MVs) has been highlighted by few recent studies in mycobacteria (50) (51), (52) and other gram positive pathogens (34). Nevertheless, in contrast to gram negative bacteria (35), EV research in gram positive bacteria, including mycobacteria, is still in its infancy, but it is burgeoning. Specifically speaking about medically important gram-positive pathogens, so far, EV-related research has been done in *Bacillus anthracis*, *Staphylococcus*, *aureus* , *Listeria monocytogenes*, *Streptococcus pneumoniae*, group A and B *Streptococci*, *Streptococcus mutans*, *Clostridium perfringens*, *Clostridium difficile* and the mycobacteria including *M. ulcerans*, *M. tuberculosis*, *M. bovis* BCG strain, *Mycobacterium kansasii*, *Mycobacterium phlei* and *M. avium* (34), (60), (61), (62), (63). Prados-Rosales *et al.* (51) documented MV production in *M. avium* through transmission electron microscopy. However, they did not investigate *M. avium* MVs further as their focus was on MVs derived from *M. tuberculosis* complex. Our study is the first in detail characterization of *M. avium* MVs produced by minimal media-led starved MAH104 as well as the phagosome environment mimicking *in vitro* system (metal mix)-led intracellular phenotype of MAH104. In addition, we investigated how could the extracellular MVs play roles in MAH104

pathogenesis. The proteomic characterization of *M. tuberculosis* (H37Rv strain) and *M. bovis* (BCG strain) by Prados-Rosales *et al.* (51) was very similar to our study, in many aspects. We used the same recipe of minimal media, published by the Prados-Rosales group in a subsequent method paper (56), to induce vesiculation in MAH104. In addition, proteomic results of MAH104 MVs, obtained with the minimal media, were consistent with their findings in MVs from H37Rv and BCG. For example, 37% of BCG, 38% of H37Rv MV-proteome (51) and 31.18% of MAH104 MV proteome, from our study, was devoted to cell wall and cell processes. Next significantly represented category was intermediate metabolism and respiration – 15% (BCG), 19% (H37Rv) (51) and 20.29% (MAH104, from our study). Other functional categories were also similarly represented among BCG and H37Rv, of their study, and MAH104 of our current study.

While minimal media connects our current study with Prados-Rosales *et al.* (51) study; it is a nutrient starvation media, which, except the starvation aspect, does not really represent the intra-phagosomal environment of a macrophage, where these mycobacterial pathogens reside and replicate, following initial infection (8), (64). We addressed this limitation by using metal mix, previously developed by our group (21). Moreover, unlike *M. tuberculosis*, whose main reservoir is always infected humans (65), and that, it spreads from person to person (66), MAC are opportunistic pathogens, ubiquitously present as free-living, within biofilms and/or within amoeba, in environments as different as house dust, showerheads, water boilers, ice machines and garden soil (2). Considering the involvement of vesiculation in bacterial communication, bacteria-bacteria co-operative and antagonistic interactions, biofilm

formation, nutrient acquisition, general survival and adapting to stressful conditions (67), it is highly likely that MAH104 produce MVs to adapt to the varied environments and lifestyles (*e.g.* free living vs. in biofilm), it persists in. Starvation would be a common stress that MAC would face in majority of environments where these environmental bacteria persist. Therefore, MVs in response to prolonged exposure of minimal media would represent more generalized vesiculation response of MAH104, with little relevance to its infectiousness and/or pathogenicity and/or virulence. However, aim of our study was to decipher the clinical significance of MAH104 vesiculation in human infections. Our rationale for using metal mix was justified by two previous studies, by our group, which found that metal mix exposure causes intracellular phenotype of MAH104, with increased expression and also direct secretion of numerous effector proteins and known MAH104 virulence factors (21), (55).

We found numerous infection-relevant MAH104 virulence proteins that were unique to the cargo of MVs, released in response to 24h metal mix exposure, and hence, absent in the cargo of MVs, released in response to 2-week minimal media exposure. Among these metal mix-specific virulence proteins, we found enhanced intracellular survival (*eis*) gene encoded Eis protein, belonging to the family of N-acyltransferase, named so because its recombination into the non-pathogenic *M. smegmatis*, enhanced their intracellular survival, within the macrophages (68). Eis protein has been described in *M. tuberculosis*, as a secreted effector protein, interacting with several host targets and associated pathways. Acyltransferase moiety, present in this protein, enables it to modulate several host innate immune responses,

in pathogen's favor. In particular, Eis inhibits autophagy, suppresses inflammation and reactive oxygen species (ROS) production by the infected macrophages, in turn, preventing their programmed cell death (69). *Eis* protein has been reported to be present in *M. tuberculosis* containing phagosome, cytosol of the infected macrophages, and even in the tuberculosis (TB) patients (using anti-eis antibody) (70), (71), clearly underscoring its significance in mycobacterial infection. Furthermore, it has also been shown to inhibit mitogen-activated T cell proliferation, and to suppress secretion of tumor necrosis factor-α (TNF-α) and interlukin-4 (IL-4) via blocking phosphorylation of extracellular signal regulated kinase (72). While Eis has not yet been characterized in MAH104, our findings suggest its export in MVs, during the first 24h of macrophage infection.

Another metal mix-specific notable MAH104 virulence protein, found in the MV cargo was trehalose synthase. Trehalose is a disaccharide, serving as a reserved carbohydrate and stress protectant. It has also been described as a byproduct of biosynthesis of mycolic acids, which is one of the major components of the mycobacterial cell wall. Findings of numerous studies support the notion that lack of complete trehalose pathway being associated with reduced pathogenic potential, although exceptions exist. Virulence of *M. tuberculosis*, *Nocardia brasiliensis*, *P. aeruginosa*, *Salmonella enterica*, *Klebsiella pneumoniae* and of numerous infamous fungal pathogens including *Candida albicans*, *Cryptococcus neoformans*, *Cryptococcus gattii*, *Aspergillus fumigatus* and *Aspergillus nidulans* has been linked to trehalose metabolism. One of the most abundant mycobacterial glycolipids, called 6,6-dimycolate (TDM) or cord factor forms when trehalose combines with the

mycolic acid. TDM has been implied in preventing phagosomal maturation, immune evasion, tissue damage and necrosis through association with the host lipids (73), (74). TDM is a well-studied immunostimulatory factor in *M. tuberculosis*. It binds to a host receptor called macrophage inducible Ca^{2+}-dependent lectin (Mincle). Upon binding to Mincle, TDM triggers pro-inflammatory cytokine and nitric oxide production by macrophages. *In vivo* administration of TDM caused elevated proinflammatory cytokine production and subsequent severe lung inflammation and granuloma formation (75). Considering these findings, it is captivating to hypothesize that trehalose synthase, delivered in the MVs, during the first 24h of infection, could catalyze trehalose synthesis, which upon combining with the mycolic acids may facilitate inflammatory pathology, including granuloma formation, seen in *M. avium* infection (18).

Five MAH104 chaperones were found only in the metal mix-induced MVs, all absent in minimal media-induced MVs. These were DnaK, HtpG, 10kDa chaperonin, 60kDa chaperonin 1 and 2. Interestingly, Prados-Rosales *et al.* (51) found DnaK and few other chaperonins in minimal media-induced *M. tuberculosis* (H37Rv) and *M. bovis* (BCG) MVs. Moreover, they detected DnaK in the lumen of BCG- and H37Rv-derived MVs through immunoblotting, visualized by electron microscopy. While we found DnaK and other chaperones in metal mix-induced MVs, we did not find them in the MVs induced by minimal media. This disparity could be because of the differences between these mycobacterial species. *M. tuberculosis* lacking transcriptional activator of heat shock proteins could not regulate phagosomal acidification, in turn, failed to replicate within the macrophages (76). Heat shock

proteins (HSPs) are important for bacterial survival upon sudden increase in the temperature of their surroundings, for example, upon entering into the host. Major function of HSPs is to act as molecular chaperones and prevent unfolding or misfolding of proteins and also facilitate protein folding (77). Considering this, such molecular chaperones may be added to MAH104 MV cargo to assist folding of other cargo proteins, until the cargo is delivered to its target site. Second possibility is that these MAH104-derived chaperones, upon MV-mediated secretion, may trigger host pro-inflammatory immune responses, which actually benefit the colonization and spread of MAH104. This later possibility is supported by the finding that *M. tuberculosis* chaperonins are highly immunogenic and potent pro-inflammatory cytokine stimulators (78). Previous study by our group, investigating MAH104 protein secretion, in response to 24h metal mix also found 10kDa and 60kDa chaperonin, directly secreted into the exposure medium (55), lending further support to the notion that MAH104 chaperones may act as immunogens.

Antioxidant enzymes, while found in all aerobically respiring organisms, are important virulence determinants for a number of pathogens to neutralize oxygen and nitrogen radicals produced by macrophages and other immune cells, as an innate immune defense against them (79). We found four antioxidant enzymes in the cargo of MAH104 MVs – superoxide dismutase (SOD), catalase (*katE*), catalase peroxidase (*katG*) and alkyl-hydroperoxide reductase (*ahpC*). Except SOD, remaining three were uniquely found in the metal mix-induced MVs, absent in the minimal media-induced MVs. Again, just like DnaK, we did not find catalase in minimal media-induced MVs in MAH104; however, Prados-Rosales *et al.* (51) found it in minimal media-induced

MVs from both *M. tuberculosis* (H37Rv) and *M. bovis* (BCG), which again, could be because of species-specific differences between these mycobacterial species. Host macrophages employ NADPH oxidase to produce highly reactive superoxide anion to kill the invading pathogen (in a process called oxidative burst). SOD neutralizes superoxide, generated during an oxidative burst, and is essential for *M. tuberculosis* to survive in activated macrophages (80). Compared to the non-pathogenic cousin *M. smegmatis*, pathogenic mycobacteria copiously produce and export SOD (81). It is notable that though much of produced SOD is exported out, it does not have a classical signal sequence, meaning it cannot be secreted via SEC pathway. Accessory secA2 pathway was found to be essential for SOD export and virulence, in *M. tuberculosis* (82). Our findings suggest MV-mediated export of SOD in MAH104. Having said that, even in MAH104, SOD was found to be directly secreted in the exposure medium, in response to 24h metal mix (55), clearly indicating that SOD export occurs through cell-bound secretion system as well as in the MV cargo, at least in MAH104, during the first 24h of macrophage infection. KatG is an interesting virulence factor in the context of antibiotic resistance and the emergence of multi-drug resistant TB cases. Numerous studies have shown that loss of KatG leads to complete attenuation of *M. tuberculosis* in various animal models, however, a specific natural mutation in KatG is associated with isoniazid resistance in *M. tuberculosis*, without the bifunctional loss of catalase-peroxidase activity (83). AhpC is a similar enzyme, scavenging peroxynitrite radical, also shown to be essential for *M. tuberculosis* survival in macrophages (84). Secreting antioxidant enzymes in MVs, during the first 24h of infection may enable MAH104 to efficiently counteract the

oxidative attack of macrophage, with minimal oxidative damage to the bacteria itself. Spontaneously released MVs from *N. meningitidis* assist them in immune evasion by overwhelming the neutrophil extracellular traps, which are actually intended for the whole bacteria, and not their MVs (85). MVs from *Haemophilus influenzae* stimulate B cells to produce antibodies, in a T cell independent manner, that do not even recognize whole *H. influenzae* bacteria, thus, diverting the host adaptive immune response towards *H. influenzae* MVs, which is actually intended for the whole bacterial cells (86). In an analogous manner, release of antioxidant enzymes-containing MVs, upon and after entry into the host cell, may divert and ultimately overwhelm NADPH oxidase-induced oxidative burst, intended for the whole bacteria, rather than their MVs, in turn helping MAH104 to evade this innate immune mechanism.

While so far discussed MAH104 virulence proteins – Eis, trehalose synthase, molecular chaperones and antioxidant enzymes (except SOD) were all exported in MVs in response to phagosomal elemental mixture and specific pH of 24h post infected macrophage (*i.e.* metal mix), but, not in response to prolonged nutrient starvation (*i.e.* minimal media), our study clearly establishes metal mix as an ideal *in vitro* medium to study MAH104 pathogenesis-relevant MVs and vesicle-bound virulence proteins. Likewise, our findings also highlight the significance of vesiculation during the early onset of MAH104 macrophage infection. This finding is consistent with the several studies in both gram positive and gram negative bacteria, and numerous resultant review articles that discuss the importance of vesiculation in bacterial virulence and pathogenesis (30), (33), (34), (35), (87). Proteins belonging to

PE/PPE family are another well-known virulence determinants of *M. tuberculosis* and other pathogenic mycobacteria, with many members known to act as cell surface antigens. Strong connection between PE/PPE family proteins and ESX (also referred to as type VII) secretion systems has been proposed (88), with the discovery that PE/PPE proteins are mainly exported through ESX-5 secretion system (89). Our study showed that a PE/PPE protein was secreted in the MV cargo in MAH104. Nevertheless, previous study by our group also found freely secreted PE/PPE proteins (55), not associated with the MVs, in response to 24h metal mix, suggesting involvement of multiple PE/PPE export pathways in MAH104. Interestingly, *M. tuberculosis* PE/PPE family protein (Rv1818c) was shown to be secreted in the exosomes, released by *M. tuberculosis*-infected macrophages and bone marrow-derived dendritic cells (90). Again, a PE/PPE family protein was found only in the MV cargo of phagosomal elemental mixture (metal mix), absent in the MV cargo of minimal media. Nevertheless, Prados-Rosales *et al.* (51) found one PE/PPE family protein in minimal media-induced MVs from *M. tuberculosis* (H37Rv) but not from *M. bovis* (BCG). Proteins belonging to this family play diverse roles in the mycobacterial pathogenesis. From initial infection to chronic phase, PE/PPE proteins have been shown to be involved in macrophage uptake, inhibition of phagosome maturation and acidification, cytokine secretion, stimulation of host cell apoptosis (through interaction with TLR2) and necrosis, dendritic cell activation and antigen processing, reviewed in detail by (88), (91), (92). It is very tempting to hypothesize that MV-mediated export of specific PE/PPE protein/s of MAH104 may stimulate macrophage apoptosis, for two solid reasons – I. mycobacterial MVs have been

shown to induce proinflammatory immune responses in a TLR2-dependent manner (51) and, II. MAH104 is known to use host cell apoptosis to spread from initially infected primary macrophage to neighboring uninfected secondary macrophages (21), (22). A more recent study showed role for a specific *M. tuberculosis* PE protein in environmental stress resistance and intracellular survival (93), which supports our finding of MV-mediated PE/PPE export, in response to metal mix. Other known mycobacterial antigens such as 29 kDa and 27kDa antigens were found in the MAH104 MV cargo of both minimal media and metal mix, consistent with the presence of 29 kDa antigen in minimal media induced MV proteome of both *M. tuberculosis* (H37Rv) and *M. bovis* (BCG) (51) suggesting that MV-mediated antigen export is probably part of more generalized stress response in these mycobacteria.

As we have seen, phagosomal elemental mixture and specific pH of 24h post-infected macrophage (*i.e.* 24h metal mix exposure) has consistently turned out to be more effective in producing MAH104 pathogenesis-relevant MVs, packaged with several virulence factors, compared to the prolonged starvation (*i.e.* 2-week minimal media exposure). However, this is not the case for all MAH104 virulence determinants, particularly of note are lipoproteins. We found only 2 known lipoproteins in the cargo of metal mix-induced MVs whereas 12 in the cargo of minimal media-induced MVs, consistent with the minimal media-induced MVs from *M. tuberculosis* (H37Rv) and *M. bovis* (BCG) (51). Physiological function of bacterial lipoproteins is to acquire ions and nutrients, facilitating survival within hostile host environment, in case of bacterial pathogens (94). And hence, it is not at all surprising that lipoproteins turned out to be a notable exception to the so far seen

pattern of more virulence factors in the metal mix-induced MVs compared to the minimal media-induced-MVs. Triacylated lipoproteins are an integral component of *M. tuberculosis* cell wall, cell membrane and MVs indeed! In addition, *M. tuberculosis* lipoprotein deletion mutants showed complete attenuation in mice (95). LprG, a cell envelope lipoprotein, was found in both minimal media and metal mix-induced MVs. It plays a crucial role in the expression of surface lipoarabinomannan – whose interaction with mannose receptors on macrophages has been suggested to be necessary for cell entry, inhibition of fusion between phagosome and lysosome and intracellular survival (96). The enrichment of lipoproteins in minimal media-induced MVs, compared to the metal mix-induced MVs could, at least partly, explain the overrepresentation of the category of "cell wall and cell processes" by the minimal media MV-proteome, compared to the metal mix MV-proteome. On the other hand, similar to the category of "virulence, detoxification and adaptation" and "PE/PPE", the category of "lipid metabolism" and to an extent also "intermediary metabolism and respiration" were overrepresented by metal mix MV-proteome, compared to the minimal media MV-proteome. Transcriptomic analysis of *M. tuberculosis* exposed to phagosome mimicking-acidic pH, found upregulation of numerous enzymes involved in the lipid metabolism (97). Further transcriptional analysis of intraphagosomal *M. tuberculosis* also found similar enzymes that led to the notion that pathogenic mycobacteria shift their carbon source from glucose or glycerol to lipids, during the onset of macrophage infection, and for the subsequent intracellular growth (64). Host lipids, but not carbohydrates, serve as the carbon source for intracellular survival and persistence of a cattle pathogen *M. avium subsp. paratuberculosis* as well (98). Lipid

and fatty acid metabolizing capabilities of *M. tuberculosis* are impressive with around 250 distinct enzymes involved in fatty acid metabolism compared to only 50, present in the *E. coli* (26). Interestingly, we found the glyoxylate cycle enzyme isocitrate lyase only in the metal mix-induced MV-proteome, absent in the minimal media-induced MVs, of MAH104. It is a fully characterized enzyme in both *M. avium* and *M. tuberculosis* (99). This single enzyme has attracted a lot of attention in TB research, and as a potential anti-TB drug target, with the discovery that it is involved in fatty acid catabolism and is necessary for *M. tuberculosis* virulence and persistence in the murine model of TB (100), (101). Our data suggests MV-mediated export of isocitrate lyase upon sensing phagosomal elemental mixture and pH but not starvation, in MAH104. Dependency on fatty acids during an infection of murine model of TB, is considered as a hallmark of *in vivo* carbon metabolism of *M. tuberculosis* (102).

As a complementary approach, we employed BONCAT labeling to identify the MAH104 secreted effectors, present in the host cell cytosol, 24h post THP1 human macrophage infection. BONCAT labeling of bacterial proteins, involves incorporation of non-canonical amino acids in place of their natural amino acid analog, during *de novo* bacterial protein synthesis. We used L-azidohomoalanine (AHA), which serves as an analog of methionine, incorporated instead of methionine in any cells (103). Host cytosol is an environment, densely packed with the host proteins whereas the abundance of bacterial effector proteins is relatively very low, making their mass spectrometric identification problematic (104). BONCAT labeling solved this problem because AHA (having an azide moiety) present in the labeled

bacterial proteins, allowed their selective enrichment, from the sample of host cell cytosol, through azide-alkyne cycloaddition reaction, also called as click-reaction (105). This click chemistry based labeling technique has been used to investigate the secreted effectors of *Yersinia enterocolitica* (106), *Salmonella typhimurium* (104) *M. tuberculosis* (20) and a protozoal pathogen *Toxoplasma gondii* (107). However, these studies used the methionine analog azidonorleucine which requires use of methionyl t-RNA synthetase mutants whereas AHA, that we used, allows labeling of wild type bacteria (107). Through this method, we found 21 MAH104 effector proteins within the cytosol of THP1 macrophage, 24h following *ex vivo* infection. 5 proteins were common between metal mix-induced MV proteome and click chemistry-tracked MAH104 secretome. This means we were able to confirm through direct macrophage infection with AHA-labeled MAH104 proteins, that at least 5 effector proteins, exported in MV cargo, are present in the host cell cytosol, 24h following macrophage infection. Among these 5 common proteins, we found a notable virulence factor, glutamine synthetase (GS) enzyme. GS mutant of *M. tuberculosis* failed to grow in human THP1 macrophages; moreover, it turned out to be avirulent in the highly susceptible guinea pig model of pulmonary TB (108). This enzyme has been characterized in *M. tuberculosis* and was found to be exported in large proportions in the phagosome of *M. tuberculosis*-infected human monocyte (109). While this enzyme has also been characterized in *M. avium* (110), there are no studies investigating involvement of GS in *M. avium* pathogenesis. Our study, for the first time presents strong evidence for potential role of GS in MAH104 pathogenesis and suggests its MV-mediated export. Two putative roles suggested for this virulence

factor include synthesis of L-glutamine, which serves as an integral cell wall component of pathogenic mycobacteria and maintenance of ammonia levels within the *M. tuberculosis*-containing phagosome, which may subsequently facilitate modulation of phagosomal pH and, inhibition of phagosome-lysosome fusion (109). GS is also required for the virulence of *M. bovis* and its mutant was not only attenuated for growth in macrophages or organs of BALB/c mice but also showed increased sensitivity to anti-TB drugs – rifampicin and D-cycloserine and, had abnormal cell surface properties (through disruption in the synthesis of poly-α-L-glutamine) and impaired capability of biofilm formation (111). GS has been a target for the development of novel anti-TB drugs, with promising results in the guinea pig model of pulmonary TB (112). The other 4 common effector proteins are involved in cell wall and cell processes and intermediary metabolism with yet unknown function in mycobacterial virulence and/or pathogenicity.

The remaining AHA-labeled 16 MAH104 effector proteins found in the host cell cytosol, but absent in the metal mix-induced MVs, thus seemingly not secreted in the MV cargo but via one of the cell-bound secretion systems, were enzymes involved in intermediary metabolism and numerous cell wall-associated secreted virulence proteins, including 3 permeases, which have been implicated in the virulence of bacterial (113), (114), and also fungal (115) pathogens. Surprisingly, while host lipids serve as an important carbon source for intracellular mycobacteria upon macrophage infection, as discussed above, and that, we found abundance of proteins including enzymes, involved in lipid and fatty acid metabolism in the cargo of metal mix-induced MVs, not a single lipid metabolism-related protein was detected

in the cytosol of MAH104 infected THP1 macrophages. This contradictory result could be explained by the origin of host cells used for the infection. THP1 cells are derived from a human monocytic leukemia (116) – cancer cell line with strikingly different metabolism than their non-cancerous counterpart present in an organism. As Eisenreich *et al.* (102) discussed in their review, in model host cells such as THP1 cell line, MAH104 might have encountered a carbon source, different from the *in vivo* non-cancerous macrophages, present in an organism. Among metal mix-induced MV-proteome and AHA-labeled secretome, only 5 proteins were common, pointing to two possibilities – I. AHA labeling may have missed several effector proteins. Choosing to use AHA restricted our discovery of MAH104 secreted effectors to only those proteins which are synthesized during *in vitro* growth on AHA-containing medium. As AHA can also label host proteins, we could not use AHA-containing medium during THP1 infection, therefore, missed out on all those MAH104 secreted effectors that are synthesized during or after the host cell infection. Realizing this limitation, we also employed a second complementary approach of FLAG-tagging few of the proteins found in the metal mix MV-proteome, by using molecular cloning, with the aim of identifying them in the host cell cytosol, by using anti-FLAG tag antibody in a western blot experiment. Though FLAG tag-incorporated overexpression constructs were successfully cloned in MAH104, we did not detect FLAG-tagged proteins in the western blotting of lysate of 24h post infected THP1 human macrophages (data not shown). II. The final destination of remaining 258 protein-carrying MVs may not be the host cell cytosol. Many of the MAH104 proteins packaged into the MVs may be destined to go out of the infected macrophage via exosomes, released by that

macrophage. Exosomes released by *M. tuberculosis*-infected macrophages activated several innate and acquired immune responses as a result of presence of numerous highly immunogenic *M. tuberculosis* proteins present in them. Treatment of host cells with the culture filtrate of *M. tuberculosis* also incited similar immune responses (117). Thus, it is highly likely that numerous proteins packaged into the MVs, during the first 24h of infection, are destined to function outside of the infected macrophage, which could possibly be involved in the spread of infection to neighboring macrophages and ultimately deep within the host tissue. We also tried to profile exosome content of THP1 macrophages, 24h and 72h post-MAH104 infection. However, we did not detect any MAH104 proteins within them (data not shown). Similarly, the other final destination of certain MAH104 effector-carrying MVs could be the host cell nucleus. Cytolethal distending toxin (CDT) carrying-MVs of periodontal pathogen *Aggregatibacter actinomycetemcomitans*, were shown to localize to the nuclear and/or perinuclear space, and release CDT into the host cell nucleus (118).

Mycobacteria are among few of the organisms that produce extremely large set of lipophilic molecules, ranging from simple fatty acids such as palmitate to highly complex mycolic acids. They possess members of every known lipid biosynthetic pathways including enzymes of common bacterial systems and those present in plants and mammals (26). Moreover, being armed with highly complex and extremely lipid-rich cell wall, mycobacterial lipids play direct roles in host-pathogen interactions, virulence and host immunomodulation (119). For example, T cell receptor signaling is inhibited by *M. tuberculosis* lipoglycans, lipoarabinomannan and

lipomannan and it was demonstrated that trafficking of these lipoglycans from intracellular tubercle bacilli to T cells occurred though MVs that ultimately inhibited activation of $CD4^+$ T cells (52). Hence, we decided to conduct lipidomic analysis of MAH104 MVs and found numerous polar and non-polar lipids in association with the MVs released in response to both minimal media and metal mix; however, no differences were detected in the MV lipid composition between the two. Phosphatidylethanolamine (PE) was the only common phospholipid that we detected in MAH104 MVs and Prados-Rosales *et al.* (51) detected in their lipidomic analysis of minimal media-induced MVs of *M. tuberculosis* (H37Rv) and *M. bovis* (BCG). The lipids detected in our study belong to the outermost layers of the mycobacterial cell wall. However, considering the proposition made by previous study (51) that cell membrane is the likely origin of MVs, further studies are needed to determine the exact lipid composition of MAH104 MVs, released in response to both prolonged starvation (*i.e.* minimal media) and the macrophage phagosomal elemental mixture and pH of 24h post MAH104 infection (*i.e.* metal mix).

Membrane vesicle research in numerous gram negative bacterial pathogens including *Bordetella pertussis, Borrelia burgdorferi, H. influenzae, H. parainfluenzae, Moraxella osloensis, Serratia marcescens, Shigella dysenteriae* and *S. flexneri, Yersinia pestis, N. gonorrhoeae, H. pylori, P. aeruginosa, S. typhimurium,* uropathogenic *E, coli* and *P. gingivalis* have found that MVs derived from all these pathogens carry DNA (44) (57), (120), (121), (122). Hence, we also investigated whether MAH104 also carry DNA within its vesicles. And, consistent with the findings from these gram-negative pathogens, we also found MAH104 MVs carrying

DNA. Our study presents strong evidence for MV-mediated export of double stranded DNA (dsDNA) in response to both minimal media and metal mix. MV-associated DNA quantification by using PicoGreen dsDNA assay was confirmed by confocal microscopic visualization of MV-associated DNA, stained with a lipophilic nucleic acid dye, SYTO-61. Consistent with previous studies, we found more DNA associated with the external surface of MVs, compared to the internal MV-lumen/cargo. Same observation was made for DNA-carrying OMVs of *H. pylori*, *P. aeruginosa*, *S. typhimurium*, uropathogenic *E, coli* and *P. gingivalis* (57). Evaluation of MVs produced during *in vitro* culture of several gram positive and gram negative bacteria for DNA carriage led Dorward & Garon (122) to conclude that DNA is packaged within MVs of only gram negative but not gram positive bacteria. Our findings directly challenge their conclusion. While they did not evaluate MVs of any mycobacteria, differences in experimental design could be behind this discrepancy. Consistent with our results, Prados-Rosales *et al.* (51) also claimed to have detected DNA in purified and intact mycobacterial MVs; however, they did not publish that data. MV-associated DNA plays a direct role in biofilm formation. *S. mutans* is one of the oral pathogens, responsible for dental caries by forming biofilms. It was found that extracellular DNA, released through bacterial MVs, played a direct role in *S. mutans* biofilm formation as DNase I treated *S. mutans* cell culture showed significantly reduced biofilm formation. Following 2-week long exposure to minimal media, we consistently observed that MAH104 cells also formed biofilms on the bottom of the flask, coupled with our finding that minimal media-induced MVs have greater amount of DNA associated with the external surfaces of MVs, make a strong

case for direct role of external MV surface associated-DNA in MAH104 biofilm formation. Although further studies will be needed to confirm this hypothesis, it has numerous implications in the context of understanding and controlling major sources of MAC infections – which are MAC biofilms present in the drinking water distribution system, household and hospital water pipes, showerheads, water boilers, ice machines and other water transporting and/or handling material, commonly found in urban areas (2), (4), (123). Similarly, this also has implications in understanding *in vivo* MAC biofilm formation in patients with underlying conditions such as cystic fibrosis (124). Nevertheless, the question remains as to how bacteria manage to get their cellular DNA associated with the external surfaces of released MVs? Explosive cell lysis of a subpopulation of MAH104 cells within its biofilm is a likely mechanism, which could be responsible for the MV external surface associated DNA, as was shown for biofilm forming cells of *P. aeruginosa* (125). Considering strong association between biofilm formation and quorum sensing, consistently documented in several gram negative and positive bacteria (126), it is irresistible to also hypothesize that probable explosive cell lysis of a subpopulation, during biofilm formation in MAH104 could be regulated by quorum sensing. Though quorum sensing in mycobacteria is almost unknown, there is some indirect evidence. Moreover, bioinformatic analysis has shown existence of LuxR homologs in *M. tuberculosis* (127). Likewise, DNA carried in MVs could also play a role in bacterial cell-to-cell communication through horizontal gene transfer as suggested previously (57).

Unlike minimal media-induced MVs, metal mix-induced MVs had significantly lower amount of DNA, associated with both external MV surfaces and internal MV lumen and/or cargo. Nevertheless, dsDNA was there, associated with MVs released in response to phagosomal elemental mixture and pH, representative of 24h post MAH104 macrophage infection, suggesting that MV-associated DNA also has certain important functions in MAH104 virulence and/or pathogenesis. DNA carried by *P. aeruginosa* OMVs was detected in the nuclear fraction of non-phagocytic lung epithelial cells, supporting this notion that vesicle mediated carriage of bacterial DNA is involved in its pathogenesis (57). A number of intracellular DNA recognizing pathways exist (mainly in the cytoplasm) that induced pro-inflammatory cascade upon sensing presence of dsDNA in the cytoplasm (128). For *M. tuberculosis* and *Legionella pneumophila* macrophage infection, it was shown that bacterial DNA enters host cell cytosol and binds to cytosolic dsDNA sensor cyclic GMP-AMP synthase (cGAS), activating type I interferon production via the endoplasmic reticulum-associated stimulator of interferon genes (STING), downstream serine threonine protein kinase (TBK1) and interferon regulatory factor 3 (IRF3) pathway (129). IRF3 deletion mutant mice, which are unable to respond to cytosolic DNA turned out to be resistant to *M. tuberculosis* infection, highlighting the importance of bacterial DNA in *M. tuberculosis* pathogenesis (130). Indeed, type I interferon production during mycobacterial infection has been considered as a pathogen-friendly immune response, detrimental to the host (28). Similarly, another cytosolic DNA sensor AIM2 (short for – absent in melanoma 2) has been shown to activate inflammasome following detection of mycobacterial DNA (131). In *M. tuberculosis*,

cytosolic contact of mycobacterial DNA has been considered to be followed by ESX-1 secreted EsxA-mediated rupture of phagosome (28). *M. avium* lack ESX-1 secretion system (23) and, based on our data, we propose that MAH104 MVs, released during the first 24h of infection, carry bacterial DNA to host cell cytosol where it interacts with one or more cytosolic DNA sensors, activating numerous pro-inflammatory immune responses, including apoptosis, through which MAH104 has been shown to spread to uninfected cells (21), (22). Further studies are needed to confirm this. Likewise, MV associated-MAH104 DNA could also enter into the host cell nucleus as was shown for the MV associated *P. aeruginosa* DNA (57). We tried to sequence the MV packaged DNA, present in the internal compartment with no success as a result of the meager quantity present inside the vesicles. Future studies need to focus on optimization of the vesicle isolation and purification protocol to get sufficient quantity of purified vesicle sample.

In summary, vesiculation is an indispensable physiological response of an opportunistic mycobacterial pathogen, MAH104 to both prolonged starvation and the hostile physicochemical environment of the 24h post-infection MAH104-containing phagosome of the macrophage. Molecular characterization implies numerous functions for MVs in MAH104 virulence, host invasion and subsequent colonization. Phagosomal environment mimicking *in vitro* system (*i.e*. metal mix) is an ideal media, far more effective than starvation causing minimal medium, to produce infection-relevant MVs in MAH104. Vesiculation in response to prolonged starvation (*i.e.* minimal media) appears to represent more generalized stress response of MAH104, aimed at acquiring nutrients, maintaining membrane integrity and biofilm

formation with vesicles enriched in metabolic enzymes, lipoproteins, other cell wall and cell processes associated proteins and internally and externally associated DNA. In contrast, vesiculation in response to phagosome mimicking system (*i.e.* metal mix) appears to represent a more host cell invasion- and colonization-focused stress response with vesicles enriched in several known virulence factors and enzymes involved in lipid and fatty acid metabolism and internally- and externally-associated MV DNA (however in lesser amounts relative to minimal media). A future study comparing the cargo of MAH104 vesicles released in response 24h metal mix and vesicles released *in vivo*, 24h following macrophage infection, is needed to definitively conclude how relevant metal mix-induced MVs are to the actual *in vivo* infection. There is always a possibility of MVs arising from cell lysis and we could not completely rule that out. However, MAH104 survival assay that we performed with minimal media and metal mix clearly showed that though MAH104 did not perform as good as it did in 10% OADC supplemented 7H9 media, it survived in both media, at least for the period of 2 weeks, as reflected by the MAH104 CFUs at the end of the 2-week long experiment. Moreover, differences in the MV cargo upon exposure to two different stress media is self-explanatory that alive MAH104 cells actively selected the MV cargo in response to specific stress that they were exposed to, and that, obtained vesicles were not mere result of stress-induced bacterial cell lysis. Nevertheless, the question remains as to why the bacteria bother to package enzymes and other virulence factors in vesicles, in an energetically expensive process of vesiculation, under stressful conditions, when conservation of energy and nutrients should be on high priority? Being naturally resistant to degradation, vesicles provide

conducive environment to help extend the activity of enzymes, virulence factors and other packaged cargo (132), at least until the cargo is delivered to its target site. Indeed, lysed and/or damaged vesicles fail to induce the robust immune response induced by intact vesicles (37). In that context, interaction of MVs with the host cell is very important in order to understand role of vesicles in delivering virulence factors to the host cells. Lipid rafts have been most frequently reported to interact with bacterial vesicles, following which, cargo of vesicles enters the host cell cytosol (35). Lipid rafts are also present on the membranes of macrophage phagosomes (133), and vesicles of MAH104 may interact with them. Focus of future studies need to be at understanding interaction of intra-phagosomal mycobacterial vesicles with the phagosomal membrane. Similarly, biogenesis and separation of a vesicle from its parent bacterium is an equally important topic. Though there are few proposed hypotheses reviewed in Brown *et al.* (34), we lack definitive information about vesicle biogenesis and vesicle separation from its parent bacterium, in lipid-rich complex cell wall harboring mycobacteria. Though many questions are yet to be answered, there is a lot of hope and future implications in understanding this highly conserved, pathogenesis-relevant, yet underappreciated aspect of microbial life (134). Following characterization of *M. tuberculosis* MVs, Prados-Rosales group investigated vaccine potential of *M. tuberculosis* vesicles, with promising results in mice. We characterized MAH104 vesicles, produced in an infection-relevant setting and our findings also have numerous implications in understanding MAC pathogenesis and the development of vaccine and novel anti-MAC therapies, while MAC diseases are on constant rise (135).

Chapter 1

REFERENCES

1. Inderlied CB, Kemper CA, Bermudez LE. 1993. The Mycobacterium avium complex. Clin Microbiol Rev 6:266-310.
2. Nishiuchi Y, Iwamoto T, Maruyama F. 2017. Infection Sources of a Common Non-tuberculous Mycobacterial Pathogen, Mycobacterium avium Complex. Front Med (Lausanne) 4:27.
3. Schorey JS, Sweet L. 2008. The mycobacterial glycopeptidolipids: structure, function, and their role in pathogenesis. Glycobiology 18:832-41.
4. Primm TP, Lucero CA, Falkinham JO, 3rd. 2004. Health impacts of environmental mycobacteria. Clin Microbiol Rev 17:98-106.
5. Cai R, Qi T, Lu H. 2014. Central nervous system infection with non-tuberculous mycobacteria: a report of that infection in two patients with AIDS. Drug Discov Ther 8:276-9.
6. Horsburgh CR, Jr. 1991. Mycobacterium avium complex infection in the acquired immunodeficiency syndrome. N Engl J Med 324:1332-8.
7. Field SK, Fisher D, Cowie RL. 2004. Mycobacterium avium complex pulmonary disease in patients without HIV infection. Chest 126:566-81.
8. Danelishvili L, Wu M, Stang B, Harriff M, Cirillo SL, Cirillo JD, Bildfell R, Arbogast B, Bermudez LE. 2007. Identification of Mycobacterium avium pathogenicity island important for macrophage and amoeba infection. Proc Natl Acad Sci U S A 104:11038-43.
9. Bermudez LE, Young LS, Enkel H. 1991. Interaction of Mycobacterium avium complex with human macrophages: roles of membrane receptors and serum proteins. Infect Immun 59:1697-702.
10. Glickman MS, Jacobs WR, Jr. 2001. Microbial pathogenesis of Mycobacterium tuberculosis: dawn of a discipline. Cell 104:477-85.
11. Koul A, Herget T, Klebl B, Ullrich A. 2004. Interplay between mycobacteria and host signalling pathways. Nat Rev Microbiol 2:189-202.
12. Danelishvili L, Bermudez LE. 2015. Mycobacterium avium MAV_2941 mimics phosphoinositol-3-kinase to interfere with macrophage phagosome maturation. Microbes Infect 17:628-37.
13. Frehel C, de Chastellier C, Lang T, Rastogi N. 1986. Evidence for inhibition of fusion of lysosomal and prelysosomal compartments with phagosomes in macrophages infected with pathogenic Mycobacterium avium. Infect Immun 52:252-62.
14. Xu S, Cooper A, Sturgill-Koszycki S, van Heyningen T, Chatterjee D, Orme I, Allen P, Russell DG. 1994. Intracellular trafficking in Mycobacterium tuberculosis and Mycobacterium avium-infected macrophages. J Immunol 153:2568-78.
15. Cambier CJ, Falkow S, Ramakrishnan L. 2014. Host evasion and exploitation schemes of Mycobacterium tuberculosis. Cell 159:1497-509.
16. Cardoso MS, Silva TM, Resende M, Appelberg R, Borges M. 2015. Lack of the Transcription Factor Hypoxia-Inducible Factor 1alpha (HIF-1alpha) in Macrophages Accelerates the Necrosis of Mycobacterium avium-Induced Granulomas. Infect Immun 83:3534-44.
17. Florido M, Appelberg R. 2006. Genetic control of immune-mediated necrosis of Mycobacterium avium granulomas. Immunology 118:122-30.
18. Ehlers S, Kutsch S, Benini J, Cooper A, Hahn C, Gerdes J, Orme I, Martin C, Rietschel ET. 1999. NOS2-derived nitric oxide regulates the size, quantity and quality of granuloma formation in Mycobacterium avium-infected mice without affecting bacterial loads. Immunology 98:313-23.
19. McNamara M, Danelishvili L, Bermudez LE. 2012. The Mycobacterium avium ESX-5 PPE protein, PPE25-MAV, interacts with an ESAT-6 family Protein, MAV_2921, and localizes to the bacterial surface. Microb Pathog 52:227-38.
20. Chande AG, Siddiqui Z, Midha MK, Sirohi V, Ravichandran S, Rao KV. 2015. Selective enrichment of mycobacterial proteins from infected host macrophages. Sci Rep 5:13430.

21. Early J, Bermudez LE. 2011. Mimicry of the pathogenic mycobacterium vacuole in vitro elicits the bacterial intracellular phenotype, including early-onset macrophage death. Infect Immun 79:2412-22.
22. Bermudez LE, Danelishvili L, Babrack L, Pham T. 2015. Evidence for genes associated with the ability of Mycobacterium avium subsp. hominissuis to escape apoptotic macrophages. Front Cell Infect Microbiol 5:63.
23. Abdallah AM, Gey van Pittius NC, Champion PA, Cox J, Luirink J, Vandenbroucke-Grauls CM, Appelmelk BJ, Bitter W. 2007. Type VII secretion--mycobacteria show the way. Nat Rev Microbiol 5:883-91.
24. Tseng TT, Tyler BM, Setubal JC. 2009. Protein secretion systems in bacterial-host associations, and their description in the Gene Ontology. BMC Microbiol 9 Suppl 1:S2.
25. Freudl R. 2013. Leaving home ain't easy: protein export systems in Gram-positive bacteria. Res Microbiol 164:664-74.
26. Cole ST, Brosch R, Parkhill J, Garnier T, Churcher C, Harris D, Gordon SV, Eiglmeier K, Gas S, Barry CE, 3rd, Tekaia F, Badcock K, Basham D, Brown D, Chillingworth T, Connor R, Davies R, Devlin K, Feltwell T, Gentles S, Hamlin N, Holroyd S, Hornsby T, Jagels K, Krogh A, McLean J, Moule S, Murphy L, Oliver K, Osborne J, Quail MA, Rajandream MA, Rogers J, Rutter S, Seeger K, Skelton J, Squares R, Squares S, Sulston JE, Taylor K, Whitehead S, Barrell BG. 1998. Deciphering the biology of Mycobacterium tuberculosis from the complete genome sequence. Nature 393:537-44.
27. Abdallah AM, Verboom T, Hannes F, Safi M, Strong M, Eisenberg D, Musters RJ, Vandenbroucke-Grauls CM, Appelmelk BJ, Luirink J, Bitter W. 2006. A specific secretion system mediates PPE41 transport in pathogenic mycobacteria. Mol Microbiol 62:667-79.
28. Groschel MI, Sayes F, Simeone R, Majlessi L, Brosch R. 2016. ESX secretion systems: mycobacterial evolution to counter host immunity. Nat Rev Microbiol 14:677-691.
29. Danelishvili L, Chinison JJJ, Pham T, Gupta R, Bermudez LE. 2017. The Voltage-Dependent Anion Channels (VDAC) of Mycobacterium avium phagosome are associated with bacterial survival and lipid export in macrophages. Sci Rep 7:7007.
30. Kuehn MJ, Kesty NC. 2005. Bacterial outer membrane vesicles and the host-pathogen interaction. Genes Dev 19:2645-55.
31. Schertzer JW, Whiteley M. 2013. Bacterial outer membrane vesicles in trafficking, communication and the host-pathogen interaction. J Mol Microbiol Biotechnol 23:118-30.
32. Kulp A, Kuehn MJ. 2010. Biological functions and biogenesis of secreted bacterial outer membrane vesicles. Annu Rev Microbiol 64:163-84.
33. Ellis TN, Kuehn MJ. 2010. Virulence and immunomodulatory roles of bacterial outer membrane vesicles. Microbiol Mol Biol Rev 74:81-94.
34. Brown L, Wolf JM, Prados-Rosales R, Casadevall A. 2015. Through the wall: extracellular vesicles in Gram-positive bacteria, mycobacteria and fungi. Nat Rev Microbiol 13:620-30.
35. Kaparakis-Liaskos M, Ferrero RL. 2015. Immune modulation by bacterial outer membrane vesicles. Nat Rev Immunol 15:375-87.
36. Bomberger JM, Maceachran DP, Coutermarsh BA, Ye S, O'Toole GA, Stanton BA. 2009. Long-distance delivery of bacterial virulence factors by Pseudomonas aeruginosa outer membrane vesicles. PLoS Pathog 5:e1000382.
37. Jun SH, Lee JH, Kim BR, Kim SI, Park TI, Lee JC, Lee YC. 2013. Acinetobacter baumannii outer membrane vesicles elicit a potent innate immune response via membrane proteins. PLoS One 8:e71751.
38. Cossart P, Sansonetti PJ. 2004. Bacterial invasion: the paradigms of enteroinvasive pathogens. Science 304:242-8.
39. Amano A, Takeuchi H, Furuta N. 2010. Outer membrane vesicles function as offensive weapons in host-parasite interactions. Microbes Infect 12:791-8.
40. Kesty NC, Mason KM, Reedy M, Miller SE, Kuehn MJ. 2004. Enterotoxigenic Escherichia coli vesicles target toxin delivery into mammalian cells. EMBO J 23:4538-49.
41. Vanaja SK, Russo AJ, Behl B, Banerjee I, Yankova M, Deshmukh SD, Rathinam VAK. 2016. Bacterial Outer Membrane Vesicles Mediate Cytosolic Localization of LPS and Caspase-11 Activation. Cell 165:1106-1119.

42. Furuta N, Tsuda K, Omori H, Yoshimori T, Yoshimura F, Amano A. 2009. Porphyromonas gingivalis outer membrane vesicles enter human epithelial cells via an endocytic pathway and are sorted to lysosomal compartments. Infect Immun 77:4187-96.
43. Parker H, Chitcholtan K, Hampton MB, Keenan JI. 2010. Uptake of Helicobacter pylori outer membrane vesicles by gastric epithelial cells. Infect Immun 78:5054-61.
44. Kaparakis M, Turnbull L, Carneiro L, Firth S, Coleman HA, Parkington HC, Le Bourhis L, Karrar A, Viala J, Mak J, Hutton ML, Davies JK, Crack PJ, Hertzog PJ, Philpott DJ, Girardin SE, Whitchurch CB, Ferrero RL. 2010. Bacterial membrane vesicles deliver peptidoglycan to NOD1 in epithelial cells. Cell Microbiol 12:372-85.
45. Jin JS, Kwon SO, Moon DC, Gurung M, Lee JH, Kim SI, Lee JC. 2011. Acinetobacter baumannii secretes cytotoxic outer membrane protein A via outer membrane vesicles. PLoS One 6:e17027.
46. Schwechheimer C, Kuehn MJ. 2015. Outer-membrane vesicles from Gram-negative bacteria: biogenesis and functions. Nat Rev Microbiol 13:605-19.
47. Roier S, Zingl FG, Cakar F, Durakovic S, Kohl P, Eichmann TO, Klug L, Gadermaier B, Weinzerl K, Prassl R, Lass A, Daum G, Reidl J, Feldman MF, Schild S. 2016. A novel mechanism for the biogenesis of outer membrane vesicles in Gram-negative bacteria. Nat Commun 7:10515.
48. Roier S, Zingl FG, Cakar F, Schild S. 2016. Bacterial outer membrane vesicle biogenesis: a new mechanism and its implications. Microb Cell 3:257-259.
49. Brennan PJ. 2003. Structure, function, and biogenesis of the cell wall of Mycobacterium tuberculosis. Tuberculosis (Edinb) 83:91-7.
50. Prados-Rosales R, Weinrick BC, Pique DG, Jacobs WR, Jr., Casadevall A, Rodriguez GM. 2014. Role for Mycobacterium tuberculosis membrane vesicles in iron acquisition. J Bacteriol 196:1250-6.
51. Prados-Rosales R, Baena A, Martinez LR, Luque-Garcia J, Kalscheuer R, Veeraraghavan U, Camara C, Nosanchuk JD, Besra GS, Chen B, Jimenez J, Glatman-Freedman A, Jacobs WR, Jr., Porcelli SA, Casadevall A. 2011. Mycobacteria release active membrane vesicles that modulate immune responses in a TLR2-dependent manner in mice. J Clin Invest 121:1471-83.
52. Athman JJ, Sande OJ, Groft SG, Reba SM, Nagy N, Wearsch PA, Richardson ET, Rojas R, Boom WH, Shukla S, Harding CV. 2017. Mycobacterium tuberculosis Membrane Vesicles Inhibit T Cell Activation. J Immunol 198:2028-2037.
53. Klimentova J, Stulik J. 2015. Methods of isolation and purification of outer membrane vesicles from gram-negative bacteria. Microbiol Res 170:1-9.
54. Wagner D, Maser J, Lai B, Cai Z, Barry CE, 3rd, Honer Zu Bentrup K, Russell DG, Bermudez LE. 2005. Elemental analysis of Mycobacterium avium-, Mycobacterium tuberculosis-, and Mycobacterium smegmatis-containing phagosomes indicates pathogen-induced microenvironments within the host cell's endosomal system. J Immunol 174:1491-500.
55. Chinison JJ, Danelishvili L, Gupta R, Rose SJ, Babrak LM, Bermudez LE. 2016. Identification of Mycobacterium avium subsp. hominissuis secreted proteins using an in vitro system mimicking the phagosomal environment. BMC Microbiol 16:270.
56. Prados-Rosales R, Brown L, Casadevall A, Montalvo-Quiros S, Luque-Garcia JL. 2014. Isolation and identification of membrane vesicle-associated proteins in Gram-positive bacteria and mycobacteria. MethodsX 1:124-9.
57. Bitto NJ, Chapman R, Pidot S, Costin A, Lo C, Choi J, D'Cruze T, Reynolds EC, Dashper SG, Turnbull L, Whitchurch CB, Stinear TP, Stacey KJ, Ferrero RL. 2017. Bacterial membrane vesicles transport their DNA cargo into host cells. Sci Rep 7:7072.
58. van Soolingen D, de Haas PE, Hermans PW, van Embden JD. 1994. DNA fingerprinting of Mycobacterium tuberculosis. Methods Enzymol 235:196-205.
59. McGarvey JA, Bermudez LE. 2001. Phenotypic and genomic analyses of the Mycobacterium avium complex reveal differences in gastrointestinal invasion and genomic composition. Infect Immun 69:7242-9.

60. Nicholas A, Jeon H, Selasi GN, Na SH, Kwon HI, Kim YJ, Choi CW, Kim SI, Lee JC. 2017. Clostridium difficile-derived membrane vesicles induce the expression of pro-inflammatory cytokine genes and cytotoxicity in colonic epithelial cells in vitro. Microb Pathog 107:6-11.
61. Surve MV, Anil A, Kamath KG, Bhutda S, Sthanam LK, Pradhan A, Srivastava R, Basu B, Dutta S, Sen S, Modi D, Banerjee A. 2016. Membrane Vesicles of Group B Streptococcus Disrupt Feto-Maternal Barrier Leading to Preterm Birth. PLoS Pathog 12:e1005816.
62. Resch U, Tsatsaronis JA, Le Rhun A, Stubiger G, Rohde M, Kasvandik S, Holzmeister S, Tinnefeld P, Wai SN, Charpentier E. 2016. A Two-Component Regulatory System Impacts Extracellular Membrane-Derived Vesicle Production in Group A Streptococcus. MBio 7.
63. Lee EY, Choi DY, Kim DK, Kim JW, Park JO, Kim S, Kim SH, Desiderio DM, Kim YK, Kim KP, Gho YS. 2009. Gram-positive bacteria produce membrane vesicles: proteomics-based characterization of Staphylococcus aureus-derived membrane vesicles. Proteomics 9:5425-36.
64. Schnappinger D, Ehrt S, Voskuil MI, Liu Y, Mangan JA, Monahan IM, Dolganov G, Efron B, Butcher PD, Nathan C, Schoolnik GK. 2003. Transcriptional Adaptation of Mycobacterium tuberculosis within Macrophages: Insights into the Phagosomal Environment. J Exp Med 198:693-704.
65. Wirth T, Hildebrand F, Allix-Beguec C, Wolbeling F, Kubica T, Kremer K, van Soolingen D, Rusch-Gerdes S, Locht C, Brisse S, Meyer A, Supply P, Niemann S. 2008. Origin, spread and demography of the Mycobacterium tuberculosis complex. PLoS Pathog 4:e1000160.
66. Fennelly KP, Martyny JW, Fulton KE, Orme IM, Cave DM, Heifets LB. 2004. Cough-generated aerosols of Mycobacterium tuberculosis: a new method to study infectiousness. Am J Respir Crit Care Med 169:604-9.
67. Kim JH, Lee J, Park J, Gho YS. 2015. Gram-negative and Gram-positive bacterial extracellular vesicles. Semin Cell Dev Biol 40:97-104.
68. Wei J, Dahl JL, Moulder JW, Roberts EA, O'Gaora P, Young DB, Friedman RL. 2000. Identification of a Mycobacterium tuberculosis gene that enhances mycobacterial survival in macrophages. J Bacteriol 182:377-84.
69. Shin DM, Jeon BY, Lee HM, Jin HS, Yuk JM, Song CH, Lee SH, Lee ZW, Cho SN, Kim JM, Friedman RL, Jo EK. 2010. Mycobacterium tuberculosis eis regulates autophagy, inflammation, and cell death through redox-dependent signaling. PLoS Pathog 6:e1001230.
70. Dahl JL, Wei J, Moulder JW, Laal S, Friedman RL. 2001. Subcellular localization of the Iitracellular survival-enhancing Eis protein of Mycobacterium tuberculosis. Infect Immun 69:4295-302.
71. Samuel LP, Song CH, Wei J, Roberts EA, Dahl JL, Barry CE, 3rd, Jo EK, Friedman RL. 2007. Expression, production and release of the Eis protein by Mycobacterium tuberculosis during infection of macrophages and its effect on cytokine secretion. Microbiology 153:529-40.
72. Lella RK, Sharma C. 2007. Eis (enhanced intracellular survival) protein of Mycobacterium tuberculosis disturbs the cross regulation of T-cells. J Biol Chem 282:18671-5.
73. Kalscheuer R, Weinrick B, Veeraraghavan U, Besra GS, Jacobs WR, Jr. 2010. Trehalose-recycling ABC transporter LpqY-SugA-SugB-SugC is essential for virulence of Mycobacterium tuberculosis. Proc Natl Acad Sci U S A 107:21761-6.
74. Tournu H, Fiori A, Van Dijck P. 2013. Relevance of trehalose in pathogenicity: some general rules, yet many exceptions. PLoS Pathog 9:e1003447.
75. Ishikawa E, Ishikawa T, Morita YS, Toyonaga K, Yamada H, Takeuchi O, Kinoshita T, Akira S, Yoshikai Y, Yamasaki S. 2009. Direct recognition of the mycobacterial glycolipid, trehalose dimycolate, by C-type lectin Mincle. J Exp Med 206:2879-88.
76. Estorninho M, Smith H, Thole J, Harders-Westerveen J, Kierzek A, Butler RE, Neyrolles O, Stewart GR. 2010. ClgR regulation of chaperone and protease systems is essential for Mycobacterium tuberculosis parasitism of the macrophage. Microbiology 156:3445-55.
77. Stewart GR, Wernisch L, Stabler R, Mangan JA, Hinds J, Laing KG, Young DB, Butcher PD. 2002. Dissection of the heat-shock response in Mycobacterium tuberculosis using mutants and microarrays. Microbiology 148:3129-38.
78. Lewthwaite JC, Coates AR, Tormay P, Singh M, Mascagni P, Poole S, Roberts M, Sharp L, Henderson B. 2001. Mycobacterium tuberculosis chaperonin 60.1 is a more potent cytokine

stimulator than chaperonin 60.2 (Hsp 65) and contains a CD14-binding domain. Infect Immun 69:7349-55.
79. Fang FC. 2004. Antimicrobial reactive oxygen and nitrogen species: concepts and controversies. Nat Rev Microbiol 2:820-32.
80. Piddington DL, Fang FC, Laessig T, Cooper AM, Orme IM, Buchmeier NA. 2001. Cu,Zn superoxide dismutase of Mycobacterium tuberculosis contributes to survival in activated macrophages that are generating an oxidative burst. Infect Immun 69:4980-7.
81. Harth G, Horwitz MA. 1999. Export of recombinant Mycobacterium tuberculosis superoxide dismutase is dependent upon both information in the protein and mycobacterial export machinery. A model for studying export of leaderless proteins by pathogenic mycobacteria. J Biol Chem 274:4281-92.
82. Braunstein M, Espinosa BJ, Chan J, Belisle JT, Jacobs WR, Jr. 2003. SecA2 functions in the secretion of superoxide dismutase A and in the virulence of Mycobacterium tuberculosis. Mol Microbiol 48:453-64.
83. Pym AS, Saint-Joanis B, Cole ST. 2002. Effect of katG mutations on the virulence of Mycobacterium tuberculosis and the implication for transmission in humans. Infect Immun 70:4955-60.
84. Master SS, Springer B, Sander P, Boettger EC, Deretic V, Timmins GS. 2002. Oxidative stress response genes in Mycobacterium tuberculosis: role of ahpC in resistance to peroxynitrite and stage-specific survival in macrophages. Microbiology 148:3139-44.
85. Lappann M, Danhof S, Guenther F, Olivares-Florez S, Mordhorst IL, Vogel U. 2013. In vitro resistance mechanisms of Neisseria meningitidis against neutrophil extracellular traps. Mol Microbiol 89:433-49.
86. Deknuydt F, Nordstrom T, Riesbeck K. 2014. Diversion of the host humoral response: a novel virulence mechanism of Haemophilus influenzae mediated via outer membrane vesicles. J Leukoc Biol 95:983-91.
87. Pathirana RD, Kaparakis-Liaskos M. 2016. Bacterial membrane vesicles: Biogenesis, immune regulation and pathogenesis. Cell Microbiol 18:1518-1524.
88. Sampson SL. 2011. Mycobacterial PE/PPE proteins at the host-pathogen interface. Clin Dev Immunol 2011:497203.
89. Abdallah AM, Verboom T, Weerdenburg EM, Gey van Pittius NC, Mahasha PW, Jimenez C, Parra M, Cadieux N, Brennan MJ, Appelmelk BJ, Bitter W. 2009. PPE and PE_PGRS proteins of Mycobacterium marinum are transported via the type VII secretion system ESX-5. Mol Microbiol 73:329-40.
90. Balaji KN, Goyal G, Narayana Y, Srinivas M, Chaturvedi R, Mohammad S. 2007. Apoptosis triggered by Rv1818c, a PE family gene from Mycobacterium tuberculosis is regulated by mitochondrial intermediates in T cells. Microbes Infect 9:271-81.
91. Fishbein S, van Wyk N, Warren RM, Sampson SL. 2015. Phylogeny to function: PE/PPE protein evolution and impact on Mycobacterium tuberculosis pathogenicity. Mol Microbiol 96:901-16.
92. Delogu G, Brennan MJ, Manganelli R. 2017. PE and PPE Genes: A Tale of Conservation and Diversity. Adv Exp Med Biol 1019:191-207.
93. Singh P, Rao RN, Reddy JR, Prasad RB, Kotturu SK, Ghosh S, Mukhopadhyay S. 2016. PE11, a PE/PPE family protein of Mycobacterium tuberculosis is involved in cell wall remodeling and virulence. Sci Rep 6:21624.
94. Nguyen MT, Gotz F. 2016. Lipoproteins of Gram-Positive Bacteria: Key Players in the Immune Response and Virulence. Microbiol Mol Biol Rev 80:891-903.
95. Becker K, Sander P. 2016. Mycobacterium tuberculosis lipoproteins in virulence and immunity - fighting with a double-edged sword. FEBS Lett 590:3800-3819.
96. Gaur RL, Ren K, Blumenthal A, Bhamidi S, Gonzalez-Nilo FD, Jackson M, Zare RN, Ehrt S, Ernst JD, Banaei N. 2014. LprG-mediated surface expression of lipoarabinomannan is essential for virulence of Mycobacterium tuberculosis. PLoS Pathog 10:e1004376.
97. Fisher MA, Plikaytis BB, Shinnick TM. 2002. Microarray analysis of the Mycobacterium tuberculosis transcriptional response to the acidic conditions found in phagosomes. J Bacteriol 184:4025-32.

98. Thirunavukkarasu S, Plain KM, de Silva K, Begg D, Whittington RJ, Purdie AC. 2014. Expression of genes associated with cholesterol and lipid metabolism identified as a novel pathway in the early pathogenesis of Mycobacterium avium subspecies paratuberculosis-infection in cattle. Vet Immunol Immunopathol 160:147-57.
99. Honer Zu Bentrup K, Miczak A, Swenson DL, Russell DG. 1999. Characterization of activity and expression of isocitrate lyase in Mycobacterium avium and Mycobacterium tuberculosis. J Bacteriol 181:7161-7.
100. McKinney JD, Honer zu Bentrup K, Munoz-Elias EJ, Miczak A, Chen B, Chan WT, Swenson D, Sacchettini JC, Jacobs WR, Jr., Russell DG. 2000. Persistence of Mycobacterium tuberculosis in macrophages and mice requires the glyoxylate shunt enzyme isocitrate lyase. Nature 406:735-8.
101. Munoz-Elias EJ, McKinney JD. 2005. Mycobacterium tuberculosis isocitrate lyases 1 and 2 are jointly required for in vivo growth and virulence. Nat Med 11:638-44.
102. Eisenreich W, Dandekar T, Heesemann J, Goebel W. 2010. Carbon metabolism of intracellular bacterial pathogens and possible links to virulence. Nat Rev Microbiol 8:401-12.
103. Zhang J, Wang J, Ng S, Lin Q, Shen HM. 2014. Development of a novel method for quantification of autophagic protein degradation by AHA labeling. Autophagy 10:901-12.
104. Grammel M, Zhang MM, Hang HC. 2010. Orthogonal alkynyl amino acid reporter for selective labeling of bacterial proteomes during infection. Angew Chem Int Ed Engl 49:5970-4.
105. Beatty KE, Xie F, Wang Q, Tirrell DA. 2005. Selective dye-labeling of newly synthesized proteins in bacterial cells. J Am Chem Soc 127:14150-1.
106. Mahdavi A, Szychowski J, Ngo JT, Sweredoski MJ, Graham RL, Hess S, Schneewind O, Mazmanian SK, Tirrell DA. 2014. Identification of secreted bacterial proteins by noncanonical amino acid tagging. Proc Natl Acad Sci U S A 111:433-8.
107. Wier GM, McGreevy EM, Brown MJ, Boyle JP. 2015. New method for the orthogonal labeling and purification of Toxoplasma gondii proteins while inside the host cell. MBio 6:e01628.
108. Tullius MV, Harth G, Horwitz MA. 2003. Glutamine synthetase GlnA1 is essential for growth of Mycobacterium tuberculosis in human THP-1 macrophages and guinea pigs. Infect Immun 71:3927-36.
109. Harth G, Clemens DL, Horwitz MA. 1994. Glutamine synthetase of Mycobacterium tuberculosis: extracellular release and characterization of its enzymatic activity. Proc Natl Acad Sci U S A 91:9342-6.
110. Alvarez ME, McCarthy CM. 1984. Glutamine synthetase from Mycobacterium avium. Can J Microbiol 30:353-9.
111. Chandra H, Basir SF, Gupta M, Banerjee N. 2010. Glutamine synthetase encoded by glnA-1 is necessary for cell wall resistance and pathogenicity of Mycobacterium bovis. Microbiology 156:3669-77.
112. Harth G, Horwitz MA. 2003. Inhibition of Mycobacterium tuberculosis glutamine synthetase as a novel antibiotic strategy against tuberculosis: demonstration of efficacy in vivo. Infect Immun 71:456-64.
113. Jakubovics NS, Smith AW, Jenkinson HF. 2000. Expression of the virulence-related Sca (Mn2+) permease in Streptococcus gordonii is regulated by a diphtheria toxin metallorepressor-like protein ScaR. Mol Microbiol 38:140-53.
114. Dintilhac A, Alloing G, Granadel C, Claverys JP. 1997. Competence and virulence of Streptococcus pneumoniae: Adc and PsaA mutants exhibit a requirement for Zn and Mn resulting from inactivation of putative ABC metal permeases. Mol Microbiol 25:727-39.
115. Ramanan N, Wang Y. 2000. A high-affinity iron permease essential for Candida albicans virulence. Science 288:1062-4.
116. Tsuchiya S, Yamabe M, Yamaguchi Y, Kobayashi Y, Konno T, Tada K. 1980. Establishment and characterization of a human acute monocytic leukemia cell line (THP-1). Int J Cancer 26:171-6.
117. Giri PK, Kruh NA, Dobos KM, Schorey JS. 2010. Proteomic analysis identifies highly antigenic proteins in exosomes from M. tuberculosis-infected and culture filtrate protein-treated macrophages. Proteomics 10:3190-202.

118. Rompikuntal PK, Thay B, Khan MK, Alanko J, Penttinen AM, Asikainen S, Wai SN, Oscarsson J. 2012. Perinuclear localization of internalized outer membrane vesicles carrying active cytolethal distending toxin from Aggregatibacter actinomycetemcomitans. Infect Immun 80:31-42.
119. Barry CE, 3rd. 2001. Interpreting cell wall 'virulence factors' of Mycobacterium tuberculosis. Trends Microbiol 9:237-41.
120. Renelli M, Matias V, Lo RY, Beveridge TJ. 2004. DNA-containing membrane vesicles of Pseudomonas aeruginosa PAO1 and their genetic transformation potential. Microbiology 150:2161-9.
121. Dorward DW, Garon CF, Judd RC. 1989. Export and intercellular transfer of DNA via membrane blebs of Neisseria gonorrhoeae. J Bacteriol 171:2499-505.
122. Dorward DW, Garon CF. 1990. DNA Is Packaged within Membrane-Derived Vesicles of Gram-Negative but Not Gram-Positive Bacteria. Appl Environ Microbiol 56:1960-2.
123. von Reyn CF, Waddell RD, Eaton T, Arbeit RD, Maslow JN, Barber TW, Brindle RJ, Gilks CF, Lumio J, Lahdevirta J, et al. 1993. Isolation of Mycobacterium avium complex from water in the United States, Finland, Zaire, and Kenya. J Clin Microbiol 31:3227-30.
124. Catherinot E, Roux AL, Vibet MA, Bellis G, Ravilly S, Lemonnier L, Le Roux E, Bernede-Bauduin C, Le Bourgeois M, Herrmann JL, Guillemot D, Gaillard JL, group OMA. 2013. Mycobacterium avium and Mycobacterium abscessus complex target distinct cystic fibrosis patient subpopulations. J Cyst Fibros 12:74-80.
125. Turnbull L, Toyofuku M, Hynen AL, Kurosawa M, Pessi G, Petty NK, Osvath SR, Carcamo-Oyarce G, Gloag ES, Shimoni R, Omasits U, Ito S, Yap X, Monahan LG, Cavaliere R, Ahrens CH, Charles IG, Nomura N, Eberl L, Whitchurch CB. 2016. Explosive cell lysis as a mechanism for the biogenesis of bacterial membrane vesicles and biofilms. Nat Commun 7:11220.
126. Parsek MR, Greenberg EP. 2005. Sociomicrobiology: the connections between quorum sensing and biofilms. Trends Microbiol 13:27-33.
127. Polkade AV, Mantri SS, Patwekar UJ, Jangid K. 2016. Quorum Sensing: An Under-Explored Phenomenon in the Phylum Actinobacteria. Front Microbiol 7:131.
128. Hornung V, Latz E. 2010. Intracellular DNA recognition. Nat Rev Immunol 10:123-30.
129. Watson RO, Bell SL, MacDuff DA, Kimmey JM, Diner EJ, Olivas J, Vance RE, Stallings CL, Virgin HW, Cox JS. 2015. The Cytosolic Sensor cGAS Detects Mycobacterium tuberculosis DNA to Induce Type I Interferons and Activate Autophagy. Cell Host Microbe 17:811-819.
130. Manzanillo PS, Shiloh MU, Portnoy DA, Cox JS. 2012. Mycobacterium tuberculosis activates the DNA-dependent cytosolic surveillance pathway within macrophages. Cell Host Microbe 11:469-80.
131. Saiga H, Kitada S, Shimada Y, Kamiyama N, Okuyama M, Makino M, Yamamoto M, Takeda K. 2012. Critical role of AIM2 in Mycobacterium tuberculosis infection. Int Immunol 24:637-44.
132. Alves NJ, Turner KB, Medintz IL, Walper SA. 2016. Protecting enzymatic function through directed packaging into bacterial outer membrane vesicles. Sci Rep 6:24866.
133. Gorgojo J, Harvill ET, Rodriguez ME. 2014. Bordetella parapertussis survives inside human macrophages in lipid raft-enriched phagosomes. Infect Immun 82:5175-84.
134. Deatherage BL, Cookson BT. 2012. Membrane vesicle release in bacteria, eukaryotes, and archaea: a conserved yet underappreciated aspect of microbial life. Infect Immun 80:1948-57.
135. Donohue MJ. 2018. Increasing nontuberculous mycobacteria reporting rates and species diversity identified in clinical laboratory reports. BMC Infect Dis 18:163.

Chapter 1

Supplementary Information

Proteomics of exosomes of infected THP1 human macrophages

Exosomes were collected during 2 time-points of 24h and 72h post infection and the cargo proteins were analyzed using mass spectrometry, as described in the methods. However, only host (human) proteins were detected and no MAH104 proteins were detected (data not shown). List of host proteins found within exosomes of 24h and 72h post MAH104 infection and uninfected controls is given in supplementary table S2 & S3 respectively. Heat map of gene ontology biological process terms for uniquely synthesized proteins during MAH104 infection and exported in exosomes during 24h and 72h post MAH104 infection by THP1 human macrophages is shown in supplementary fig S2 &S3. Similarly, Venn diagrams showing unique and common proteins between exosomes of 24h and 72h post MAH104 infected THP1 macrophages and uninfected controls are also given in supplementary figure S4 & S5 respectively.

Table S1: MAH104 proteins found in the MVs, released in response to 2-week Metal mix exposure

Accession	Description	MW [kDa]	# Peptides
A0A0H2ZZ02	Fatty acid synthase	327.953	51
A0QL48	DNA-directed RNA polymerase subunit beta	146.936	30
A0QL35	Elongation factor Tu	43.744	20
A0A0H2ZZY3	Linear gramicidin synthetase subunit D	366.21	23
A0A0H2ZYX8	Acetyl-/propionyl-coenzyme A carboxylase alpha chain	62.376	16
A0QKR2	60 kDa chaperonin 1	55.763	14
A0QLP6	60 kDa chaperonin 2	56.58	18
A0QIW5	Polyribonucleotide nucleotidyltransferase	79.549	15
A0A0H2ZSP8	Glyceraldehyde-3-phosphate dehydrogenase	36.073	11
A0A0H2ZZP6	Glycerol kinase	55.077	13
A0QL49	DNA-directed RNA polymerase subunit beta	129.679	22
A0A0H3A1B6	Wag31 protein	26.99	10
A0QGA4	Catalase-peroxidase	81.611	13
A0A0H3A2U5	Aconitate hydratase 1	101.051	14
A0QL36	Elongation factor G	77.184	14
A0QKU5	DNA-directed RNA polymerase subunit alpha	37.682	9
A0A0H2ZZD1	Putative acyl-CoA dehydrogenase	64.545	11
A0QCI6	Malate dehydrogenase	34.583	9
A0A0H3A1M4	Acetyl-CoA carboxylase carboxyltransferase	56.721	12
A0A0H2ZT47	DNA gyrase subunit A	92.284	12
A0A0H2ZTC2	Propionyl-CoA carboxylase beta chain	59.044	6
A0A0H2ZRC1	Adenosylhomocysteinase	54.46	10
A0A0H3A0Y7	3-oxoacyl-[acyl-carrier-protein] synthase 1	42.401	9
A0A0H2ZYD4	MoxR protein	40.705	10
A0A0H3A1U9	Carbamoyl-phosphate synthase L chain, ATP binding domain	70.45	12
A0QCX8	ATP synthase subunit beta	53.064	12
A0QBI3	Putative phosphoserine aminotransferase	39.702	8
A0QC23	Serine hydroxymethyltransferase	44.927	11
A0A0H2ZTV9	Erythronolide synthase, modules 3 and 4	434.377	12
A0A0H3A236	Negative regulator of genetic competence ClpC/mecB	90.716	13
A0A0H2ZV88	D-3-phosphoglycerate dehydrogenase	54.461	10
A0A0H2ZVK4	Phosphoenolpyruvate carboxykinase [GTP]	67.574	10
A0A0H2ZZY4	Major membrane protein 1	33.651	7
A0QHH8	Phosphoribosyl isomerase A	25.346	9
A0A0H2ZUE2	Cysteine desulfurase	69.893	10
A0QLV0	F420-dependent glucose-6-phosphate dehydrogenase	37.331	10
A0A0H3A0U3	Propionyl-CoA carboxylase beta chain	57.306	8
A0A0H2ZTY5	Linear gramicidin synthetase subunit D	1113.385	14

A0A0H3A1C3	Glycerol-3-phosphate dehydrogenase	63.034	10
A0QKU6	30S ribosomal protein S4	23.48	9
A0A0H2ZZC7	Polyketide synthase	192.863	11
A0A0H2ZUC5	DNA gyrase subunit B	74.485	7
A0A0H2ZWD4	Fatty acid desaturase	31.484	7
A0QGK3	Probable phosphoketolase	89.322	8
A0A0H2ZSV5	Enoyl-[acyl-carrier-protein] reductase [NADH]	28.679	4
A0A0H2ZVS4	Putative acyl-CoA dehydrogenase	76.024	7
A0A0H2ZT90	Isocitrate dehydrogenase, NADP-dependent	83.086	6
A0A0H2ZXW9	3-oxoacyl-[acyl-carrier-protein] synthase 2	42.863	4
A0QLK3	2,3-bisphosphoglycerate-dependent phosphoglycerate mutase	27.143	5
A0QI75	Alanine--tRNA ligase	96.875	5
A0A0H2ZZ95	Hydrolase, peptidase M42 family protein	44.301	8
A0A0H3A2P2	Oxidoreductase, short chain dehydrogenase/reductase family protein	47.243	7
A0A0H2ZYT8	Isocitrate lyase	85.19	7
A0QHY4	Phosphoglycerate kinase	42.411	6
A0A0H2ZW23	Aspartate transaminase	46.538	6
A0A0H2ZX40	Ribonucleoside-diphosphate reductase	80.349	9
A0A0H2ZS36	Methyltransferase type 11	26.295	7
A0A0H2ZWB5	Glycoside hydrolase	76.659	5
A0A0H2ZRT1	NAD-glutamate dehydrogenase	178.746	11
A0A0H2ZY16	30S ribosomal protein S1	52.989	7
A0A0H2ZS48	Thiamine pyrophosphate enzyme	59.551	5
A0A0H2ZS23	Acyl carrier protein	12.477	4
A0A0H2ZWE8	Acetyl-CoA acetyltransferase	40.494	5
A0A0H2ZZV9	Succinate dehydrogenase	70.481	5
A0A0H2ZYG8	Aspartate aminotransferase	45.621	6
D5JGI7	Laminin-binding histone-like protein	21.923	4
A0QJB3	Polyphosphate kinase	81.966	7
A0A0H2ZV13	Glutamine-dependent NAD(+) synthetase	75.457	6
A0A0H2ZUZ8	Putative oxidoreductase YdbC	31.579	6
A0A0H3A275	Acyl-CoA dehydrogenase domain protein	42.58	6
A0A0H2ZTD3	O-methyltransferase	22.988	6
A0A0H3A362	Universal stress protein family protein	30.583	5
A0A0H2ZRE0	Putative acyl-CoA dehydrogenase	66.52	6
A0A0H2ZTD7	NADH-quinone oxidoreductase	83.977	7
A0A0H3A172	Fatty acid desaturase	39.199	9
A0QEJ0	Chaperone protein HtpG	72.795	8
A0A0H3A293	Cysteine desulfurase family protein	41.656	6
A0A0H2ZQN4	ATP-dependent Clp protease proteolytic subunit	23.277	3
A0A0H2ZYK8	Cysteine synthase	32.326	8
A0QBX4	Enolase	44.846	6
A0A0H3A1A9	Dihydrolipoyl dehydrogenase	49.504	7

A0QJC6	Ketol-acid reductoisomerase (NADP(+))	35.991	6
A0A0H3A3T5	Cyclopropane-fatty-acyl-phospholipid synthase 1	34.315	5
A0QI26	S-adenosylmethionine synthase	43.279	6
A0A0H3A179	Lysine--tRNA ligase	55.12	5
A0A0H2ZX04	Methylmalonate-semialdehyde dehydrogenase	54.049	6
A0QGN2	Glycine dehydrogenase (decarboxylating)	99.898	7
A0A0H3A2N1	Acetyl-coenzyme A synthetase	71.398	6
A0A0H2ZS53	L-carnitine dehydratase/bile acid-inducible protein F	42.946	5
A0A0H2ZXF9	Non-homologous end joining protein Ku	34.021	7
A0A0H2ZU32	Branched-chain-amino-acid aminotransferase	40.005	5
A0QHA8	Argininosuccinate synthase	43.753	3
A0A0H2ZRQ6	Dehydrogenase	36.467	3
A0A0H2ZXU2	Alcohol dehydrogenase B	39.776	4
A0QMB9	Succinate-semialdehyde dehydrogenase [NADP(+)]	49.978	6
A0A0H3A456	Fatty acid desaturase	38.983	6
A0A0H2ZZG1	Inosine-5'-monophosphate dehydrogenase	54.727	6
A0A0H2ZYT9	Uncharacterized protein	33.352	3
A0A0H2ZZ49	35kd antigen	29.442	5
A0A0H2ZZV2	Aldo/keto reductase	35.09	3
A0A0H2ZYI7	Oxidoreductase, short chain dehydrogenase/reductase family protein	29.746	4
A0A0H2ZT78	Acetyl-CoA acetyltransferase	42.718	7
A0A0H3A258	Asparagine synthase (Glutamine-hydrolyzing)	63.198	4
A0A0H2ZVK0	Peroxisomal multifunctional enzyme type 2	29.887	4
A0A0H2ZX18	ABC-transporter protein, ATP binding component	61.981	6
A0A0H2ZXS5	3-Hydroxyacyl-CoA dehydrogenase	26.396	5
A0QCX7	ATP synthase gamma chain	33.556	3
A0A0H2ZV52	Anti-anti-sigma factor	33.006	4
A0QFB2	Proteasome-associated ATPase	67.534	5
A0A0H3A1F1	2-hydroxy-6-oxo-6-phenylhexa-2,4-dienoate hydrolase	32.07	4
A0A0H3A378	General stress protein 69	35.513	5
A0A0H3A1F5	Phosphoribosylformylglycinamidine synthase subunit PurQ	23.669	4
A0Q999	Serine--tRNA ligase	45.727	3
A0A0H3A0Z0	Adenylosuccinate lyase	51.12	4
A0A0H2ZYE5	Transcriptional regulator, Crp/Fnr family protein	24.78	6
A0A0H3A2Q9	Putative acyl-CoA dehydrogenase	41.349	6
A0A0H3A2C4	Uncharacterized protein	94.413	6
A0A0H2ZUT1	RifB protein	220.279	6
A0A0H3A0J9	RNA polymerase sigma factor SigA	54.15	4
A0A0H2ZV07	Uncharacterized protein	20.903	4
A0QGM8	Malate synthase G	80.28	6
A0A0H2ZSP0	Methoxy mycolic acid synthase 1	33.019	4
A0A0H2ZUY6	2-isopropylmalate synthase	65.633	3
A0A0H2ZVV6	Glutamine synthetase	53.651	5

A0A0H2ZWY7	Transcription termination factor Rho	64.416	5
A0A0H3A2U4	3-hydroxybutyryl-CoA dehydrogenase	31.816	3
A0A0H2ZS43	IMP dehydrogenase family protein	39.51	3
A0QJC2	3-isopropylmalate dehydrogenase	35.625	4
A0QBP0	Succinate--CoA ligase [ADP-forming] subunit beta	40.942	5
A0A0H3A0J8	Glutamate decarboxylase	50.958	4
A0A0H2ZV74	Aldehyde dehydrogenase	51.37	4
A0A0H2ZQK2	Enoyl-CoA hydratase	25.935	4
A0A0H2ZWT4	Uncharacterized protein	46.107	4
A0A0H2ZSN9	Ribonuclease J	59.591	4
A0A0H2ZYT7	Alpha-glucan phosphorylase	95.974	5
A0A0H2ZQJ7	Ribosome-binding ATPase YchF	37.672	4
A0A0H3A439	Bifunctional purine biosynthesis protein PurH	56.528	5
A0A0H3A4W6	LprG protein	24.405	3
A0A0H2ZV42	Malonyl CoA-acyl carrier protein transacylase	30.616	4
A0QHC1	50S ribosomal protein L20	14.65	2
A0QAK7	Trehalose-6-phosphate synthase	55.168	3
A0QL15	50S ribosomal protein L2	30.418	3
A0A0H2ZWB2	Eptc-inducible aldehyde dehydrogenase	54.731	4
A0A0H2ZW06	Sulfate adenylyltransferase	47.155	3
A0A0H2ZWW6	Uncharacterized protein	32.763	3
A0A0H2ZSU0	N5-carboxyaminoimidazole ribonucleotide synthase	42.686	4
A0A0H2ZWV4	Homoserine dehydrogenase	45.642	4
A0A0H2ZT32	3-oxoacyl-[acyl-carrier-protein] synthase 2	44.044	3
A0A0H3A4Z6	Putative acyl-CoA dehydrogenase	76.514	2
A0QBT9	Arginine deiminase	43.214	5
A0QMH2	Dihydroxy-acid dehydratase	59.538	3
A0QGP2	Protein translocase subunit SecA	84.965	3
A0A0H2ZQW5	Dibenzothiophene desulfurization enzyme A	49.426	3
A0A0H2ZYK6	Acyl-CoA synthase	63.823	4
A0A0H3A036	Aspartate-semialdehyde dehydrogenase	36.185	3
A0A0H3A5E8	Putative acyl-CoA dehydrogenase	48.063	4
A0QCX5	ATP synthase subunit b-delta	48.45	4
A0A0H2ZWB0	Dihydrolipoamide acetyltransferase component of pyruvate dehydrogenase complex	61.732	4
A0A0H3A0S9	Pyruvate synthase	69.347	3
A0QLW6	Adenylosuccinate synthetase	46.776	3
A0A0H2ZRA2	Nitroreductase family protein	23.968	3
A0QCX6	ATP synthase subunit alpha	59.956	4
A0A0H2ZR92	Glucose-6-phosphate 1-dehydrogenase	54.413	3
A0A0H2ZX05	Uncharacterized protein	34.633	2
A0A0H2ZWZ6	Tyrosine--tRNA ligase	46.228	4
A0A0H2ZU78	Probable M18 family aminopeptidase 2	46.039	3
A0QIC8	Pyridoxal 5'-phosphate synthase subunit PdxS	31.943	3

A0A0H2ZT26	Linear gramicidin synthetase subunit B	273.203	4
A0A0H2ZRJ2	Ferredoxin-dependent glutamate synthase 1	166.4	4
A0QAB5	Cysteine--tRNA ligase	51.87	4
A0QFB7	Pup--protein ligase	51.267	3
A0QJ99	Uncharacterized oxidoreductase MAV_3816	30.321	5
A0A0H2ZV46	Uncharacterized protein	35.788	2
A0QLG2	Glutamate-1-semialdehyde 2,1-aminomutase	45.443	3
A0A0H3A2I9	Alkylhydroperoxide reductase	21.642	2
A0A0H2ZZ17	Cyclopropane-fatty-acyl-phospholipid synthase 2	34.172	3
A0A0H3A0A9	Short chain dehydrogenase	29.788	2
A0A0H2ZSE9	29 kDa antigen Cfp29	28.601	3
A0A0H2ZSV6	Uncharacterized protein	32.285	2
A0A0H3A0L0	Bacterioferritin	18.467	3
A0A0H2ZSC5	HAD-superfamily protein subfamily protein IB hydrolase	32.325	3
A0A0H3A2T7	Putative acyl-CoA dehydrogenase	49.481	4
A0A0H2ZWK2	NAD dependent epimerase/dehydratase family protein	37.538	4
A0A0H2ZYS1	Cyclopropane-fatty-acyl-phospholipid synthase 1	32.892	3
A0A0H2ZX69	Pyruvate decarboxylase	64.884	4
A0A0H2ZUZ7	Acyl-CoA synthase	69.304	4
A0A0H3A247	Methionine--tRNA ligase	58.637	3
A0A0H2ZYW5	OpcA protein	32.934	3
A0A0H2ZVT3	Retinol dehydrogenase 13	33.8	3
A0QF76	L-cysteine:1D-myo-inositol 2-amino-2-deoxy-alpha-D-glucopyranoside ligase	41.793	4
A0A0H2ZWA1	Alpha/beta hydrolase fold domain protein	39.477	3
A0A0H2ZYR0	Oxidoreductase	26.071	3
A0A0H2ZTN6	Acetyl-CoA acetyltransferase	42.584	2
A0A0H2ZRT9	Anthranilate synthase component 1	54.828	3
A0A0H3A0V1	Peptidase, M24 family protein	38.952	4
A0A0H2ZZU2	GMP synthase [glutamine-hydrolyzing]	54.317	4
A0A0H2ZUC3	Isoleucine--tRNA ligase	118.154	3
A0QL54	50S ribosomal protein L10	20.176	3
A0QHG8	Tryptophan synthase alpha chain	27.868	3
A0A0H3A1V0	3-hydroxyacyl-CoA dehydrogenase type-2	26.126	2
A0A0H2ZWN3	Monooxygenase	31.925	2
A0A0H2ZW42	Anthranilate phosphoribosyltransferase	42.018	3
A0A0H2ZW78	Short-chain dehydrogenase	27.899	3
A0A0H3A0M2	Glucose-6-phosphate 1-dehydrogenase	56.471	3
A0A0H2ZR47	Erythronolide synthase, modules 3 and 4	219.568	4
A0A0H3A3F8	Oxidoreductase, short chain dehydrogenase/reductase family protein	26.766	2
A0QL18	50S ribosomal protein L3	23.069	2
A0A0H2ZYW7	Fumarate reductase/succinate dehydrogenase flavoprotein	60.096	4
A0QL12	30S ribosomal protein S3	30.601	2
A0A0H2ZX09	Molybdopterin biosynthesis protein moeA	44.528	2

A0A0H2ZX62	Carbonic anhydrase	17.958	2
A0A0H3A158	Pigment production hydroxylase	43.188	3
A0A0H2ZTR9	UDP-galactopyranose mutase	45.947	4
A0A0H2ZYM4	30S ribosomal protein S2	30.135	4
A0A0H2ZVW4	Methionine synthase	137.811	3
A0QJD1	Aspartyl/glutamyl-tRNA(Asn/Gln) amidotransferase subunit B	54.503	3
A0QHI0	Imidazoleglycerol-phosphate dehydratase	22.57	2
A0A0H2ZXI8	3-dehydroquinate synthase	37.55	2
A0QL02	50S ribosomal protein L14	13.419	2
A0A0H3A039	Alpha oxoglutarate ferredoxin oxidoreductase, beta subunit	39.094	3
A0A0H3A0A3	Alanine dehydrogenase/pyridine nucleotide transhydrogenase	37.28	3
A0QH68	CTP synthase	63.103	3
A0A0H3A106	FMN-dependent monooxygenase	37.234	2
A0A0H2ZT43	NADH-quinone oxidoreductase subunit F	48.794	3
A0A0H2ZUN7	Diacylglycerol O-acyltransferase	52.259	3
A0A0H2ZZS6	Acyl-CoA thioesterase II	31.202	2
A0A0H3A005	Thioredoxin reductase	38.556	3
A0A0H2ZT73	DNA polymerase I	99.522	2
A0QI01	Putative sporulation transcription regulator WhiA	34.911	2
A0A0H2ZUJ9	Phosphotransferase enzyme family protein	38.378	2
A0A0H2ZW11	Phospho-2-dehydro-3-deoxyheptonate aldolase	50.6	3
A0QM57	Putative S-adenosyl-L-methionine-dependent methyltransferase MAV_4873	32.841	3
A0A0H2ZUI2	Succinyl-CoA:3-ketoacid-coenzyme A transferase 1	47.594	3
A0A0H2ZU16	Uncharacterized protein	30.302	2
A0A0H3A2G7	Probable enoyl-CoA hydratase	27.896	2
A0A0H2ZS95	3-oxoacyl-(Acyl-carrier-protein) reductase	26.635	2
A0A0H2ZYW6	Fructose-1,6-bisphosphatase	37.656	2
A0A0H2ZS17	Mcr protein	38.55	3
A0A0H2ZWJ8	Acyl-CoA oxidase	71.487	3
A0A0H2ZXP2	Putative acyl-CoA dehydrogenase	65.77	2
A0A0H3A078	Asparagine synthase (Glutamine-hydrolyzing)	71.413	3
A0A0H2ZXA6	Aminotransferase	39.26	2
A0A0H2ZQI0	Isocitrate lyase	46.988	2
A0A0H3A0K4	YceI like family protein	19.287	2
A0A0H3A4J9	Epoxide hydrolase	41.824	2
A0A0H3A494	ATPase family protein associated with various cellular activities (AAA)	34.944	2
A0A0H3A225	3-beta hydroxysteroid dehydrogenase/isomerase family protein	39.631	2
A0A0H3A4C4	Methyltransferase MtfC	29.998	2
A0A0H2ZZ08	Lactate 2-monooxygenase	41.143	3
A0A0H3A3J0	Universal stress protein family protein	31.256	2
A0A0H2ZYL6	Putative molybdenum cofactor synthesis protein	16.654	3
A0A0H2ZUB1	Acetyl-CoA acetyltransferase	40.898	2
A0A0H2ZZ86	Uncharacterized protein	30.681	2

A0A0H3A4P5	ABC1 family protein	48.813	2
A0A0H2ZSD8	PPE family protein	38.582	2
A0A0H3A2R8	Signal recognition particle protein	54.28	3
A0A0H2ZRH9	DNA polymerase III subunit gamma/tau	65.432	2
A0A0H2ZZG6	Carbamoyl-phosphate synthase small chain	39.678	2
A0QJB6	3-isopropylmalate dehydratase small subunit	21.89	2
A0A0H2ZYJ4	Uncharacterized protein	36.758	2
A0A0H3A2U7	Putative flavin-containing monoamine oxidase AofH	47.935	2
A0A0H2ZZB0	Catalase	80.004	2
A0QL19	30S ribosomal protein S10	11.424	2
A0A0H3A425	Dienelactone hydrolase family protein	21.835	3
A0QKU8	30S ribosomal protein S13	14.3	3
A0QHA7	Argininosuccinate lyase	49.709	2
A0QKR3	10 kDa chaperonin	10.742	2
A0A0H3A0N4	Gnat-family protein acetyltransferase	64.592	3
A0A0H2ZWL5	Succinate dehydrogenase	29.851	2
A0A0H2ZZ99	Possible ketoacyl reductase	27.959	2
A0A0H2ZU50	MmcI protein	28.545	3
A0A0H2ZSD9	Acyl-CoA dehydrogenase	41.754	3
A0A0H2ZY07	Uncharacterized protein	30.719	2
A0A0H3A334	DNA ligase	85.272	2
A0A0H2ZTI8	TetR-family protein transcriptional regulator	25.078	2
A0A0H2ZUY1	Valine--tRNA ligase	98.769	2
A0A0H3A3H5	Electron transfer protein, beta subunit	27.83	2
A0A0H2ZSX9	Adenine specific DNA methylase Mod	74.233	2
A0A0H3A1U7	Propionyl-CoA carboxylase beta chain	50.071	2
A0A0H2ZY31	Limonene 1,2-monooxygenase	42.013	2
A0A0H2ZZV4	Uncharacterized protein	47.57	2
A0A0H3A2S9	Phenylalanine--tRNA ligase beta subunit	87.725	2
A0A0H2ZT48	Putative acyl-CoA dehydrogenase	63.369	2
A0A0H2ZRI7	4-aminobutyrate transaminase	47.248	2
A0A0H3A0K0	Uncharacterized protein	27.09	2
A0A0H2ZTQ3	Amidohydrolase	41.618	2
A0A0H3A2P8	UPF0336 protein MAV_4646	18.948	2
A0QIY9	Proline--tRNA ligase	63.544	2
A0QLX9	Orotate phosphoribosyltransferase	18.836	2
A0A0H2ZV97	UvrABC system protein B	80.884	2
A0A0H3A4W0	Malto-oligosyltrehalose synthase	82.638	2
A0A0H2ZU93	4-hydroxy-3-methylbut-2-en-1-yl diphosphate synthase (flavodoxin)	38.15	2
A0QID4	Threonine--tRNA ligase	76.279	2
A0A0H3A1L3	ATPase, AAA family protein	67.192	2
A0A0H3A0K2	Pyridoxamine 5'-phosphate oxidase family protein	18.899	2
A0A0H2ZXY3	Aldehyde dehydrogenase (NAD) family protein	54.406	3

A0A0H2ZTL6	RNA polymerase sigma factor	35.91	2
A0A0H2ZRL8	Myo-inositol-1-phosphate synthase	40.216	2
A0A0H2ZYN4	MaoC like domain protein	30.22	2
A0A0H2ZSR1	ATP-dependent Clp protease proteolytic subunit	21.651	2
A0A0H2ZW37	Uncharacterized protein	39.41	3
A0A0H3A2S6	Modulator of DNA gyrase	54.682	2
A0A0H2ZXC6	Long-chain specific acyl-CoA dehydrogenase	43.221	2
A0A0H2ZUX4	ESAT-6-like protein OS=Mycobacterium avium (strain 104) GN=MAV_1177 PE=3 SV=1	9.88	2
A0A0H2ZYN3	5-carboxymethyl-2-hydroxymuconate delta-isomerase	28.381	2
A0A0H2ZQF4	Linear gramicidin synthetase subunit D	237.443	3
A0A0H2ZYA7	HesB/YadR/YfhF family protein	12.487	2
A0A0H3A163	Chromosome partition protein Smc	128.989	2
A0QBE6	Alpha-keto-acid decarboxylase	60.351	3
A0A0H3A071	Glycine cleavage T-protein (Aminomethyl transferase)	38.393	2
A0A0H2ZR81	3-alpha-(Or 20-beta)-hydroxysteroid dehydrogenase	25.905	2
A0A0H3A1U0	TrkB protein	23.604	2
A0QKJ4	Adenosine deaminase	40.509	2
A0A0H3A011	Peptidase family protein M13	73.344	2
A0QF50	UDP-N-acetylmuramoylalanine--D-glutamate ligase	49.72	2
A0A0H3A0E2	Pyruvate dehydrogenase E1 component	103.283	2
A0A0H2ZXZ9	Rne protein	102.42	3
A0QKT3	50S ribosomal protein L13	16.157	2
A0A0H2ZX25	Dehydrogenase	67.174	2
A0A0H2ZZI0	Cell division ATP-binding protein FtsE	25.801	2
A0A0H2ZV25	Mg/Co/Ni transporter MgtE	46.517	2
A0A0H3A0F4	Glycine--tRNA ligase	52.476	2
A0A0H3A3F3	DoxX subfamily protein, putative	36.076	2
A0A0H3A3S6	Transferase	42.906	2
A0A0H2ZW38	Oxidoreductase, zinc-binding	35.913	2
A0QJU9	NADH-quinone oxidoreductase subunit C	26.619	2
A0A0H3A0Q3	Short chain dehydrogenase	32.139	2
A0A0H2ZZG2	Uncharacterized protein	16.544	2
A0A0H3A1V1	Putative acyl-CoA dehydrogenase	43.727	2
A0A0H2ZS46	ATP-dependent RNA helicase DeaD	61.302	2
A0A0H2ZWI2	Rieske 2Fe-2S family protein	57.274	2
A0A0H3A2A3	NADP-dependent alcohol dehydrogenase c	37.131	2
A0A0H3A304	MaoC like domain protein	30.431	2
A0A0H2ZXB3	Pyruvate carboxylase	120.415	2
A0A0H2ZUH3	4-alpha-glucanotransferase	80.345	2
A0QHY0	Phosphoenolpyruvate carboxylase	102.484	2
A0A0H2ZWQ2	Succinate dehydrogenase flavoprotein subunit	64.318	2

Table S2: (A) Host (human) proteins found in the exosomes collected 24h post MAH104 infection of THP1 macrophage and (B) uninfected control.

(A)

Accession	Description	MW [kDa]	# Peptides
P02751	fibronectin [OS=Homo sapiens]	262.5	11
P60709	Actin, cytoplasmic 1 [OS=Homo sapiens]	41.7	9
P35527	Keratin, type I cytoskeletal 9 [OS=Homo sapiens]	62	7
H6VRG1	keratin 1 [OS=Homo sapiens]	66.1	9
P13645	Keratin, type I cytoskeletal 10 [OS=Homo sapiens]	58.8	6
P01024	Complement C3 [OS=Homo sapiens]	187	5
B2RDY9	Adenylyl cyclase-associated protein [OS=Homo sapiens]	51.6	4
P62736	Actin, aortic smooth muscle [OS=Homo sapiens]	42	6
P02774-3	Isoform 3 of Vitamin D-binding protein [OS=Homo sapiens]	55.1	3
A0A024R9Q1	thrombospondin 1, isoform CRA_a [OS=Homo sapiens]	129.3	6
P11142-1	Heat shock cognate 71 kDa protein [OS=Homo sapiens]	70.9	5
B7Z507	cDNA FLJ51036, highly similar to Matrix metalloproteinase-9 [OS=Homo sapiens]	71.5	6
B7Z747	cDNA FLJ51120, highly similar to Matrix metalloproteinase-9 [OS=Homo sapiens]	66.1	6
P35908	Keratin, type II cytoskeletal 2 epidermal [OS=Homo sapiens]	65.4	5
C0JYY2	apolipoprotein B (including Ag(x) antigen) [OS=Homo sapiens]	515.2	5
P63104-1	14-3-3 protein zeta/delta [OS=Homo sapiens]	27.7	3
A0A0U4BW16	non-muscle myosin heavy chain 9 [OS=Homo sapiens]	226.4	4
P06733-1	alpha-enolase [OS=Homo sapiens]	47.1	3
P06396	Gelsolin [OS=Homo sapiens]	85.6	4
P07355-2	Isoform 2 of Annexin A2 [OS=Homo sapiens]	40.4	3
B7Z8Q2	cDNA FLJ55606, highly similar to Alpha-2-HS-glycoprotein [OS=Homo sapiens]	46.6	2
A8K9C4	elongation factor 1-alpha [OS=Homo sapiens]	50.2	3
A0A0F7G8J1	Plasminogen [OS=Homo sapiens]	90.6	2
B2RDG0	Proteasome subunit alpha type [OS=Homo sapiens]	29.4	3
D3DRR6	inter-alpha (globulin) inhibitor H2, isoform CRA_a [OS=Homo sapiens]	106.5	3
P01023	alpha-2-macroglobulin [OS=Homo sapiens]	163.2	2
P11021	78 kDa glucose-regulated protein [OS=Homo sapiens]	72.3	2
B2R950	cDNA, FLJ94213, highly similar to Homo sapiens pregnancy-zone protein (PZP), mRNA [OS=Homo sapiens]	163.8	2
P02452	Collagen alpha-1(I) chain [OS=Homo sapiens]	138.9	3
Q15582	Transforming growth factor-beta-induced protein ig-h3 [OS=Homo sapiens]	74.6	2
A8JZY9	tubulin alpha chain [OS=Homo sapiens]	50.1	2
P00734	Prothrombin [OS=Homo sapiens]	70	2
O00391	Sulfhydryl oxidase 1 [OS=Homo sapiens]	82.5	2
A0A1S5UZ07	Talin-1 [OS=Homo sapiens]	271.3	2
A0A0G2JPR0	Complement C4-A [OS=Homo sapiens]	192.8	2
B1AHL2	Fibulin-1 [OS=Homo sapiens]	78.3	2

P14618	Pyruvate kinase PKM [OS=Homo sapiens]	57.9	2
A0A1B0GU03	Uncharacterized protein [OS=Homo sapiens]	62.7	2
O43707	Alpha-actinin-4 [OS=Homo sapiens]	104.8	2
A8K3I0	cDNA FLJ78437, highly similar to Homo sapiens cartilage oligomeric matrix protein (COMP), mRNA [OS=Homo sapiens]	82.8	2
D6RAR4	Hepatocyte growtH factor activator [OS=Homo sapiens]	71.4	2
P49720	proteasome subunit beta type-3 [OS=Homo sapiens]	22.9	2
P31946	14-3-3 protein beta/alpha [OS=Homo sapiens]	28.1	2

(B)

Accession	Description	MW [kDa]	# Peptides
P13645	Keratin, type I cytoskeletal 10 [OS=Homo sapiens]	58.8	9
B4DPP6	cDNA FLJ54371, highly similar to Serum albumin [OS=Homo sapiens]	70.3	2
H6VRG2	keratin 1 [OS=Homo sapiens]	66	10
P02751	fibronectin [OS=Homo sapiens]	262.5	8
P35527	Keratin, type I cytoskeletal 9 [OS=Homo sapiens]	62	7
P35908	Keratin, type II cytoskeletal 2 epidermal [OS=Homo sapiens]	65.4	7
A0A024R9Q1	thrombospondin 1, isoform CRA_a [OS=Homo sapiens]	129.3	7
B2RDY9	Adenylyl cyclase-associated protein [OS=Homo sapiens]	51.6	4
P60709	Actin, cytoplasmic 1 [OS=Homo sapiens]	41.7	6
P01024	Complement C3 [OS=Homo sapiens]	187	3
P02774-3	Isoform 3 of Vitamin D-binding protein [OS=Homo sapiens]	55.1	2
P00734	Prothrombin [OS=Homo sapiens]	70	3
P06733-1	alpha-enolase [OS=Homo sapiens]	47.1	4
B7Z8Q2	cDNA FLJ55606, highly similar to Alpha-2-HS-glycoprotein [OS=Homo sapiens]	46.6	2
P11142-1	Heat shock cognate 71 kDa protein [OS=Homo sapiens]	70.9	4
C0JYY2	apolipoprotein B (including Ag(x) antigen) [OS=Homo sapiens]	515.2	2
P08238	Heat shock protein HSP 90-beta [OS=Homo sapiens]	83.2	3
A0A0U4BW16	non-muscle myosin heavy chain 9 [OS=Homo sapiens]	226.4	4
A8K3I0	cDNA FLJ78437, highly similar to Homo sapiens cartilage oligomeric matrix protein (COMP), mRNA [OS=Homo sapiens]	82.8	4
P12109	Collagen alpha-1(VI) chain [OS=Homo sapiens]	108.5	2
P01023	alpha-2-macroglobulin [OS=Homo sapiens]	163.2	2
P06396	Gelsolin [OS=Homo sapiens]	85.6	3
A8JZY9	tubulin alpha chain [OS=Homo sapiens]	50.1	2
A0A1K0GXZ1	Globin C1 [OS=Homo sapiens]	19.2	2
P07355-2	Isoform 2 of Annexin A2 [OS=Homo sapiens]	40.4	2
A0A0G2JPR0	Complement C4-A [OS=Homo sapiens]	192.8	2
P63104-1	14-3-3 protein zeta/delta [OS=Homo sapiens]	27.7	2
P62805	histone H4 [OS=Homo sapiens]	11.4	2
D3DRR6	inter-alpha (globulin) inhibitor H2, isoform CRA_a [OS=Homo sapiens]	106.5	2
B2R950	cDNA, FLJ94213, highly similar to Homo sapiens pregnancy-zone protein (PZP), mRNA [OS=Homo sapiens]	163.8	2

A0A0F7G8J1	Plasminogen [OS=Homo sapiens]	90.6	2
P36955	Pigment epithelium-derived factor [OS=Homo sapiens]	46.3	2
P11021	78 kDa glucose-regulated protein [OS=Homo sapiens]	72.3	2
P23142	Fibulin-1 [OS=Homo sapiens]	77.2	2
P02452	Collagen alpha-1(I) chain [OS=Homo sapiens]	138.9	2
P08779	Keratin, type I cytoskeletal 16 [OS=Homo sapiens]	51.2	2
P14780	Matrix metalloproteinase-9 [OS=Homo sapiens]	78.4	2
Q59EJ3	heat shock 70kDa protein 1A variant [OS=Homo sapiens]	77.4	2

Table S3: (A) Host (human) proteins found in the exosomes collected 72h post MAH104 infection of THP1 macrophage and (B) uninfected control.

(A)

Accession	Description	MW [kDa]	# Peptides
B4DPP6	cDNA FLJ54371, highly similar to Serum albumin [OS=Homo sapiens]	70.3	3
P13645	Keratin, type I cytoskeletal 10 [OS=Homo sapiens]	58.8	10
P02751-15	Isoform 15 of Fibronectin [OS=Homo sapiens]	272.2	11
P01024	Complement C3 [OS=Homo sapiens]	187	12
P35579-1	Myosin-9 [OS=Homo sapiens]	226.4	11
P35527	Keratin, type I cytoskeletal 9 [OS=Homo sapiens]	62	9
B2RDY9	Adenylyl cyclase-associated protein [OS=Homo sapiens]	51.6	7
P60709	Actin, cytoplasmic 1 [OS=Homo sapiens]	41.7	7
H6VRG1	keratin 1 [OS=Homo sapiens]	66.1	7
P35908	Keratin, type II cytoskeletal 2 epidermal [OS=Homo sapiens]	65.4	7
P11142-1	Heat shock cognate 71 kDa protein [OS=Homo sapiens]	70.9	7
A0A024R9Q1	thrombospondin 1, isoform CRA_a [OS=Homo sapiens]	129.3	8
A0A1S5UZ07	Talin-1 [OS=Homo sapiens]	271.3	7
P14618	Pyruvate kinase PKM [OS=Homo sapiens]	57.9	6
A8K3K1	cDNA FLJ78096, highly similar to Homo sapiens actin, alpha, cardiac muscle (ACTC), mRNA [OS=Homo sapiens]	42	4
P07355-2	Isoform 2 of Annexin A2 [OS=Homo sapiens]	40.4	5
P02774-3	Isoform 3 of Vitamin D-binding protein [OS=Homo sapiens]	55.1	2
P12814-1	Alpha-actinin-1 [OS=Homo sapiens]	103	5
P36222	Chitinase-3-like protein 1 [OS=Homo sapiens]	42.6	5
P61158	actin-related protein 3 [OS=Homo sapiens]	47.3	5
P13647	keratin, type II cytoskeletal 5 [OS=Homo sapiens]	62.3	4
B7Z8Q2	cDNA FLJ55606, highly similar to Alpha-2-HS-glycoprotein [OS=Homo sapiens]	46.6	2
Q15582	Transforming growth factor-beta-induced protein ig-h3 [OS=Homo sapiens]	74.6	4
P08670	Vimentin [OS=Homo sapiens]	53.6	2
P02649	Apolipoprotein E [OS=Homo sapiens]	36.1	5
P04083	annexin A1 [OS=Homo sapiens]	38.7	4
P63104-1	14-3-3 protein zeta/delta [OS=Homo sapiens]	27.7	3
P23142	Fibulin-1 [OS=Homo sapiens]	77.2	5

C0JYY2	apolipoprotein B (including Ag(x) antigen) [OS=Homo sapiens]	515.2	5
B2RDG0	Proteasome subunit alpha type [OS=Homo sapiens]	29.4	4
P01023	alpha-2-macroglobulin [OS=Homo sapiens]	163.2	2
P14780	Matrix metalloproteinase-9 [OS=Homo sapiens]	78.4	4
B2R950	cDNA, FLJ94213, highly similar to Homo sapiens pregnancy-zone protein (PZP), mRNA [OS=Homo sapiens]	163.8	2
B4DR52	Histone H2B [OS=Homo sapiens]	18	2
E9PK25	Cofilin-1 [OS=Homo sapiens]	22.7	3
P00734	Prothrombin [OS=Homo sapiens]	70	2
P36955	Pigment epithelium-derived factor [OS=Homo sapiens]	46.3	3
A8K3I0	cDNA FLJ78437, highly similar to Homo sapiens cartilage oligomeric matrix protein (COMP), mRNA [OS=Homo sapiens]	82.8	4
P04075-2	Isoform 2 of Fructose-bisphosphate aldolase A [OS=Homo sapiens]	45.2	2
P08758	annexin A5 [OS=Homo sapiens]	35.9	3
P08238	Heat shock protein HSP 90-beta [OS=Homo sapiens]	83.2	3
A0A1B0GU03	Uncharacterized protein [OS=Homo sapiens]	62.7	3
P68371	Tubulin beta-4B chain [OS=Homo sapiens]	49.8	3
P06733-1	alpha-enolase [OS=Homo sapiens]	47.1	2
A0A0C4DFU2	superoxide dismutase [OS=Homo sapiens]	24.7	3
A0A1K0GXZ1	Globin C1 [OS=Homo sapiens]	19.2	3
A8JZY9	tubulin alpha chain [OS=Homo sapiens]	50.1	3
A0A087WVQ6	Clathrin heavy chain [OS=Homo sapiens]	191.9	3
P68366	Tubulin alpha-4A chain [OS=Homo sapiens]	49.9	3
P62805	histone H4 [OS=Homo sapiens]	11.4	2
P02545	Prelamin-A/C [OS=Homo sapiens]	74.1	3
A8K9C4	elongation factor 1-alpha [OS=Homo sapiens]	50.2	3
A0A0F7G8J1	Plasminogen [OS=Homo sapiens]	90.6	2
P00558	phosphoglycerate kinase 1 [OS=Homo sapiens]	44.6	2
A0A0U1RRH7	Histone H2A [OS=Homo sapiens]	18.5	2
P12109	Collagen alpha-1(VI) chain [OS=Homo sapiens]	108.5	2
P11021	78 kDa glucose-regulated protein [OS=Homo sapiens]	72.3	2
P08779	Keratin, type I cytoskeletal 16 [OS=Homo sapiens]	51.2	2
O43707	Alpha-actinin-4 [OS=Homo sapiens]	104.8	3
P50897	Palmitoyl-protein thioesterase 1 [OS=Homo sapiens]	34.2	2
D3DRR6	inter-alpha (globulin) inhibitor H2, isoform CRA_a [OS=Homo sapiens]	106.5	2
B4DI54	cDNA FLJ56386, highly similar to Heat shock 70 kDa protein 1L [OS=Homo sapiens]	77.5	2
O15511-2	Isoform 2 of Actin-related protein 2/3 complex subunit 5 [OS=Homo sapiens]	16.6	2
P23526-1	Adenosylhomocysteinase [OS=Homo sapiens]	47.7	2
B2R7F8	Plasminogen [OS=Homo sapiens]	90.5	2
P05452	Tetranectin [OS=Homo sapiens]	22.5	2
P04406-1	glyceraldehyde-3-phosphate dehydrogenase [OS=Homo sapiens]	36	2
O14818-1	Proteasome subunit alpha type-7 [OS=Homo sapiens]	27.9	2
A0A0C4DG17	40S ribosomal protein SA [OS=Homo sapiens]	33.3	2
D6RAR4	Hepatocyte growtH factor activator [OS=Homo sapiens]	71.4	2

A0A0G2JPR0	Complement C4-A [OS=Homo sapiens]	192.8	2
B3KNB4	cDNA FLJ14168 fis, clone NT2RP2001440, highly similar to 14-3-3 protein gamma [OS=Homo sapiens]	28.2	2
P28066-1	Proteasome subunit alpha type-5 [OS=Homo sapiens]	26.4	2
A0A0U4BCF5	Complement factor I [OS=Homo sapiens]	65.3	2
P16104	Histone H2AX [OS=Homo sapiens]	15.1	2
P02452	Collagen alpha-1(I) chain [OS=Homo sapiens]	138.9	2
G9K388	YWHAE/FAM22A fusion protein [OS=Homo sapiens]	41.2	2
B4DLV7	Rab GDP dissociation inhibitor [OS=Homo sapiens]	51.1	2
J3KMX3	Alpha-fetoprotein [OS=Homo sapiens]	70.4	2
P06748	Nucleophosmin [OS=Homo sapiens]	32.6	2
P55072	Transitional endoplasmic reticulum ATPase [OS=Homo sapiens]	89.3	2
P27348	14-3-3 protein theta [OS=Homo sapiens]	27.7	2
Q16658	Fascin [OS=Homo sapiens]	54.5	2
B2R4P2	cDNA, FLJ92164, highly similar to Homo sapiens peroxiredoxin 1 (PRDX1), mRNA [OS=Homo sapiens]	22.2	2
P01031	Complement C5 [OS=Homo sapiens]	188.2	2
P07900-2	Isoform 2 of Heat shock protein HSP 90-alpha [OS=Homo sapiens]	98.1	2

(B)

Accession	Description	MW [kDa]	# Peptides
B2RDY9	Adenylyl cyclase-associated protein [OS=Homo sapiens]	51.6	11
P35579-1	Myosin-9 [OS=Homo sapiens]	226.4	13
P13645	Keratin, type I cytoskeletal 10 [OS=Homo sapiens]	58.8	13
P35527	Keratin, type I cytoskeletal 9 [OS=Homo sapiens]	62	11
A0A024R9Q1	thrombospondin 1, isoform CRA_a [OS=Homo sapiens]	129.3	14
B4DPP6	cDNA FLJ54371, highly similar to Serum albumin [OS=Homo sapiens]	70.3	3
P02751-15	Isoform 15 of Fibronectin [OS=Homo sapiens]	272.2	11
A0A1S5UZ07	Talin-1 [OS=Homo sapiens]	271.3	12
P60709	Actin, cytoplasmic 1 [OS=Homo sapiens]	41.7	9
H6VRG1	keratin 1 [OS=Homo sapiens]	66.1	10
P01024	Complement C3 [OS=Homo sapiens]	187	6
P35908	Keratin, type II cytoskeletal 2 epidermal [OS=Homo sapiens]	65.4	9
A8JZY9	tubulin alpha chain [OS=Homo sapiens]	50.1	6
P02649	Apolipoprotein E [OS=Homo sapiens]	36.1	7
P68366	Tubulin alpha-4A chain [OS=Homo sapiens]	49.9	6
P14618	Pyruvate kinase PKM [OS=Homo sapiens]	57.9	7
A8K3I0	cDNA FLJ78437, highly similar to Homo sapiens cartilage oligomeric matrix protein (COMP), mRNA [OS=Homo sapiens]	82.8	5
P11142-1	Heat shock cognate 71 kDa protein [OS=Homo sapiens]	70.9	5
P36222	Chitinase-3-like protein 1 [OS=Homo sapiens]	42.6	4
Q59EJ3	heat shock 70kDa protein 1A variant [OS=Homo sapiens]	77.4	4
P12814-4	Isoform 4 of Alpha-actinin-1 [OS=Homo sapiens]	107.1	7
P68371	Tubulin beta-4B chain [OS=Homo sapiens]	49.8	6

P02774-3	Isoform 3 of Vitamin D-binding protein [OS=Homo sapiens]	55.1	2
P07437	tubulin beta chain [OS=Homo sapiens]	49.6	6
P23142	Fibulin-1 [OS=Homo sapiens]	77.2	6
A8K3K1	cDNA FLJ78096, highly similar to Homo sapiens actin, alpha, cardiac muscle (ACTC), mRNA [OS=Homo sapiens]	42	5
B2R7F8	Plasminogen [OS=Homo sapiens]	90.5	4
P00734	Prothrombin [OS=Homo sapiens]	70	3
C0JYY2	apolipoprotein B (including Ag(x) antigen) [OS=Homo sapiens]	515.2	4
P36955	Pigment epithelium-derived factor [OS=Homo sapiens]	46.3	4
E9PK25	Cofilin-1 [OS=Homo sapiens]	22.7	3
P11021	78 kDa glucose-regulated protein [OS=Homo sapiens]	72.3	3
Q15582	Transforming growth factor-beta-induced protein ig-h3 [OS=Homo sapiens]	74.6	4
A0A0G2JPR0	Complement C4-A [OS=Homo sapiens]	192.8	4
P07355-2	Isoform 2 of Annexin A2 [OS=Homo sapiens]	40.4	4
P12109	Collagen alpha-1(VI) chain [OS=Homo sapiens]	108.5	3
A0A087WVQ6	Clathrin heavy chain [OS=Homo sapiens]	191.9	4
P62805	histone H4 [OS=Homo sapiens]	11.4	3
P35443	Thrombospondin-4 [OS=Homo sapiens]	105.8	3
B5BU38	Annexin [OS=Homo sapiens]	38.7	3
P31146	Coronin-1A [OS=Homo sapiens]	51	3
P05452	Tetranectin [OS=Homo sapiens]	22.5	2
A0A1K0GXZ1	Globin C1 [OS=Homo sapiens]	19.2	2
D3DRR6	inter-alpha (globulin) inhibitor H2, isoform CRA_a [OS=Homo sapiens]	106.5	3
B7Z8Q2	cDNA FLJ55606, highly similar to Alpha-2-HS-glycoprotein [OS=Homo sapiens]	46.6	2
P63104-1	14-3-3 protein zeta/delta [OS=Homo sapiens]	27.7	2
P01023	alpha-2-macroglobulin [OS=Homo sapiens]	163.2	2
A8K9C4	elongation factor 1-alpha [OS=Homo sapiens]	50.2	3
G3V5Z7	Proteasome subunit alpha type [OS=Homo sapiens]	28.1	3
P02452	Collagen alpha-1(I) chain [OS=Homo sapiens]	138.9	2
P06899	Histone H2B type 1-J [OS=Homo sapiens]	13.9	3
P06396	Gelsolin [OS=Homo sapiens]	85.6	2
P06733-1	alpha-enolase [OS=Homo sapiens]	47.1	2
P23526-1	Adenosylhomocysteinase [OS=Homo sapiens]	47.7	3
A0A0U1RRH7	Histone H2A [OS=Homo sapiens]	18.5	2
B7Z6Z4	Myosin light polypeptide 6 [OS=Homo sapiens]	26.7	3
P04406-1	glyceraldehyde-3-phosphate dehydrogenase [OS=Homo sapiens]	36	3
P61160-1	Actin-related protein 2 [OS=Homo sapiens]	44.7	3
P61626	lysozyme c [OS=Homo sapiens]	16.5	2
P17987	T-complex protein 1 subunit alpha [OS=Homo sapiens]	60.3	3
A0A0A0MRJ7	Coagulation factor V [OS=Homo sapiens]	252.1	2
B4DLV7	Rab GDP dissociation inhibitor [OS=Homo sapiens]	51.1	2
P49327	Fatty acid synthase [OS=Homo sapiens]	273.3	2
A8K4Z4	60S acidic ribosomal protein P0 [OS=Homo sapiens]	34.2	2
O60701	UDP-glucose 6-dehydrogenase [OS=Homo sapiens]	55	2

J3KMX3	Alpha-fetoprotein [OS=Homo sapiens]	70.4	2
P55072	Transitional endoplasmic reticulum ATPase [OS=Homo sapiens]	89.3	2
A0A1B0GU03	Uncharacterized protein [OS=Homo sapiens]	62.7	2
P01344-3	Isoform 3 of Insulin-like growth factor II [OS=Homo sapiens]	26.3	2
P16104	Histone H2AX [OS=Homo sapiens]	15.1	2
O14818-1	Proteasome subunit alpha type-7 [OS=Homo sapiens]	27.9	2
P07737	profilin-1 [OS=Homo sapiens]	15	2
P61158	actin-related protein 3 [OS=Homo sapiens]	47.3	2
A0A0F7G8J1	Plasminogen [OS=Homo sapiens]	90.6	2
P05543	thyroxine-binding globulin [OS=Homo sapiens]	46.3	2
O15511-2	Isoform 2 of Actin-related protein 2/3 complex subunit 5 [OS=Homo sapiens]	16.6	2
P51570-2	Isoform 2 of Galactokinase [OS=Homo sapiens]	45.3	2
B2R950	cDNA, FLJ94213, highly similar to Homo sapiens pregnancy-zone protein (PZP), mRNA [OS=Homo sapiens]	163.8	2
Q08380	Galectin-3-binding protein [OS=Homo sapiens]	65.3	2
P07900-2	Isoform 2 of Heat shock protein HSP 90-alpha [OS=Homo sapiens]	98.1	2
P50990	T-complex protein 1 subunit theta [OS=Homo sapiens]	59.6	2
P04075-2	Isoform 2 of Fructose-bisphosphate aldolase A [OS=Homo sapiens]	45.2	2
Q5U0B9	stem cell growth factor; lymphocyte secreted C-type lectin [OS=Homo sapiens]	35.6	2
P48740-2	Isoform 2 of Mannan-binding lectin serine protease 1 [OS=Homo sapiens]	81.8	2
P25789	Proteasome subunit alpha type-4 [OS=Homo sapiens]	29.5	2
A0A161I202	lactoferrin [OS=Homo sapiens]	78.3	2

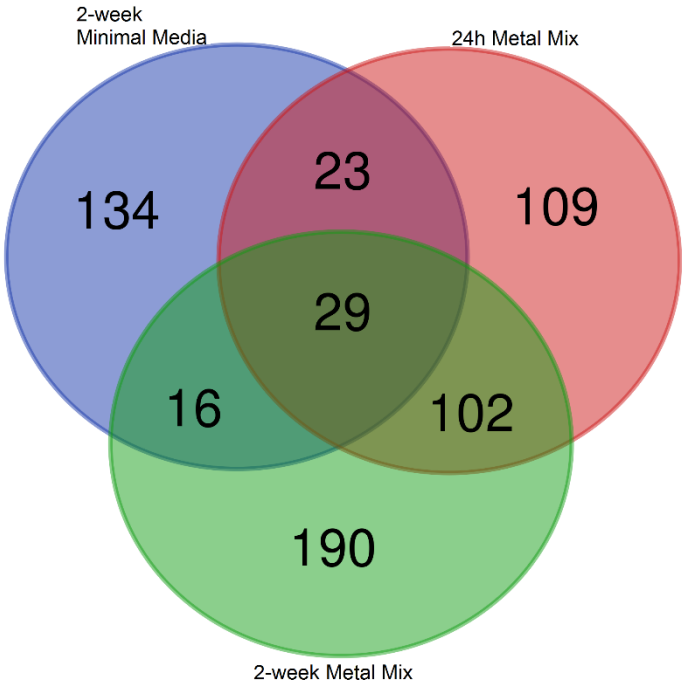

Figure S1: Venn diagram showing common and unique proteins found in MAH104 MVs released in response to 2-week minimal media exposure, 24h metal mix exposure and 2-week metal mix exposure. The Venn diagrams were created by using Ghent University, Gent, Belgium operated Bioinformatics & Evolutionary Genomics website (http://bioinformatics.psb.ugent.be/webtools/Venn/)

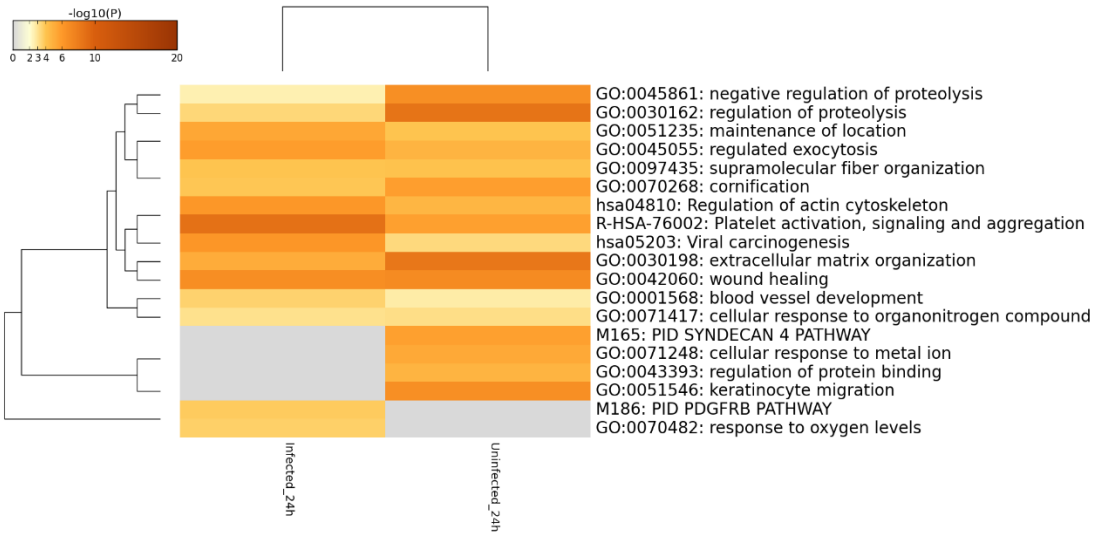

Figure S2: Heat map of Gene Ontology: The Metascape (http://metascape.org) bioinformatic analysis was used to perform enrichment analyses of GO Biological Process terms for human macrophage proteins uniquely synthesized during M. avium infection at 24h. *p values <0.05.

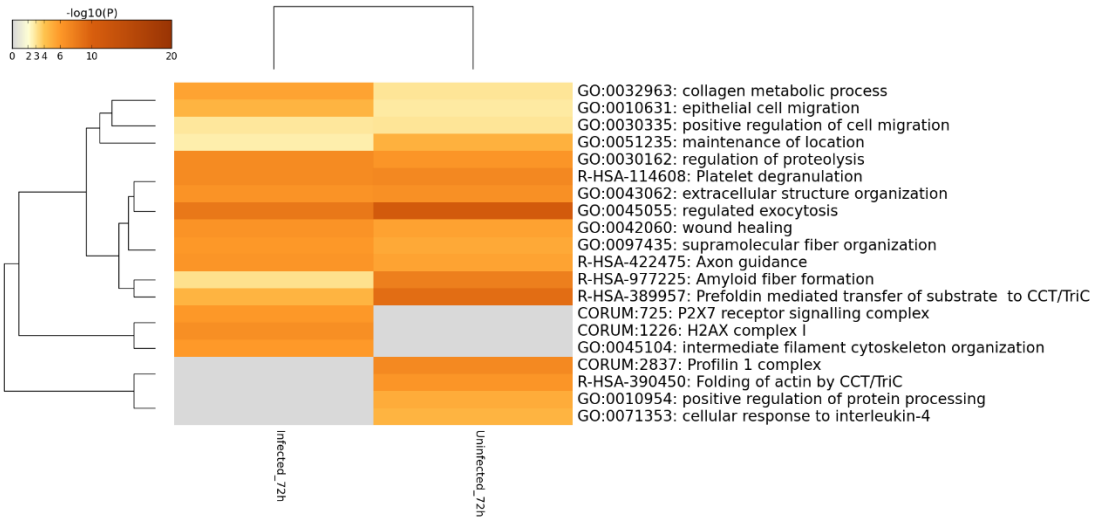

Figure S3: Heat map of Gene Ontology: The Metascape (http://metascape.org) bioinformatic analysis was used to perform enrichment analyses of GO Biological Process terms for human macrophage proteins uniquely synthesized during M. avium infection at 72h. *p values <0.05.

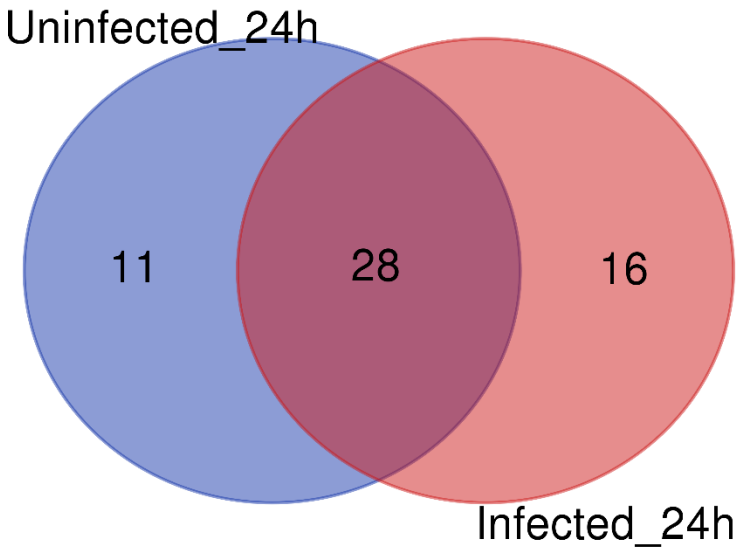

Figure S4: Venn diagram showing common and unique proteins found in exosomes of MAH104 infected THP1 human macrophages and uninfected control. The Venn diagrams were created by using Ghent University, Gent, Belgium operated Bioinformatics & Evolutionary Genomics website (http://bioinformatics.psb.ugent.be/webtools/Venn/)

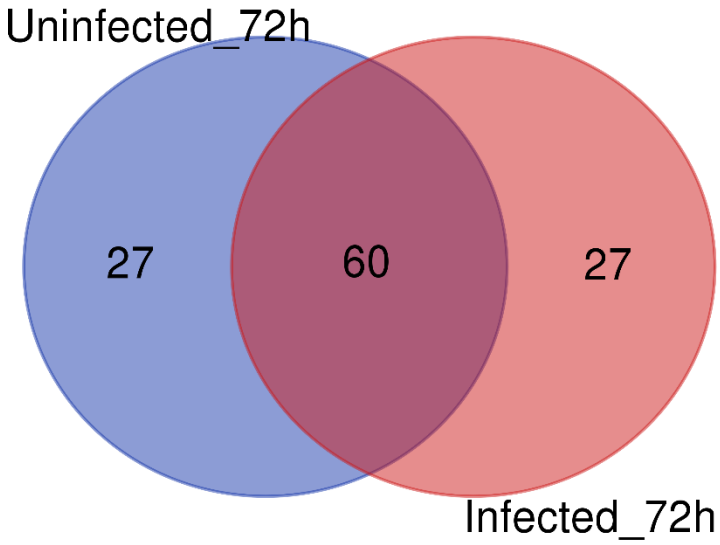

Figure S4: Venn diagram showing common and unique proteins found in exosomes of MAH104 infected THP1 human macrophages and uninfected control. The Venn diagrams were created by using Ghent University, Gent, Belgium operated Bioinformatics & Evolutionary Genomics website (http://bioinformatics.psb.ugent.be/webtools/Venn/)